# Data Analysis and Experimental Design for Accelerated Life Testing with Heterogeneous Group Effects

by

Kangwon Seo

A Dissertation Presented in Partial Fulfillment
of the Requirements for the Degree
Doctor of Philosophy

Approved May 2017 by the
Graduate Supervisory Committee:

Rong Pan, Chair
Douglas C. Montgomery
J. Rene Villalobos
Steven E. Rigdon

ARIZONA STATE UNIVERSITY

August 2017

ABSTRACT

In accelerated life tests (ALTs), complete randomization is hardly achievable because of economic and engineering constraints. Typical experimental protocols such as subsampling or random blocks in ALTs result in a grouped structure, which leads to correlated lifetime observations. In this dissertation, generalized linear mixed model (GLMM) approach is proposed to analyze ALT data and find the optimal ALT design with the consideration of heterogeneous group effects.

Two types of ALTs are demonstrated for data analysis. First, constant-stress ALT (CSALT) data with Weibull failure time distribution is modeled by GLMM. The marginal likelihood of observations is approximated by the quadrature rule; and the maximum likelihood (ML) estimation method is applied in iterative fashion to estimate unknown parameters including the variance component of random effect. Secondly, step-stress ALT (SSALT) data with random group effects is analyzed in similar manner but with an assumption of exponentially distributed failure time in each stress step. Two parameter estimation methods, from the frequentist's and Bayesian points of view, are applied; and they are compared with other traditional models through simulation study and real example of the heterogeneous SSALT data. The proposed random effect model shows superiority in terms of reducing bias and variance in the estimation of life-stress relationship.

The GLMM approach is particularly useful for the optimal experimental design of ALT while taking the random group effects into account. In specific, planning ALTs under nested design structure with random test chamber effects are studied. A greedy two-phased approach shows that different test chamber assignments to stress conditions substantially impact on the estimation of unknown parameters. Then, the $D$-optimal test plan with two test chambers is constructed by applying the quasi-likelihood approach. Lastly, the optimal ALT planning is expanded for the case

of multiple sources of random effects so that the crossed design structure is also considered, along with the nested structure.

*This dissertation is dedicated to:*

*my parents, parents-in-law, sister and brother,*

*Eva and Grace, and my wife*

# ACKNOWLEDGMENTS

All of my efforts, frustration, happiness, helplessness during last few years for research achievements are all melted in this dissertation. There are many people to whom I want to express my gratitude for this achievement.

First and foremost, I want to thank Dr. Rong Pan for being the chair of my Ph.D. committee. I am grateful for all opportunities that he has provided me. He allowed me to work on research under his supervision and gave me opportunities to delve into various kinds of research topics. He also supported, encouraged, and cared me with open mind. Without him, this dissertation would not have been possible.

I also would like to thank Dr. Douglas Montgomery, Dr. Rene Villalobos, and Dr. Steven Rigdon for spending time and guiding me as the committee members of this dissertation. Especially I have learned a lot from Dr. Montgomery, not only his knowledge but also his attitude as a scholar. His continuous curiosity and respect for students' opinions always inspired me.

In addition, I also wish to thank Dr. Cheryl Jennings, Dr. Koo-hyun Park, and Dr. Kewei Chen for their supports and care during my endeavor. Their encouragements and commendation have become a strong motivation to endure this long journey.

Lastly I would never have been able to complete this dissertation without dedication and love of my family. My parents, Kyung-il Seo and Sara Min, my parents-in-law, Myung-ki Park and Soon-ok Yim, my elder sister and brother, Iris Seo and Jangwon Seo have always trusted and concerned me. I especially wish to express my deep gratitude to my two lovely daughters, Eva and Grace, and my wife, Seoyeon Park, for their endurance, trust, and love during my graduate study.

TABLE OF CONTENTS

CHAPTER Page

CHAPTER Page

LIST OF TABLES

LIST OF FIGURES

Figure Page

# Chapter 1

# INTRODUCTION

Lifetime estimation and prediction of a product have long been a great concern for reliability engineers. Information extracted from products' life tests plays a fundamental role for all reliability-related decision making such as establishing warranty policy or evaluating new product designs. Due to the impractical time duration of a life test of products in usual environmental condition, accelerated life tests (ALTs), by which test units are exposed to higher-than-usual stress levels, are widely used to obtain failure time observations in manageable test time. In a sense that lifetime (i.e., the response variable) depends on stress conditions (i.e., explanatory variables), a regression type of model is used for statistical inference of ALT data.

ALT is a special type of experiment as it has some interesting characteristics which are distinct from typical experiments. First, failure time data need to be modeled by a positive continuous random variable, which means that the response variable is not normally distributed. In many cases, a log-location-scale family, such as Weibull or log-normal distribution, is considered for the failure time distribution model. Secondly, in spite of being accelerated, lifetime of some test units are still longer than the test duration; and it causes right-censored data, where the exact failure time is unobserved. Lastly, the inference obtained in the test region should be extrapolated to the usual stress region, which is located beyond the region where the data is collected. Despite all of these challenges, data analysis and efficient experimental designs for ALT have been well-studied in the literature (see e.g., Nelson, 2009; Meeker and Escobar, 2014).

Among other modeling approaches for ALT data, the generalized linear model (GLM) (McCullagh and Nelder, 1989) has been recently applied to data analysis and optimal planning of ALTs (Aitkin and Clayton, 1980; Lee and Pan, 2010; Monroe *et al.*, 2011; Yang and Pan, 2013). The GLM provides a structured framework for statistical inferences and experimental design of ALTs. For example, most popular statistical software packages are capable for the parameter estimation of a GLM model. Despite its usefulness, the GLM approach for ALT assumes that the observations are independent of each other. In practice, however, complete randomization of an ALT is easily violated by, for example, different sources of test materials or use of non-homogeneous test stands, which all leads to the involvement of unwanted nuisance factors into the test. For more information about the experimental protocols which hinder the independent reliability data, see e.g., Vining (2013). As a result, ALT data obtained from the same group (e.g., observations from the same test chamber) are expected to be correlated.

In this thesis, failure time data analysis and optimal experimental designs for ALTs with restricted randomization are discussed. In particular, ALT data is modeled taking correlations between observations into account. The generalized linear mixed model (GLMM) approach, which is a natural expansion of GLM for random effect models, is suggested to accommodate a heterogeneous group effect of ALTs with right-censoring plan. Although, most recently, data analysis for correlated ALT data has been studied by several researchers (León *et al.*, 2007; Pan and Kozakai, 2013; Freeman and Vining, 2010; Kensler *et al.*, 2015), the experimental design for ALT under the mixed effect model, to the best of my knowledge, has not been studied yet. In this aspect, the GLMM provides a useful framework for planning correlated ALTs, so does the GLM for the independent ALTs.

The remainder of this thesis is structured as follows. Chapter 2 describes the GLMM approach for analyzing constant-stress ALT (CSALT) data with random group effects. The iterative maximum likelihood method for parameter estimation is presented; and the asymptotic variance-covariance matrix of the estimated parameters is derived. The marginal likelihood of GLMM involves an integration without a closed form. The quadrature method is used to approximate it by which the fast evaluation of the likelihood function is available. The proposed model is applied to two real reliability data, which are examples of subsampling and random blocks, respectively.

Chapter 3 extends the GLMM approach to the analysis of step-stress ALT (SSALT) data. By the memoryless property of the exponential distribution, SSALT data is transformed to the pseudo-CSALT data. Two different methods are examined for the parameter estimation from the frequentist and Bayesian perspectives, but both are based on the deterministic approach. Traditional fixed effect models and the proposed random effect model are compared by the simulation study and real SSALT data.

In Chapter 4, the chamber-to-chamber variation is addressed for planning ALTs. When an ALT is conducted with multiple test chambers, an assignment of test chambers to each stress condition is important. This experiment can be seen as a type of nested designs where the stress conditions are nested in the test chambers. First, impacts of different test chamber assignment plans are illustrated by two-phased approach. Second, the quasi-likelihood approach, enabled by GLMM, is introduced to construct the $D$-optimal design. A specific example of ALT with two stress factors is considered with two test chambers tested on four different stress conditions.

Chapter 5 addresses, extending the idea of Chapter 4, the $D$-optimal design with multiple sources of random group effects. In real world applications, it is not unusual to have products provided by different suppliers be tested on different test chambers.

In this case, the observations are grouped not only by test chambers but also by suppliers. A similar example with Chapter 4, but with an additional random effect, is described to illustrate the construction of the $D$-optimal design.

Finally, contributions of this thesis and future research is described in Chapter 6.

Chapter 2

# DATA ANALYSIS FOR ACCELERATED LIFE TESTS WITH CONSTRAINED RANDOMIZATION

Accelerated life tests (ALTs) often involve experimental protocols with constrained randomization such as subsampling or random block. As a result, lifetime data may involve a grouped structure among the observations. In this chapter, we develop a generalized linear mixed model (GLMM) approach for analyzing ALT data with a grouped structure in order to reflect random effects of groups in the model. The GLMM approach provides a flexible way to model censored failure time data with random effects. Particularly, for the Weibull failure time distribution, we describe an iterative procedure for the model parameters estimation and derive the asymptotic variance-covariance matrix using the approximated likelihood function. Two examples of lifetime data with subsampling and random block are analyzed by the proposed method, which is implemented by modern computer software.

## 2.1 Introduction

### *2.1.1 Problem*

Randomization is one of the basic principles of experimental design. A completely randomized design assumes all experimental responses to be independent of each other. Planning an accelerated life test (ALT) with multiple stress factors can be treated as an experimental design problem, thus it should follow this principle. In

reality, however, ALT experiments are inevitably going to violate the randomization assumption because of the engineering and economic constraints of such tests. Typical experimental protocols in ALTs include subsampling or random block, and both lead to a grouped structure among observations. Data analysis that does not take into account any of these constrained randomization conditions may result in incorrect inferences on parameters of interest.

Recently, there have been several attempts to take into account experimental protocols (e.g., subsampling or random block) in reliability data analysis. Freeman and Vining (2010) described a two-stage method for analyzing reliability data from designed experiments containing subsampling. León *et al.* (2007) used Bayesian Monte Carlo Markov Chain (MCMC) methods to make inferences from an ALT where the test units come from different batches and the batch effect is random. Freeman and Vining (2013) provided a Weibull nonlinear mixed model (NLMM) methodology for incorporating random effects in the analysis. They applied quadrature approximation on the expectation of the likelihood function over random effects. Pan and Kozakai (2013) proposed a semiparametric model with random effects and the Bayesian piecewise exponential inference method. Xiao and Tang (2013) suggested a method that incorporates the idea of frailty, which accounts for the subsampling effect, and the technique of multiple imputations to deal with censored data. Wang *et al.* (2015) presented an improved two-stage approach using bootstrapping and an unbiasing factor.

In this chapter, we propose a generalized linear mixed model (GLMM) approach to analyzing multiple-stress ALT data with constrained randomization. The idea is based on Aitkin and Clayton (1980) in which they reformulated likelihood functions of right censored survival data under exponential, Weibull or extreme value distribution as a generalized linear model (GLM). Monroe *et al.* (2011) and Yang and Pan (2013)

utilized the GLM approach for the experimental designs of ALTs. We extend the inference procedure of Aitkin and Clayton (1980) to mixed models so that random effects can be accommodated. This approach shares the same principle of fitting the grouped failure time data by maximizing the approximated likelihood with the NLMM method (Freeman and Vining, 2013), the most recent approach among the frequentist methods. However, our approach has several advantages over the other approaches. These advantages are (1) it provides more flexible ways to model failure time data as the failure time distribution is not specified in advance and censored observations can be easily accommodated; (2) it enjoys the use of GLMMs, a well-developed non-linear mixed model, and the computing algorithms that have been implemented in several statistical software packages; and (3) it opens the opportunity for the experimental design study of ALT with random effects as GLM has been used for fixed effects model in Monroe *et al.* (2011) and Yang and Pan (2013).

### *2.1.2 Motivating Examples*

Zelen (1959) described the glass capacitor life test experiment, which was conducted with two stress variables, voltage and temperature. The dataset consists of 64 failure/censoring time observations under 8 different stress combinations. In a complete randomized design, each glass capacitor should be randomly assigned to a test stand and tested at the same time; instead, Zelen's data were generated from 8 test stands with 8 glass capacitors (i.e., subsamples) per test stand. In this case, correlation may exist among failure times from the same test stand.

Another well-known ALT experiment with constrained randomization is provided by Gerstle and Kunz (1983), in which they studied the reliability of pressure vessels wrapped by different spools (i.e., random blocks). A total of 108 pressure vessels were tested at four different pressure levels and 8 spools were used to wrap pressure vessels.

Since different spools may have different strength, lifetimes of pressure vessels with the same spool may be correlated.

## 2.2 Methodology

In this section, we describe the method for analyzing failure time data with a grouped structure by the GLMM approach. The basic principle for parameter estimation is maximizing the expected log-likelihood function; thus, the marginal log-likelihood function or its approximation needs to be obtained by integrating out random effect variables. Given its popularity, the case of Weibull failure time distribution will be shown in this section, but the method can be easily extended to other distributions. The asymptotic variance-covariance matrix of the estimated parameters is also derived for statistical inferences.

### *2.2.1 Generalized Linear Mixed Model Approach*

Suppose we conduct an experiment in which randomization is constrained by subsampling or random blocks, thus there exists groups in the data. Let $t_{ij}$ be the failure time of the $j$th test unit in the $i$th group with $i = 1, \ldots, m$ and $j = 1, \ldots, n_j$, and $\mathbf{x}_{ij} = (1, x_{ij}^1, \ldots, x_{ij}^p)'$ be the corresponding vector of explanatory variables (i.e., stress condition). A normal random variable $u_i$ is introduced to reflect the random effects among groups. That is,

$$u_i \sim \text{iid. } N(0, \sigma_u^2).$$

Let $f(t|u)$, $F(t|u)$, $R(t|u) = 1 - F(t|u)$ and $h(t|u) = f(t|u)/R(t|u)$ be probability density function (pdf), cumulative density function (cdf), reliability function and hazard function of failure time $t$, all conditional on the group effect $u$, respectively. The Cox's proportional hazard (PH) model (Cox, 1972) can be extended to the mixed

model as follows:

$$h(t_{ij}|u_i) = h_0(t_{ij}) \exp(\eta_{ij}) \tag{2.1}$$

where $\eta_{ij} = \mathbf{x}'_{ij}\boldsymbol{\beta} + u_i$ is a linear predictor which includes the random effect as its intercept. Thus, the conditional pdf of failure time is

$$f(t_{ij}|u_i) = h_0(t_{ij}) \exp(\eta_{ij} - H_0(t_{ij})e^{\eta_{ij}}) \tag{2.2}$$

where $H_0(t_{ij}) = \int_{-\infty}^{t} h_0(v_{ij})\, \mathrm{d}v_{ij}$ and it is the cumulative baseline hazard function.

For right censored failure time data, let $c_{ij}$ be an indicator variable taking the value 1 if $t_{ij}$ is a failed observation, and 0 if $t_{ij}$ is a censored observation. We assume that the failure times of a given group are independent of each other within the group. Hence, the marginal likelihood of entire observations in all groups can be written as

$$\begin{aligned}
L &= \prod_{i=1}^{m} \int_{-\infty}^{\infty} \prod_{j=1}^{n_i} f(t_{ij}|u_i)^{c_{ij}} R(t_{ij}|u_i)^{1-c_{ij}} \pi(u_i)\, \mathrm{d}u_i \\
&= \prod_{i=1}^{m} \int_{-\infty}^{\infty} \prod_{j=1}^{n_i} h(t_{ij}|u_i)^{c_{ij}} R(t_{ij}|u_i) \pi(u_i)\, \mathrm{d}u_i \\
&= \prod_{i=1}^{m} \int_{-\infty}^{\infty} \prod_{j=1}^{n_i} [h_0(t_{ij})e^{\eta_{ij}}]^{c_{ij}} \exp(-H_0(t_{ij})e^{\eta_{ij}}) \pi(u_i)\, \mathrm{d}u_i \\
&= \prod_{i=1}^{m} \int_{-\infty}^{\infty} \prod_{j=1}^{n_i} \left(\mu_{ij}^{c_{ij}} e^{-\mu_{ij}}\right) [h_0(t_{ij})/H_0(t_{ij})]^{c_{ij}} \pi(u_i)\, \mathrm{d}u_i
\end{aligned} \tag{2.3}$$

where $\mu_{ij} = H_0(t_{ij})e^{\eta_{ij}}$ and $\pi(u_i)$ is the normal pdf of $u_i$. The term in the round bracket of the likelihood function Eq. (2.3) is the kernel of the likelihood function for Poisson distributed random variable with mean $\mu_{ij}$. The second term does not involve the parameters of fixed effects $\boldsymbol{\beta}$ and of random effects $\sigma_u^2$, but may depend on other unknown parameters in the baseline hazard function. Therefore, the parameter estimators, $\hat{\boldsymbol{\beta}}$ and $\hat{\sigma}_u^2$, that maximize the likelihood function (or log-likelihood function) are the same as those that maximize the likelihood function (or log-likelihood function) from the Poisson distribution.

Given $u_i$, we can treat the indicator variable $c_{ij}$ as from Poisson distribution with conditional mean $\mu_{ij} = \mathbb{E}[c_{ij}|u_i]$, and the GLMM formulation is written as

- The response variable : $c_{ij}|u_i \sim \text{ind. } Poisson(\mu_{ij})$;
- The linear predictor : $\eta_{ij} = \mathbf{x}'_{ij}\boldsymbol{\beta} + u_i$;
- The random effects distribution : $u_i \sim \text{iid. } N(0, \sigma_u^2)$;
- The link function : $\log \mu_{ij} = \eta_{ij} + \log H_0(t_{ij})$,

where the second term in the right hand side of the link function is an offset term.

We maximize the log-likelihood function in an iterative fashion. Given initial estimates of the unknown parameters in $H_0(t_{ij})$, the ML estimates of $\boldsymbol{\beta}$ and $\sigma_u^2$ are obtained from GLMM parameter estimation method which can be conducted by software packages such as R or SAS. With these estimates of $\boldsymbol{\beta}$ and $\sigma_u^2$, the updated estimates of the unknown parameters in $H_0(t_{ij})$ can be obtained from the likelihood equations with respect to these parameters, and this sequence of steps continued until convergence.

### *2.2.2 Weibull Distribution*

The PH model is a semiparametric model, that is, the baseline hazard function is typically unspecified. Thus, the GLMM formulation is applicable on any right censored data set as long as the PH assumption of Eq. (2.1) is acceptable. Meanwhile, it is well-known that, for Weibull distribution, the PH model is equivalent to the accelerated failure time (AFT) model which is one of the most popular models in the reliability field. For this reason, we focus on the Weibull distribution in this chapter, although it is also possible to use other distributions (e.g., extreme value distribution) by changing the baseline hazard function (see Aitkin and Clayton, 1980).

The pdf of Weibull distribution is obtained as follows from Eq. (2.2) by specifying $H_0(t_{ij}) = t_{ij}^{\alpha}$ with an unknown shape parameter $\alpha > 0$ that is assumed to be common to all failure times in different groups.

$$f(t_{ij}|u_i) = \alpha\lambda_{ij}t_{ij}^{\alpha-1}\exp\left(-\lambda_{ij}t_{ij}^{\alpha}\right), \quad t_{ij} > 0$$

where $\lambda_{ij} = e^{\eta_{ij}}$ is a scale parameter (or intrinsic failure rate) modeled as log-linear relationship with the linear predictor. From Eq. (2.3), the likelihood function is

$$L = \prod_{i=1}^{m}\int_{-\infty}^{\infty}\prod_{j=1}^{n_i}\left(\mu_{ij}^{c_{ij}}e^{-\mu_{ij}}\right)\left[\alpha/t_{ij}\right]^{c_{ij}}\pi(u_i)\,\mathrm{d}u_i$$

where $\mu_{ij} = t_{ij}^{\alpha}e^{\eta_{ij}}$, thus the link function is

$$\log\mu_{ij} = \eta_{ij} + \alpha\log t_{ij},$$

and the log-likelihood is

$$\log L = \sum_{i=1}^{m}\sum_{j=1}^{n_i}c_{ij}(\log\alpha - \log t_{ij}) + \sum_{i=1}^{m}\log\int_{-\infty}^{\infty}\prod_{j=1}^{n_i}\left(\mu_{ij}^{c_{ij}}e^{-\mu_{ij}}\right)\pi(u_i)\,\mathrm{d}u_i. \tag{2.4}$$

Note that Eq. (2.4) includes the integration with respect to the random effect $u_i$, which may not be evaluated analytically.

### *2.2.3 Maximum Likelihood Estimation*

The likelihood equations can be derived by setting the partial derivatives of Eq. (2.4) with respect to each unknown parameter equal to zeros, which are given, by exchangeability between integral and derivative, as follows:

$$\frac{\partial\log L}{\partial\alpha} = \frac{\sum_{i=1}^{m}\sum_{j=1}^{n_i}c_{ij}}{\alpha} - \sum_{i=1}^{m}\left\{\frac{\int_{-\infty}^{\infty}p_i(u_i)\,q_i(u_i)\,\pi(u_i)\,\mathrm{d}u_i}{\int_{-\infty}^{\infty}p_i(u_i)\,\pi(u_i)\,\mathrm{d}u_i}\right\} = 0, \tag{2.5a}$$

$$\frac{\partial\log L}{\partial\beta_k} = -\sum_{i=1}^{m}\left\{\frac{\int_{-\infty}^{\infty}p_i(u_i)\,r_i^k(u_i)\,\pi(u_i)\,\mathrm{d}u_i}{\int_{-\infty}^{\infty}p_i(u_i)\,\pi(u_i)\,\mathrm{d}u_i}\right\} = 0, \tag{2.5b}$$

$$\frac{\partial\log L}{\partial\sigma_u^2} = -\sum_{i=1}^{m}\left\{\frac{\int_{-\infty}^{\infty}p_i(u_i)\,s(u_i)\,\pi(u_i)\,\mathrm{d}u_i}{\int_{-\infty}^{\infty}p_i(u_i)\,\pi(u_i)\,\mathrm{d}u_i}\right\} = 0, \tag{2.5c}$$

where

$$p_i(u_i) = \prod_{j=1}^{n_i} \left(\mu_{ij}^{c_{ij}} e^{-\mu_{ij}}\right), \tag{2.6a}$$

$$q_i(u_i) = \sum_{j=1}^{n_i} \log t_{ij}(\mu_{ij} - c_{ij}), \tag{2.6b}$$

$$r_i^k(u_i) = \sum_{j=1}^{n_i} \log x_{ijk}(\mu_{ij} - c_{ij}), \tag{2.6c}$$

$$s(u_i) = \frac{1}{2\sigma_u^2} - \frac{u_i^2}{2\sigma_u^4}, \tag{2.6d}$$

for each group $i = 1, \ldots, m$. From Eq. (2.5a), the ML estimate of $\alpha$ satisfies

$$\hat{\alpha} = \frac{\sum_{i=1}^{m} \sum_{j=1}^{n_i} c_{ij}}{\sum_{i=1}^{m} \left\{ \frac{\int_{-\infty}^{\infty} p_i(u_i)\, q_i(u_i)\, \pi(u_i)\, \mathrm{d}u_i}{\int_{-\infty}^{\infty} p_i(u_i)\, \pi(u_i)\, \mathrm{d}u_i} \right\}} \tag{2.7}$$

The integrals in the denominator cannot be simplified further or be expressed in a closed analytical form; thus, some numerical integration method is needed. As seen in Eq. (2.7), each integration is a single-dimension integral with respect to a normal density, which can be evaluated accurately using Gauss-Hermite (G-H) quadrature (McCulloch *et al.*, 2008). It can be seen that the denominator of Eq. (2.7) is a sum of ratios of two integrals of the form

$$\int_{-\infty}^{\infty} g(u_i) \frac{e^{-u_i^2/(2\sigma_u^2)}}{\sqrt{2\pi\sigma_u^2}}\, \mathrm{d}u_i \tag{2.8}$$

which, by a variable transformation of $u_i = \sqrt{2}\sigma_u v$, can be written as

$$\int_{-\infty}^{\infty} \frac{g(\sqrt{2}\sigma_u v)}{\sqrt{\pi}} e^{-v^2}\, \mathrm{d}v \equiv \int_{-\infty}^{\infty} g^*(v) e^{-v^2}\, \mathrm{d}v. \tag{2.9}$$

G-H quadrature approximates the integral in Eq. (2.9) as a weighted sum:

$$\int_{-\infty}^{\infty} g^*(v) e^{-v^2}\, \mathrm{d}v \approx \sum_{k=1}^{d} g^*(x_k)\, w_k, \tag{2.10}$$

where $d$ is the number of quadrature points, $x_k$'s are the evaluation points and $w_k$'s are the corresponding weights. For more specific definitions of $x_k$ and $w_k$, see McCulloch

*et al.* (2008), chapter 14. Given $d$, $x_k$'s and $w_k$'s can be calculated using existing software packages. By applying Eq. (2.10), the ratio of the integrals in Eq. (2.7) is approximated by

$$\frac{\int_{-\infty}^{\infty} p_i(u_i)\, q_i(u_i)\, \pi(u_i)\, \mathrm{d}u_i}{\int_{-\infty}^{\infty} p_i(u_i)\, \pi(u_i)\, \mathrm{d}u_i} \approx \frac{\sum_{k=1}^{d} p_i(\sqrt{2}\sigma_u x_k)\, q_i(\sqrt{2}\sigma_u x_k)\, w_k}{\sum_{k=1}^{d} p_i(\sqrt{2}\sigma_u x_k)\, w_k} \tag{2.11}$$

See Subsection 2.3.2 for the determination of the number of quadrature points.

Now, we can iteratively maximize the log-likelihood function with respect to unknown parameters, $\alpha$, $\beta_k$'s and $\sigma_u^2$. It begins from an initial value of $\alpha^{(0)}$ which is often set to 1 (i.e., a model with exponential distribution is fitted), then fits GLMM model with $\alpha^{(0)}$ to estimate $\beta_k^{(0)}$'s and $\sigma_u^{2(0)}$, calculate the updated $\alpha^{(0)\prime}$ using Eq. (2.7), and fits GLMM again with $\alpha^{(1)} = (\alpha^{(0)} + \alpha^{(0)\prime})/2$ to obtain $\beta_k^{(1)}$'s and $\sigma_u^{2(1)}$ (Aitkin and Clayton, 1980). This procedure continues until the difference of the new value of $\alpha$ with the previous one is substantially small.

### *2.2.4 Asymptotic Variance-covariance Matrix*

The asymptotic variance-covariance matrix of the parameter estimates can be obtained by the inverse of the observed Fisher information matrix (i.e., the negative second derivatives of the log-likelihood function). For notational convenience, let $\pi(u_i) = \pi$ in Eq. (2.3), $p_i(u_i) = p_i$, $q_i(u_i) = q_i$, $r_i^k(u_i) = r_i^k$ and $s(u_i) = s$ in Eq. (2.6). In addition, let

$$\begin{aligned}
qq_i &= \sum_{j=1}^{n_i} \mu_{ij} \log^2 t_{ij}, \\
qr_i^k &= \sum_{j=1}^{n_i} \mu_{ij}\, x_{ijk} \log t_{ij}, \\
r^k r_i^l &= \sum_{j=1}^{n_i} \mu_{ij}\, x_{ijk}\, x_{ijl}, \\
ss &= -\frac{1}{2\sigma_u^4} + \frac{u_i^2}{\sigma_u^6}
\end{aligned}$$

for each group $i = 1, \ldots, m$. Then the second derivatives of the log-likelihood function are derived as follows:

$$\frac{\partial^2 \log L}{\partial \alpha^2} = -\frac{\sum_{i=1}^{m}\sum_{j=1}^{n_i} c_{ij}}{\alpha^2} - \sum_{i=1}^{m}\left\{ \frac{(\int_{-\infty}^{\infty} p_i\, q_i\, \pi\, \mathrm{d}u_i)^2}{(\int_{-\infty}^{\infty} p_i\, \pi\, \mathrm{d}u_i)^2} - \frac{\int_{-\infty}^{\infty} p_i\, (q_i^2 - qq_i)\, \pi\, \mathrm{d}u_i}{\int_{-\infty}^{\infty} p_i\, \pi\, \mathrm{d}u_i} \right\},$$

$$\frac{\partial^2 \log L}{\partial \beta_k \partial \beta_l} = -\sum_{i=1}^{m}\left\{ \frac{\int_{-\infty}^{\infty} p_i\, r_i^k\, \pi\, \mathrm{d}u_i \int_{-\infty}^{\infty} p_i\, r_i^l\, \pi\, \mathrm{d}u_i}{(\int_{-\infty}^{\infty} p_i\, \pi\, \mathrm{d}u_i)^2} - \frac{\int_{-\infty}^{\infty} p_i\, (r_i^k\, r_i^l - r^k r_i^l)\, \pi\, \mathrm{d}u_i}{\int_{-\infty}^{\infty} p_i\, \pi\, \mathrm{d}u_i} \right\},$$

$$\frac{\partial^2 \log L}{\partial (\sigma_u^2)^2} = -\sum_{i=1}^{m}\left\{ \frac{(\int_{-\infty}^{\infty} p_i\, s\, \pi\, \mathrm{d}u_i)^2}{(\int_{-\infty}^{\infty} p_i\, \pi\, \mathrm{d}u_i)^2} - \frac{\int_{-\infty}^{\infty} p_i\, (s^2 - ss)\, \pi\, \mathrm{d}u_i}{\int_{-\infty}^{\infty} p_i\, \pi\, \mathrm{d}u_i} \right\},$$

$$\frac{\partial^2 \log L}{\partial \alpha \partial \beta_k} = -\sum_{i=1}^{m}\left\{ \frac{\int_{-\infty}^{\infty} p_i\, q_i\, \pi\, \mathrm{d}u_i \int_{-\infty}^{\infty} p_i\, r_i^k\, \pi\, \mathrm{d}u_i}{(\int_{-\infty}^{\infty} p_i\, \pi\, \mathrm{d}u_i)^2} - \frac{\int_{-\infty}^{\infty} p_i\, (q_i\, r_i^k - q r_i^k)\, \pi\, \mathrm{d}u_i}{\int_{-\infty}^{\infty} p_i\, \pi\, \mathrm{d}u_i} \right\},$$

$$\frac{\partial^2 \log L}{\partial \alpha \partial \sigma_u^2} = -\sum_{i=1}^{m}\left\{ \frac{\int_{-\infty}^{\infty} p_i\, q_i\, \pi\, \mathrm{d}u_i \int_{-\infty}^{\infty} p_i\, s\, \pi\, \mathrm{d}u_i}{(\int_{-\infty}^{\infty} p_i\, \pi\, \mathrm{d}u_i)^2} - \frac{\int_{-\infty}^{\infty} p_i\, q_i\, s\, \pi\, \mathrm{d}u_i}{\int_{-\infty}^{\infty} p_i\, \pi\, \mathrm{d}u_i} \right\},$$

$$\frac{\partial^2 \log L}{\partial \beta_k \partial \sigma_u^2} = -\sum_{i=1}^{m}\left\{ \frac{\int_{-\infty}^{\infty} p_i\, r_i^k\, \pi\, \mathrm{d}u_i \int_{-\infty}^{\infty} p_i\, s\, \pi\, \mathrm{d}u_i}{(\int_{-\infty}^{\infty} p_i\, \pi\, \mathrm{d}u_i)^2} - \frac{\int_{-\infty}^{\infty} p_i\, r_i^k\, s\, \pi\, \mathrm{d}u_i}{\int_{-\infty}^{\infty} p_i\, \pi\, \mathrm{d}u_i} \right\}.$$

Let the second derivatives of the log-likelihood function evaluated at the ML estimates be

$$\left.\frac{\partial^2 \log L}{\partial \beta_k \partial \beta_l}\right|_{\boldsymbol{\theta}=\hat{\boldsymbol{\theta}}} = -a_{kl}, \qquad \left.\frac{\partial^2 \log L}{\partial \beta_k \partial \sigma_u^2}\right|_{\boldsymbol{\theta}=\hat{\boldsymbol{\theta}}} = -b_k, \qquad \left.\frac{\partial^2 \log L}{\partial (\sigma_u^2)^2}\right|_{\boldsymbol{\theta}=\hat{\boldsymbol{\theta}}} = -c,$$
$$\left.\frac{\partial^2 \log L}{\partial \alpha \partial \beta_k}\right|_{\boldsymbol{\theta}=\hat{\boldsymbol{\theta}}} = -d_k, \qquad \left.\frac{\partial^2 \log L}{\partial \alpha \partial \sigma_u^2}\right|_{\boldsymbol{\theta}=\hat{\boldsymbol{\theta}}} = -e, \qquad \left.\frac{\partial^2 \log L}{\partial \alpha^2}\right|_{\boldsymbol{\theta}=\hat{\boldsymbol{\theta}}} = -f,$$

where $\boldsymbol{\theta} = (\boldsymbol{\beta}, \sigma_u^2, \alpha)$ is the parameter vector and $\hat{\boldsymbol{\theta}}$ is the ML estimates of the parameters. Then the asymptotic variance-covariance matrix of the estimated parameters is obtained by

$$\mathrm{Avar}(\hat{\boldsymbol{\beta}}, \hat{\sigma}_u^2, \hat{\alpha}) = \begin{bmatrix} A & \mathbf{b} & \mathbf{d} \\ \mathbf{b}' & c & e \\ \mathbf{d}' & e' & f \end{bmatrix}^{-1} \tag{2.12}$$

where $A$ is a $(p+1) \times (p+1)$ matrix whose elements are $a_{kl}$; $\mathbf{b} = (b_0, \cdots, b_p)'$; and $\mathbf{d} = (d_0, \cdots, d_p)'$.

One advantage of using GLMM is that common statistical software calculates the Hessian matrix during the optimization iteration, and we can retrieve this matrix, which is composed of $A$, $\mathbf{b}$ and $c$, from the GLMM output. Thus, we only need to calculate $\mathbf{d}$, $e$ and $f$. Again, we approximate integrals included in second derivatives using G-H quadrature.

## 2.3 Implementation

### *2.3.1 Life-stress Relationship*

One of the major challenges in ALTs is the need for extrapolation of the results obtained from the region of accelerated test stress conditions into the region of use stress conditions. Physical acceleration models which study the failure mechanisms of materials under different types of stress variables play an important role for the life-stress relationship that is necessary for the extrapolation. For example, the generalized Eyring model can be used to describe the relationship of life with temperature and another stress variable such as humidity or voltage, which is the case of the glass capacitor lifetime experiment introduced in Subsection 2.1.2. The inverse power model is another life-stress relationship, which is frequently used for a non-thermal accelerating variable like voltage or pressure. We can use the inverse power model for the pressure vessel reliability study, the second example in Subsection 2.1.2, as pressure has been used for a stress variable. For more details of these models, see Escobar and Meeker (2006).

Although each physical model has its own form, most of them suggest the use of natural stress variables as the explanatory variables of the regression model, so that the extrapolation is physically reasonable. The Eyring model leads to the natural stress variables for temperature given as $s = 1/kT$, where $k = 8.62 \times 10^{-5} eV/K$

is Boltzmann's constant and $T = \text{temp}\,^\circ\text{C} + 273.15$ is the temperature in degrees Kelvin, and the log transformation for another stress variable (e.g., $s = \ln(\text{Voltage})$ in our first example). The inverse power model also implies the log transformation of a stress variable (e.g., $s = \ln(\text{Pressure})$ in our second example).

### *2.3.2 Number of Quadrature Points*

The number of quadrature points, $d$, used in Eq. (2.11) is a tuning parameter that needs to be determined for updating $\alpha$ using Eq. (2.7). It is known that 20 quadrature points are usually enough for a good degree of approximation for a single integral (McCulloch *et al.*, 2008). However, a ratio of two integrals could be more sensitive to $d$, depending on the magnitude of these integrals, especially when both of them are small. We investigated the accuracy of quadrature approximation with different number of quadrature points by comparing them with those from the Monte Carlo (MC) sampling. The Strong Law of Large Number (SLLN) implies that the integral of Eq. (2.8) can be approximated by the sample average as follows:

$$\int_{-\infty}^{\infty} g(u_i)\pi(u_i)\,\mathrm{d}u_i = \mathbb{E}[g(u_i)] \approx \frac{1}{M}\sum_{r=1}^{M} g(u_i).$$

For large $M$ the average converges almost surely to the expectation.

In our study, we found that more than 100 quadrature points were needed for convergence to the result from the MC sampling. For example, given the estimated parameter values from the first iteration of the analysis of pressure vessel data, Figure 2.1 shows the approximated ratio of integrals in Eq. (2.11) for spool 2 ($i = 2$) by G-H quadrature with different $d$ (varying from 1 to 200), and it also shows the converging result by MC sampling. One can see that, when $d$ is less than 100, the result from quadrature approximation fluctuates, but it appears to converge to the

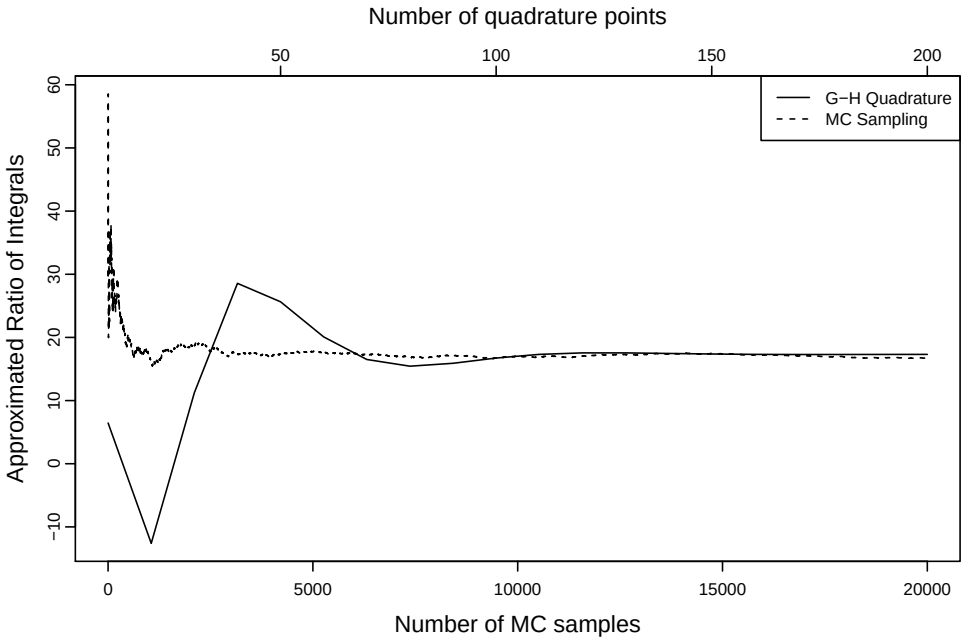


**Figure 2.1:** Approximated ratio of integrals by G-H quadrature and MC sampling

MC sampling result when $d$ is greater than 100. Based on this finding, we used 100 quadrature points to ensure the accuracy of G-H quadrature.

### *2.3.3 Analysis of Glass Capacitor Data*

As described in Subsection 2.1.2, eight glass capacitors were tested under each of the eight stress level combinations of temperature-voltage. After the fourth failure for each stress condition, the test was terminated (i.e., type-II censoring). Zelen (1959) did not explicitly describe the experimental protocol for the life test of glass capacitors; however, it is reasonable to assume that test units with the same stress levels had been tested on the same test stand simultaneously because of time and cost limitations. In this case, the experimental unit is the test stand but the observational unit is each capacitor, and hence subsampling is involved in the test. Table 2.1

summarizes the result of the test. Note that the stress variables from the original data (temp °C and Volt) were transformed to the natural stress variables. In addition to the data given in Table 2.1, we generated the indicator variable $c_{ij}$'s for censoring as described in Subsection 2.2.1, and used them as responses of GLMM fitting. We assume that there is no interaction between the two stress variables. Therefore, the linear predictor and the link function in this example are given as $\eta_{ij} = \beta_0 + \beta_1 s_{ij}^1 + \beta_2 s_{ij}^2 + u_i$ and $\log \mu_{ij} = \eta_{ij} + \alpha \log t_{ij}$, respectively, where $i = 1, \ldots, 8$ is the index of test stand and $j = 1, \ldots, 8$ is the index of test unit.

**Table 2.1:** Life test data of glass capacitors

| Test stand | $s^1 = 1/kT$ | $s^2 = \ln V$ | Failure time (hrs) |
|---|---|---|---|
| 1 | 26.19 | 5.30 | 439, 904, 1,092, 1,105 |
| 2 | 26.19 | 5.52 | 572, 690, 904, 1,090 |
| 3 | 26.19 | 5.70 | 315, 315, 439, 628 |
| 4 | 26.19 | 5.86 | 258, 258, 347, 588 |
| 5 | 25.61 | 5.30 | 959, 1,065, 1,065, 1,087 |
| 6 | 25.61 | 5.52 | 216, 315, 455, 473 |
| 7 | 25.61 | 5.70 | 241, 315, 332, 380 |
| 8 | 25.61 | 5.86 | 241, 241, 435, 455 |

We used SAS PROC GLIMMIX for the GLMM fitting. There are several estimation methods PROC GLIMMIX provides, and one of the methods is using maximum likelihood by G-H quadrature, which is suitable for our purpose. We also implemented the iteration procedure using SAS/IML and 100 quadrature points were used for a calculation of updated $\alpha$. Iteration stopped when $\alpha^{(i)\prime} - \alpha^{(i)} \leq 10^{-5}$.

A total number of 8 iterations were taken for the convergence. Table 2.2 shows the parameter estimates for fixed effects from the last iteration, and the estimated shape parameter is $\hat{\alpha} = 2.812$. The variance of the random effect $\sigma_u^2$ is estimated as zero while Freeman and Vining (2013) reported a non-zero estimate of $\sigma_u^2$. We found that the approximated value of the log-likelihood function in Eq. (2.4) evaluated at the ML estimates of our method is slightly larger than the one of Freeman and Vining (2013), so more accurate results. Therefore we conclude that no random effects exist among test stands in this example. In this case, we can remove the random effect term from the linear predictor and fit the data by simple fixed effects model using GLM.

**Table 2.2:** Parameter estimates for fixed effects

| Parameter | Estimate | Std. error | t value | p-value |
|---|---|---|---|---|
| $\beta_0$ | $-5.39$ | 16.15 | $-0.33$ | 0.7497 |
| $\beta_1$ | $-1.51$ | 0.61 | $-2.46$ | 0.0173 |
| $\beta_2$ | 4.56 | 0.79 | 5.81 | $< .0001$ |

### *2.3.4 Analysis of Pressure Vessel Data*

This dataset consists of the lifetimes of 108 pressure vessels being tested at four different stresses of the wrapping fiber (23.4, 25.5, 27.6 and 29.7 MegaPascals). The pressure vessels were manufactured in batches by 8 different spools and each spool was used to wrap a number of pressure vessels. Table 2.3 shows a part of the dataset, and the entire one can be found in Gerstle and Kunz (1983). Again, we transformed the stress variable by taking log. Test units that had not yet failed at 41,000 hours were right-censored (type-I censoring) and there exist 11 censored observations at the stress level of $s = 3.15$. The linear predictor is given as $\eta_{ij} = \beta_0 + \beta_1 s_{ij}^1 + u_i$, where

$i = 1, \ldots, 8$ is the index of spool and $j = 1, \ldots, n_i$ is the index of test unit. The other conditions are the same as in the previous section.

**Table 2.3:** Life test data of pressure vessels (part), failure time with an asterisk * indicates a censored data.

| $s = \ln Mpa$ | Spool | Failure time | Number of test units |
|---|---|---|---|
| 3.39 | 2 | 2.2 | 39 |
| | 7 | 4.0 | |
| | ⋮ | ⋮ | |
| | 4 | 1802.1 | |
| 3.32 | 3 | 19.1 | 24 |
| | 3 | 24.3 | |
| | ⋮ | ⋮ | |
| | 4 | 6177.5 | |
| 3.24 | 6 | 225.2 | 24 |
| | 7 | 503.6 | |
| | ⋮ | ⋮ | |
| | 1 | 31008.0 | |
| 3.15 | 7 | 4000.0 | 21 |
| | 7 | 5376.0 | |
| | ⋮ | ⋮ | |
| | 8 | 41000.0* | |

A total of 12 iterations were required for the convergence. Table 2.4 shows the estimates of the regression coefficients and the variance of random effect reported by the output of GLMM model from SAS. In addition, the predicted random effects for

each spool (i.e., $\hat{u}_i, i = 1, \ldots, 8$) as well as those standard errors are shown in Table 2.5, which are another output of SAS. We can observe that there exists significant variations of spool effects in, e.g., spool 4 or spool 7. By Eq. (2.7) and Eq. (2.11), the estimated shape parameter is $\hat{\alpha} = 1.251$.

**Table 2.4:** Parameter estimates of pressure vessel data

| Parameter | Estimate | Std. error | t value | p-value |
|---|---|---|---|---|
| $\beta_0$ | $-103.91$ | 4.3097 | $-24.11$ | $< .0001$ |
| $\beta_1$ | 28.8143 | 1.2909 | 22.32 | $< .0001$ |
| $\sigma_u^2$ | 2.4077 | 1.2504 | | |

**Table 2.5:** Predicted random effects of each spool

| Spool | Estimate | Std. error | t value | p-value |
|---|---|---|---|---|
| 1 | $-1.6977$ | 0.6125 | $-2.77$ | 0.0067 |
| 2 | 0.8552 | 0.5885 | 1.45 | 0.1493 |
| 3 | 1.7441 | 0.6192 | 2.82 | 0.0059 |
| 4 | $-2.3128$ | 0.6141 | $-3.77$ | 0.0003 |
| 5 | 0.0679 | 0.6355 | 0.11 | 0.9151 |
| 6 | 0.3222 | 0.6124 | 0.53 | 0.6000 |
| 7 | 2.3484 | 0.6226 | 3.77 | 0.0003 |
| 8 | $-0.9985$ | 0.6131 | $-1.63$ | 0.1065 |

The standard errors in Table 2.4 may underestimate the variances of estimated parameters because the GLMM model does not contain the estimation of $\alpha$. In order to obtain the complete asymptotic variance-covariance matrix of the parameter estimates, we extracted the Hessian matrix from the last GLMM fitting output of

SAS (Table 2.6). Indeed, because SAS optimizes $-2\log L$ (deviance), we need to multiply 1/2 to the Hessian matrix to obtain $A$, $\mathbf{b}$ and $c$ in Eq. (2.12).

**Table 2.6:** Hessian matrix of $-2\log L$

| | $\beta_0$ | $\beta_1$ | $\sigma_u^2$ |
|---|---|---|---|
| $\beta_0$ | 6.4003 | 21.1875 | 0.000424 |
| $\beta_1$ | 21.1875 | 71.3389 | −0.02047 |
| $\sigma_u^2$ | 0.000424 | −0.02047 | 1.2796 |

In the meantime, we obtained $\mathbf{d} = (22.62, 62.81)'$, $e = -2.06$ and $f = 502.24$ by calculating corresponding second derivatives in Subsection 2.2.4 using G-H quadrature. After combining the results and taking the inverse, we get the following variance-covariance matrix:

$$\text{Avar}(\hat{\beta}_0, \hat{\beta}_1, \hat{\sigma}_u^2, \hat{\alpha}) = \begin{bmatrix} 78.56 & -21.90 & -2.99 & -0.81 \\ -21.90 & 6.14 & 0.82 & 0.22 \\ -2.99 & 0.82 & 1.70 & 0.04 \\ -0.81 & 0.22 & 0.04 & 0.01 \end{bmatrix}$$

and the standard errors can be obtained by $se(\hat{\beta}_0) = \sqrt{78.56} = 8.86$, $se(\hat{\beta}_1) = \sqrt{6.14} = 2.48$, $se(\hat{\sigma}_u^2) = \sqrt{1.70} = 1.31$, and $se(\hat{\alpha}) = \sqrt{0.01} = 0.10$. We can observe the calculated standard errors of $\hat{\beta}_0$, $\hat{\beta}_1$ and $\hat{\sigma}_u^2$ are bigger than those in Table 2.4.

## 2.4 Conclusions

In this chapter, we proposed a GLMM approach to the ALT data analysis with constrained randomization. This approach provides a structured framework for modeling censored failure time data with random effects and it can be easily implemented in statistical software. Our model is developed under the proportional hazard assumption, which is essentially a semiparametric model, thus it can be applied to

many other failure time distributions in addition to the Weibull distribution. In the examples above, we utilized physical acceleration models to derive the life-stress relationship, which has been overlooked by previous researches on similar problems. Furthermore, it is expected that the proposed GLMM approach can assist in the experimental design study of ALTs with random effects.

Chapter 3

# ANALYZING STEP-STRESS ACCELERATED LIFE TESTING DATA WITH HETEROGENEOUS GROUP EFFECTS

Step-stress accelerated life testing (SSALT) is a special type of experiments that test a product's lifetime with time-varying stress levels. Typical testing protocols deployed in SSALTs cannot implement complete randomization of experiments; instead, they often result in grouped structures of experimental units and, thus, correlated observations. In this chapter we propose a generalized linear mixed model (GLMM) approach to take into account the random group effect in SSALT. Failure times are assumed to be exponentially distributed under any stress level. Two parameter estimation methods, adaptive Gaussian quadrature (AGQ) and the integrated nested Laplace approximation (INLA), are introduced. A simulation study is conducted to compare the proposed random effect model with the traditional model, which pools data groups together, and with the fixed effect model. We also compare AGQ and INLA's with different priors for parameter estimation. Results show that the proposed model can validate the existence of group-to-group variation. Lastly the GLMM model is applied to a real data and it shows that disregarding experimental protocols in SSALT may result in large bias in the estimation of the effect of stress variables.

## 3.1 Introduction

### *3.1.1 Background and Motivation*

Life tests for highly reliable products or materials require an extremely long time for observing any failures. Accelerated life testing (ALT) attempts to address this problem by elevating some environmental stresses so as to obtain failure time data quickly. In contrast to constant-stress ALT (CSALT), where the stress applied on a test unit is fixed at a single level, step-stress accelerated life testing (SSALT) varies stress levels over the testing period, typically in an increasing pattern, as long as the test unit has not failed yet. Therefore, the testing method will push the test unit to failure with more and more severe stresses and further reduce the total testing time.

Most previous studies on statistical analysis of SSALT data have been conducted based on the assumption that lifetimes of test units are independent of each other. Only by a completely randomized experiment would this assumption be valid. In reality, however, it is almost impossible to guarantee the complete randomization in ALT due to the limited availability of test equipment and test units, as well as budget and time constraints. Some experimental protocols such as subsampling or random blocks can be seen as a compromise between available resource and complete randomization. Subsampling arises from discordance between experimental units and observational units (Vining, 2013); for example, it occurs when multiple test units are located on the same test stand, while testing stresses are applied on test stands, not individual test units. Random blocks may come from a batch manufacturing or different raw materials used by test units. Figure 3.1 illustrates these experimental protocols. One can see that both the protocols result in a grouped structure among the observations, and in this case lifetimes within the same group may be correlated. If these correlations were ignored in data analysis, inaccurate result would be obtained.

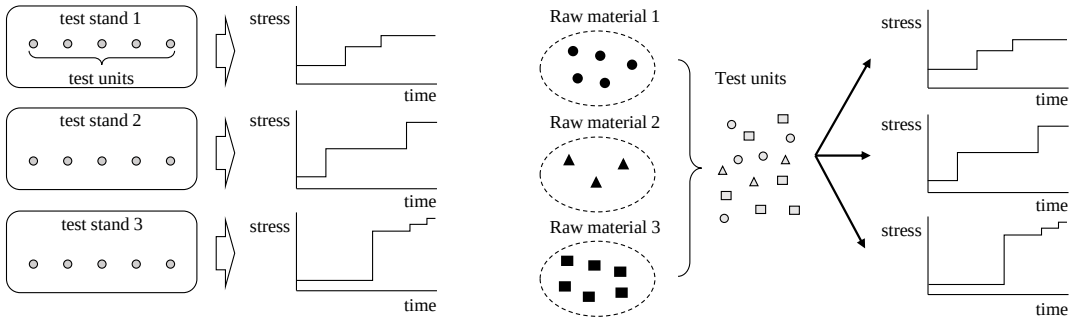


**(a)** Subsampling **(b)** Random blocks

**Figure 3.1:** Experimental protocols causing a grouped structure in SSALT

Motivating examples of such grouping structure in SSALT can be found in the literature. Zhao and Elsayed (2005) illustrate an SSALT experiment to obtain lifetimes of light emitting diodes (LEDs), where each experimental set is made of a board containing $4 \times 8$ LEDs. Although Zhao and Elsayed (2005) exploit only a single set of test units, multiple experimental sets may be tested in different test chambers to obtain more data. In these cases, it is reasonable to assume that observations from 32 test units tested at the same test chamber are correlated. Another example can be found in Nelson (1980), in which the SSALT data of power cable insulation with time-varying stress of voltage is described. This dataset contains the failure or censored time of a total of 21 test units of 7 test groups with 3 test units each. Test units within a same group tested at the same test stand, and different groups may have different stress profiles, which leads to the case of subsampling.

Information extracted from products' life tests plays a fundamental role for all reliability-related decision making such as establishing warranty policy or evaluating new product designs. Such decisions based on erroneous finding may cause incalculable harm to manufacturers. Therefore more accurate estimations and predictions of product reliability from the more realistic model are required.

### *3.1.2 Previous Work*

Traditional ways to model SSALT can be summarized based on their assumptions on how the varying stress affects a product's lifetime. The cumulative exposure (CE) model (Nelson, 1980) assumes that the survived test units will fail according to the cumulative density function (cdf) for current stress level starting at the previously accumulated cdf level. Alternatively, Khamis and Higgins (1999) proposed a transformed exponential model, called KH model, motivated by its mathematical simplicity. It turns out that, by the KH model, the stress makes a direct impact on the hazard rate of the product's lifetime according to the proportional hazard (PH) model. Sha and Pan (2014) illustrated the difference of these two models by depicting the composite cumulative hazard function of SSALT. Graphically, the CE model forms the composite cumulative failure rate by a horizontal shift of the individual cumulative hazard function segment under CSALT with corresponding stress; while the PH model makes it by vertical shift. However, for exponentially distributed lifetimes, these two models are the same because an exponential random variable has a linear cumulative failure rate, which produces the identical result by either horizontal or vertical shift.

The presence of group effects among observations leads to a random effect model since we are interested in a whole population of all possible groups, while not in specific groups that emerged from the experiment; thus, these groups are regarded as samples from a population. For CSALT, several studies have been conducted to take into account these random group effects during the past few years. León *et al.* (2007) illustrated Bayesian analysis using Markov chain Monte Carlo (MCMC) with an application concerning random blocks. They compared fixed and random group effect models and showed that the random group effect model provided more precise

estimates and predictions. Pan and Kozakai (2013) had a discussion of the frailty modeling approach to the same dataset. Freeman and Vining (2010, 2013) proposed a nonlinear mixed model (NLMM) to incorporate random effects. Their simulation study revealed that the proposed method was more robust in various scenarios compared to traditional methods with the independence assumption. Kensler *et al.* (2015) extended the NLMM method further to reflect experiments containing subsampling and random blocks simultaneously. Another extension can be found in Lv *et al.* (2015) where they incorporated different failure mechanisms by allowing the shape parameter of the Weibull lifetime distribution to be dependent on accelerating stresses. Wang *et al.* (2015) studied the bias in the lower percentile estimate when there was subsampling in right censored reliability data and they proposed a two-stage bootstrapping approach to establish an unbiasing factor. Seo and Pan (2016) described a generalized linear mixed model (GLMM) approach for right-censored CSALT data with random group effects. They argued that the GLMM was more flexible to model failure time data and easier to implement for the parameter estimation. Most recently, Rodríguez-Borbón *et al.* (2017) used a proportional hazard model with error effect to analyze the ALT data from a knock sensor accelerated life test.

While CSALT with constrained randomization has been previously discussed, similar models for SSALT have not received much attention in literature. In this chapter, we propose a generalized linear mixed model (GLMM) approach to analyze failure time data from SSALTs with heterogeneous group effects. We assume that 1) lifetimes at individual stress levels are exponentially distributed; and 2) lifetimes can be right-censored by Type-I (i.e., termination of predetermined testing time) or Type-II (i.e., obtaining predetermined number of failures) censoring. We introduce a random group effect to the previously studied SSALT model and build GLMM formulation from the conditional likelihood function. Two GLMM parameter estimation methods,

from the frequentist and Bayesian points of view, respectively, are introduced. Finally, the proposed estimation methods are assessed and compared with other traditional methods through a simulation study.

## 3.2 SSALT Model

Lee and Pan (2010) proposed a generalized linear model (GLM) approach for SSALT with exponentially distributed lifetimes under a constant stress, but only with fixed effects. They have shown that the likelihood of a single observation from SSALT can be constructed by likelihoods of each stress step segment's observations under CSALT. They then built the GLM with Poisson response using an indicator variable for censoring. In this section, we extend this model to accommodate the random group effects.

### *3.2.1 SSALT with Random Effects*

Suppose we have a total of $N = \sum_{i=1}^{m} n_i$ test units where $m$ is the number of groups formed by experimental protocols and $n_i$ is the number of test units in the $i$th group. The $j$th test unit in the $i$th group is tested under the SSALT planned with $l$ steps of stress levels. Note that $l$ could vary depending on the stress profile that the $ij$th unit is tested on, but, for convenience, we use the notation without a subscript $ij$ unless it is necessary. Let $x_{ijk}$, $k = 1, \ldots, l$ be stress levels corresponding to each step, which are changed at the time points $\xi_{ij1}, \ldots, \xi_{ij,l-1}$. We assume that the stress factor is represented as a form of a natural variable by a suitable physical acceleration model (e.g., log transformation by inverse power law). In addition, We introduce normal random variables $u_i$'s to reflect each group effect. That is,

$$u_i \sim \text{iid. } N(0, \sigma_u^2),\ i = 1, \ldots, m, \tag{3.1}$$

where $\sigma_u^2$ is a variance component of group effect and it is one of the unknown parameters in the model.

Let $t_{ijk}$ be the failure time of the $ij$th test unit under the constant stress level $x_{ijk}$, which is exponentially distributed with a failure rate $\lambda_{ijk}$. The failure rate $\lambda_{ijk}$ is related to stress level $x_{ijk}$ through a log linear function given by

$$\log(\lambda_{ijk}) = \beta_0 + \beta_1 x_{ijk} + u_i, \tag{3.2}$$

where $\beta_0$ and $\beta_1$ are unknown regression parameters reflecting the fixed effect size of the stress; $u_i$ causes random variation of the intercept. The conditional probability density function (pdf) and reliability function of $t_{ijk}$ given $u_i$ under individual constant stress levels are then given, respectively, by

$$f_{\text{cs}}(t_{ijk}|u_i) = \lambda_{ijk}\exp(-\lambda_{ijk}t_{ijk}), \quad t_{ijk} > 0 \tag{3.3}$$

$$R_{\text{cs}}(t_{ijk}|u_i) = \exp(-\lambda_{ijk}t_{ijk}), \quad t_{ijk} > 0 \tag{3.4}$$

where the subscript cs indicates a constant stress.

Now let $t_{ij}$, without the subscript $k$, be the failure time of the $ij$th test unit under the step-stress profile applied to the unit. By either CE or PH model, we can show that the conditional pdf of $t_{ij}$ given $u_i$ is given by

$$f_{\text{ss}}(t_{ij}|u_i)$$
$$= \begin{cases} \lambda_{ij1}\exp\{-\lambda_{ij1}t_{ij}\}, & 0 \le t_{ij} < \xi_{ij1} \\ \lambda_{ij2}\exp\{-\lambda_{ij2}(t_{ij}-\xi_{ij1}) - \lambda_{ij1}\xi_{ij1}\}, & \xi_{ij1} \le t_{ij} < \xi_{ij2} \\ \lambda_{ij3}\exp\{-\lambda_{ij3}(t_{ij}-\xi_{ij2}) - \lambda_{ij2}(t_{ij}-\xi_{ij1}) - \lambda_{ij1}\xi_{ij1}\}, & \xi_{ij2} \le t_{ij} < \xi_{ij3} \\ \cdots & \\ \lambda_{ijl}\exp\{-\lambda_{ijl}(t_{ij}-\xi_{ij,l-1})\cdots - \lambda_{ij2}(t_{ij}-\xi_{ij1}) - \lambda_{ij1}\xi_{ij1}\}, & \xi_{ij,l-1} \le t_{ij} < \infty, \end{cases}$$

and it can be rewritten in terms of the pdf and reliability functions in Eq. (3.3) and (3.4) by

$$
\begin{aligned}
&f_{\mathrm{ss}}(t_{ij}|u_i) \\
&\quad = \begin{cases}
f_{\mathrm{cs}}(t_{ij}|u_i), & 0 \le t_{ij} < \xi_{ij1} \\
R_{\mathrm{cs}}(\xi_{ij1}|u_i) f_{\mathrm{cs}}(t_{ij} - \xi_{ij1}|u_i), & \xi_{ij1} \le t_{ij} < \xi_{ij2} \\
R_{\mathrm{cs}}(\xi_{ij1}|u_i) R_{\mathrm{cs}}(\xi_{ij2} - \xi_{ij1}|u_i) f_{\mathrm{cs}}(t_{ij} - \xi_{ij2}|u_i), & \xi_{ij2} \le t_{ij} < \xi_{ij3} \\
\cdots & \\
R_{\mathrm{cs}}(\xi_{ij1}|u_i) \cdots R_{\mathrm{cs}}(\xi_{ij,l-1} - \xi_{ij,l-2}|u_i) f_{\mathrm{cs}}(t_{ij} - \xi_{ij,l-1}|u_i), & \xi_{ij,l-1} \le t_{ij} < \infty.
\end{cases}
\end{aligned} \tag{3.5}
$$

Eq. (3.5) says that a single test unit's conditional likelihood of failure at the $k$th step of the stress profile can be treated as the conditional likelihoods of $k$ test units with constant stresses, in which the first $k-1$ units are survived and the last unit is failed. This equivalent likelihoods between SSALT and CSALT is due to the memoryless property of exponential distribution, which is illustrated in Figure 3.2. If we observe a unit that is working under the stress level $x_1$ at the time point $\xi_1$, the remaining lifetime of this unit under a higher stress level $x_2$ is stochastically the same as the lifetime of a new test unit under the stress level $x_2$. Likewise, if the unit survives until $\xi_2$, it can be treated as a new test unit again when the test stress level is changed to the next level $x_3$. As a result, a single observation under SSALT generates three pseudo data points under constant stresses in this example.

We define $c_{ijk} = 1$, $y_{ijk} = t_{ij} - \xi_{ij,k-1}$ if $ij$th unit is failed at $k$th step; and $c_{ijk} = 0$, $y_{ijk} = \xi_{ijk} - \xi_{ij,k-1}$ if it is survived. In other words, $c_{ijk}$ is an indicator variable for censoring and $y_{ijk}$ is the survival time at the $k$th step. In addition, let $p_{ij} \le l_{ij}$ be an index of the step where the failed or censored observation is obtained. Then the conditional likelihood of the observations on a single test unit from the SSALT is

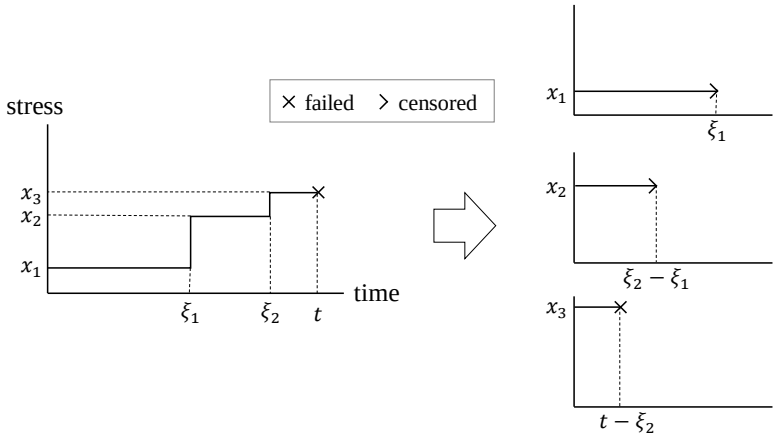


**Figure 3.2:** Memoryless property of exponential lifetime distribution in SSALT

given by

$$L_{ij|u_i} = \prod_{k=1}^{p_{ij}} f_{\text{cs}}(y_{ijk}|u_i)^{c_{ijk}} R_{\text{cs}}(y_{ijk}|u_i)^{1-c_{ijk}},$$

which is an another expression of Eq. (3.5). Let $q_i = \sum_{j=1}^{n_i} p_{ij}$ be the total number of step segments from all observations in $i$th group. The conditional likelihood of the $i$th group is then given by

$$\begin{aligned} L_{i|u_i} &= \prod_{j=1}^{n_i} \prod_{k=1}^{p_{ij}} f_{\text{cs}}(y_{ijk}|u_i)^{c_{ijk}} R_{\text{cs}}(y_{ijk}|u_i)^{1-c_{ijk}} \\ &= \prod_{s=1}^{q_i} f_{\text{cs}}(y_{is}|u_i)^{c_{is}} R_{\text{cs}}(y_{is}|u_i)^{1-c_{is}} \\ &= \prod_{s=1}^{q_i} \lambda_{is}^{c_{is}} \exp\left(-\lambda_{is} y_{is}\right), \end{aligned}$$

where $s = 1, \ldots, p_{i1}, p_{i1}+1, \ldots, p_{i1}+p_{i2}, \ldots, q_i$.

By the definition of $u_i$ in (3.1), observations from different groups are independent. Therefore, the marginal likelihood of all observations in all groups can be constructed by integrating out the random effect variable for each group and then multiplying the likelihoods of all groups, that is

$$L = \prod_{i=1}^{m} \int_{-\infty}^{\infty} \prod_{s=1}^{q_i} \lambda_{is}^{c_{is}} \exp\left(-\lambda_{is} y_{is}\right) \pi(u_i)\, \mathrm{d}u_i, \tag{3.6}$$

where $\pi(u_i) = (2\pi\sigma_u^2)^{-1/2} \exp\left(-u_i^2/(2\sigma_u^2)\right)$, the pdf of $u_i$.

### *3.2.2 GLMM Formulation*

The GLMM (McCulloch and Searle, 2001) is a class of models that include random effects into the linear predictor of a generalized linear model. It is often used for mixed models where the response conditional on the random effects is not normally distributed, but follows a distribution in the exponential family (e.g., binary or count data). The formulation of a GLMM consists of four components: the conditional distribution model of the response variable, the linear predictor that consists of fixed and random effects, the distribution model of random effects, and the link function that relates the conditional mean of the response with the linear predictor. Since the random effect is not directly observable, inference for model parameters in a GLMM is conducted based on the marginal likelihood of observed data.

Eq. (3.6) can be rewritten in terms of $\mu_{is} = \lambda_{is} y_{is}$ as

$$L = \prod_{i=1}^{m} \int_{-\infty}^{\infty} \prod_{s=1}^{q_i} \left(\mu_{is}^{c_{is}} \mathrm{e}^{-\mu_{is}}\right) y_{is}^{-c_{is}} \, \pi(u_i) \, \mathrm{d}u_i.$$

The term in the round bracket is the Poisson kernel of random variable $c_{is}$ with a conditional mean $\mu_{is} = E[c_{is}|u_i]$. From Eq. (3.2), we see that the unknown parameters are only included in this term. Therefore, the likelihood of $y_{is}$'s can be treated as if it is constructed by Poisson random variables $c_{is}$'s. We now can formulate the model according to components for GLMM as follows:

- Response variable: $c_{is}|u_i \sim \text{ind. } Poisson(\mu_{is})$;
- Linear predictor: $\eta_{is} = \beta_0 + \beta_1 x_{is} + u_i$;
- Random effect: $u_i \sim \text{iid. } N(0, \sigma_u^2)$;
- Link function: $g(\mu_{is}) = \log \mu_{is} = \eta_{is} + \log y_{is}$.

The link function is log link and it includes an offset term $\log y_{is}$. The log-likelihood is then

$$\log L = \sum_{i=1}^{m} \log \int_{-\infty}^{\infty} \prod_{s=1}^{q_i} \left( \mu_{is}^{c_{is}} \mathrm{e}^{-\mu_{is}} \right) \pi(u_i) \, \mathrm{d}u_i - \sum_{i=1}^{m} \sum_{s=1}^{q_i} c_{is} y_{is}. \tag{3.7}$$

The integration in the first term does not have a closed form. Its evaluation requires a numerical approximation.

## 3.3 Numerical Methods for Parameter Estimation

Two parameter estimation methods are briefly discussed in this section. The first one is adaptive Gaussian quarature (AGQ), which is a maximum likelihood estimation (MLE) method, proposed by Pinheiro and Bates (1995). The second one is integrated nested Laplace approximation (INLA), which is an approximate Bayesian method, by Rue *et al.* (2009). In this section, we provide the salient ideas of those two methods by tracking the procedures with SSALT data. For more comprehensive descriptions and examples, see the original papers.

### *3.3.1 Adaptive Gaussian Quadrature*

Early works for parameter estimation in GLMM, including the penalized quasi-likelihood (PQL) and the marginal quasi-likelihood (MQL) proposed by Breslow and Clayton (1993), were based on approximating GLMM to the linear mixed model (LMM), therefore an iterative algorithm for LMM can be applied to GLMM. However, it is known that these procedures produce biased estimates in certain cases, especially for binary data. On the other hand, more direct methods to evaluate intractable integrals in the likelihood function using quadrature approximation have been recognized as being more accurate and more computationally efficient.

To maximize the log-likelihood function (3.7), the integral in the first term is required to be evaluated numerically for given values of unknown parameters, $\hat{\boldsymbol{\beta}} =$

$(\hat{\beta}_0, \hat{\beta}_1)$ and $\hat{\sigma}_u^2$. Monte Carlo sampling is an easy way to approximate integrals. Let $h(u_i) = \prod_{s=1}^{q_i} (\mu_{is}^{c_{is}} \mathrm{e}^{-\mu_{is}})$ in Eq. (3.7). Then,

$$\int_{-\infty}^{\infty} h(u_i)\pi(u_i)\,\mathrm{d}u_i = E[h(u_i)] \approx \frac{1}{M}\sum_{k=1}^{M} h(u_{ik})$$

where $u_{ik}$'s are random samples drawn from the density $\pi(u_i)$. The function whose value is evaluated by random samples (i.e., $h(u_i)$ in this case) is called the target density. By the Strong Law of Large Number, this approximated quantity converges to the true value of the integral when $M \to \infty$. However it is not an efficient way to evaluate the integration for the purpose of optimization, which needs several iterations, as it requires sufficiently large number of random samples even for a single evaluation.

Meanwhile, importance sampling is known as a much more efficient stochastic integration method than Monte Carlo sampling. It introduces a proposal distribution $\omega(u_i)$ as follows.

$$\int_{-\infty}^{\infty} h(u_i)\pi(u_i)\,\mathrm{d}u_i = \int_{-\infty}^{\infty} h(u_i)\frac{\pi(u_i)}{\omega(u_i)}\omega(u_i)\,\mathrm{d}u_i$$

Now it generates random samples from $\omega(u_i)$, instead of $\pi(u_i)$. Obviously the target is changed as well by the introduction of the proposal distribution, and it is the original target weighted by the importance weights $\pi(u_i)/\omega(u_i)$. One possible choice for $\omega(u_i)$ is a distribution which resembles the original integrand $h(u_i)\pi(u_i)$.

Alternatively, the Gaussian quadrature rules can be viewed as a deterministic version of the Monte Carlo sampling. It provides an accurate approximation when the integrand includes specific kernel function. In specific, Gauss-Hermite (GH) quadrature can be used for the kernel function $\mathrm{e}^{-v^2}$, which can be seen as a kernel of $N(0, 1/2)$. Given the number of quadrature points $d$, GH quadrature approximates the integral

as follows.

$$\int_{-\infty}^{\infty} g(v)\mathrm{e}^{-v^2}\,\mathrm{d}v \approx \sum_{k=1}^{d} g(x_k)w_k$$

where $g(v)$ is an arbitrary function; $x_k$'s are fixed evaluation points; and $w_k$'s are the corresponding weights. In GH quadrature, the target function $g(v)$ is only evaluated by some predetermined evaluation points $x_k$'s instead of random samples drawn from the density $N(0, 1/2)$; and hence the weights are given to reflect the probability mass at each point. In our case, using a variable transformation, $u_i = \sqrt{2}\sigma_u v$, we obtain

$$\int_{-\infty}^{\infty} h(u_i)\pi(u_i)\,\mathrm{d}u_i = \int_{-\infty}^{\infty} h(\sqrt{2}\sigma_u v)\frac{\mathrm{e}^{-v^2}}{\sqrt{\pi}}\,\mathrm{d}v \approx \sum_{k=1}^{d} h(\sqrt{2}\sigma_u x_k)\frac{w_k}{\sqrt{\pi}}$$

where $\sqrt{2}\sigma_u x_k$ and $w_k/\sqrt{\pi}$ can be viewed as the evaluation points and weights extracted from $N(0, \sigma_u^2)$.

Likewise, AGQ is a deterministic version of the importance sampling (Pinheiro and Bates, 1995). That is, we exploit the proposal distribution which approximates $h(u_i)\pi(u_i)$; and then generate the evaluation points and weights from the proposal. More specifically AGQ approximates $h(u_i)\pi(u_i)$ to the Gaussian density with the mean centered at the mode and the variance calculated using the curvature at the mode of $h(u_i)\pi(u_i)$. The integration part of Eq. (3.7) can be written as

$$\frac{1}{\sqrt{2\pi}\sigma_u}\int_{-\infty}^{\infty} \exp\left\{-\frac{u_i^2}{2\sigma_u^2} + \sum_{s=1}^{q_i}(c_{is}\log\mu_{is} - \mu_{is})\right\}\mathrm{d}u_i. \tag{3.8}$$

This form of integrand is frequently found in the joint likelihood of the GLMM model. The first term of the exponent comes from the normal random effect and the second term is due to the data likelihood. Let $g(u_i)$ denote the function in the curly brackets. The Gaussian approximation of the integrand in Eq. (3.8) is given as

$$\exp\{g(u_i)\} \approx \exp\left\{-\frac{(u_i - u_i^*)^2}{2\sigma^{2*}}\right\} \tag{3.9}$$

where the derivation of $u_i^*$ and $\sigma^{2*}$ is provided in Appendix A.

As in the importance sampling, Eq. (3.9) is multiplied to the original integrand and divided by itself. That is,

$$\int_{-\infty}^{\infty} \exp\{g(u_i)\}\, \mathrm{d}u_i = \int_{-\infty}^{\infty} \frac{\exp\{g(u_i)\}}{\exp\left\{-\frac{(u_i-u_i^*)^2}{2\sigma^{2*}}\right\}} \exp\left\{-\frac{(u_i-u_i^*)^2}{2\sigma^{2*}}\right\} \mathrm{d}u_i \tag{3.10}$$

$$= \sqrt{2}\sigma^* \int_{-\infty}^{\infty} \exp\left\{g(u_i^* + \sqrt{2}\sigma^* v)\right\} \exp\left\{v^2\right\} \exp\left\{-v^2\right\} \mathrm{d}v \tag{3.11}$$

$$\approx \sqrt{2}\sigma^* \sum_{k=1}^{d} \exp\left\{g(u_i^* + \sqrt{2}\sigma^* x_k)\right\} \exp\left\{x_k^2\right\} w_k \tag{3.12}$$

where the variable is transformed by $v = \frac{u_i - u_i^*}{\sqrt{2}\sigma^*}$ in (3.11); and the GH quadrature rule is applied in (3.12). As a result AGQ evaluates the integration of (3.10) by the summation with $u_i^* + \sqrt{2}\sigma^* x_k$ as the evaluation points; and $\sqrt{2}\sigma^* \exp\{x_k^2\}\, w_k$ as the weights. AGQ is known as efficient quadrature method, which means it requires only a small number of evaluation points.

### *3.3.2 Integrated Nested Laplace Approximation*

Bayesian inference is particularly useful when only a small number of test units are available as in the case of ALTs. Engineers' domain knowledge from previous or similar products can be utilized through the specification of prior distributions of model parameters. For SSALT, Lee and Pan (2008) presented how an informative prior can be elicited from experts' opinions. They derived a conjugate prior and posterior distributions for a simple SSALT with Type-II censoring. However, for a general inference problem the conjugacy may not be justified beside of computational convenience; hence, it often requires some sampling methods such as MCMC to build a posterior distribution. Recent research utilizing MCMC for SSALT data include Lee and Pan (2012), Xu *et al.* (2014) and Hamada (2015).

Despite its popularity, MCMC still has some practical impediments. First, it requires substantially large amount of time to obtain a sufficient number of samples, which precludes a simulation study of Bayesian analysis. Second, it is not straightforward to determine whether the generated samples converge to the posterior distribution of interest, although theoretical results indicate that the MCMC algorithms converge in the long run (Sinharay, 2004). In our study, we found that MCMC often failed to converge even with a very long run when we applied it on the GLMM model of SSALT. In addition, it produced large correlation among subsequent samples and failed to achieve good mixing of samples. To overcome these problems, we consider an approximate Bayesian method using Laplace approximation, in which no sampling is needed. Some early work of this approach to ALTs include Achcar (1993). In this chapter, we apply INLA, where it is originally developed to account for approximate Bayesian inference of latent Gaussian models. INLA has been applied to various statistical models including GLMM, and previous studies show that it provides fast and accurate approximation to MCMC results (Holand *et al.*, 2013; Grilli *et al.*, 2015; Fong *et al.*, 2010).

In INLA, as in most Bayesian approaches for regression models, Gaussian priors for coefficients of fixed effects are assigned, i.e., $\beta_0 \sim N(0, \tau_0^{-1})$ and $\beta_1 \sim N(0, \tau_1^{-1})$; and a non-Gaussian prior is assigned for the precision parameter of random effects, where the typical choice is a Gamma distribution, i.e., $\tau_u = 1/\sigma_u^2 \sim \pi(\tau_u) = Gamma(a, b)$ with the unnormalized density $\tau_u^{(a-1)} e^{-b\tau_u}$. Let $\boldsymbol{z} = (\beta_0, \beta_1, u_1, \ldots, u_m)^T$ denote the vector of all Gaussian random variables; $\mathbf{Q}(\tau_u) = diag(\tau_0, \tau_1, \tau_u, \ldots, \tau_u)$ be the $(m + 2) \times (m + 2)$ precision matrix of $\boldsymbol{z}$; and $\mathbf{D}$ be the observed data containing $c_{is}$'s and

$y_{is}$'s. The joint posterior of $\boldsymbol{z}$ and $\tau_u$ is then given as

$$\begin{aligned}\pi(\boldsymbol{z}, \tau_u|\mathbf{D}) &\propto \pi(\boldsymbol{z}, \tau_u, \mathbf{D}) \\ &= \pi(\tau_u)\pi(\boldsymbol{z}|\tau_u)\prod_{i=1}^{m}\pi(\mathbf{D}_i|\boldsymbol{z}, \tau_u) \\ &\propto \pi(\tau_u)|\mathbf{Q}(\tau_u)|^{1/2}\exp\left\{-\frac{1}{2}\boldsymbol{z}^T\mathbf{Q}(\tau_u)\boldsymbol{z} + \sum_{i=1}^{m}\sum_{s=1}^{q_i}(c_{is}\log\mu_{is} - \mu_{is})\right\}.\end{aligned}$$

We wish to obtain the posterior marginal of the precision $\pi(\tau_u|\mathbf{D})$, and using that we also want to obtain the posterior marginal of each Gaussian variables, $z_p$'s, by integrating out $\tau_u$ from the joint as follows:

$$\pi(z_p|\mathbf{D}) = \int \pi(z_p|\tau_u, \mathbf{D})\,\pi(\tau_u|\mathbf{D})\,\mathrm{d}\tau_u, \quad p = 1, \ldots, m, m+1, m+2. \tag{3.13}$$

The INLA applies Laplace approximations to each density of the integrand in Eq. (3.13). Then it exploits the numerical integration to combine two densities. That is,

$$\pi(z_p|\mathbf{D}) \approx \tilde{\pi}_{INLA}(z_p|\mathbf{D}) = \int \tilde{\pi}_{LA}(z_p|\tau_u, \mathbf{D})\,\tilde{\pi}_{LA}(\tau_u|\mathbf{D})\,\mathrm{d}\tau_u \tag{3.14}$$

$$\approx \sum_{k=1}^{d}\tilde{\pi}_{LA}(z_p|\tau_u^k, \mathbf{D})\,\tilde{\pi}_{LA}(\tau_u^k|\mathbf{D})\,\Delta_k, \tag{3.15}$$

where $\tilde{\pi}$ denotes an approximated density; the subscript $LA$ indicates the Laplace approximation; $d$ is the number of evaluation points for the numerical integration; and $\Delta_k$'s are area weights. Appendix A provides more details of $\tilde{\pi}_{LA}(z_p|\tau_u, \mathbf{D})$ and $\tilde{\pi}_{LA}(\tau_u|\mathbf{D})$. Eq. (3.15) implies that the posterior marginal of a Gaussian variable is constructed by a mixture of densities $\tilde{\pi}(z_p|\tau_u^k, \mathbf{D})$ weighted by $\tilde{\pi}_{LA}(\tau_u^k|\mathbf{D})\,\Delta_k$ at selected points.

## 3.4 Simulation Study

### *3.4.1 Simulation Design*

The objectives of this simulation study are 1) to compare different models with or without the random group effect, and 2) to compare two parameter estimation

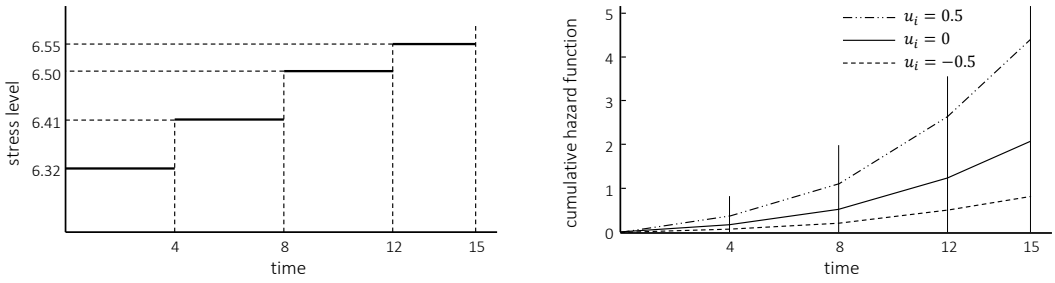


**(a)** SSALT for simulation

**(b)** Cumulative hazard functions with different random effects

**Figure 3.3:** Simulation setting

methods for GLMM described in Section 3.3, with various prior distribution settings. We presume a 4-step progressive SSALT experiment with a single stress factor, which has a similar stress profile to the one of Zhao and Elsayed (2005) introduced in Subsection 3.1.1, but with modified stress levels and step-change time points. In specific, stress levels are postulated as $(x_1, x_2, x_3, x_4) = (6.32, 6.41, 6.50, 6.55)$; and so are step-change time points as $(\xi_1, \xi_2, \xi_3) = (4, 8, 12)$ with the test termination time at $\xi_4 = 15$. We assume that all test units across all groups are tested under the same stress profile, and all groups contain the same number of test units (i.e., $n_1 = \cdots = n_m = n$). In addition, the following acceleration model is assumed for test units in the $i$th group and at the $k$th stress level.

$$\log(\lambda_{ijk}) = -55 + 8.2x_k + u_i, \quad j = 1, \ldots, n. \tag{3.16}$$

Figure 3.3 illustrates (a) the stress profile of the SSALT and (b) examples of the cumulative hazard functions with different random effects, which are $u_i = 0.5$, 0, and $-0.5$.

Several magnitudes of variance components are considered and they are $\sigma_u = 0.2, 0.5, 0.8, 1.1$ and 1.4. A total of 1,000 data sets are generated for each $\sigma_u$ value.

For each dataset, the number of groups $m$ and the number of test units within a group $n$ are generated from the discrete uniform with the range of $[3, 8]$ and $[5, 10]$, respectively; hence, the total number of test units can be varied from 15 to 80. Simulation data cannot be generated from standard parametric distributions since the cdf of the failure time under step-stress is a piecewise function; hence, we obtain data by the inverse of cdf. The detailed procedure for generating the simulation data is provided in Appendix A.

We attempt to fit each dataset using three different models. The first model is a pooled group model with a linear predictor $\log(\lambda_{ik}) = \beta_0 + \beta_1 x_k$, in which all test units are assumed to be independent and the correlations of observations within groups are ignored. The second model accommodates the fixed group effect through $\log(\lambda_{ik}) = \beta_0 + \beta_1 x_k + b_i$ with $b_i$'s being fixed unknown effects. This model can be used when we are only interested in the specific groups within the experiment rather than a population of group effects. For a pooled and fixed group models, the parameters are estimated by GLM method (Lee and Pan, 2010). The third model is a random group effect model that is considered in this chapter. We try AGQ with 20 quadrature points and two INLA's with different prior distributions for the estimation of $\beta$'s and $\sigma_u$. The flat normal priors with large variances $N(0, 1000)$ are given as priors of $\beta$'s for both INLA models. This is often used as a non-informative prior of regression coefficients. On the other hand, in terms of the prior distribution of the precision parameter $\tau_u = 1/\sigma_u^2$, the first INLA model uses $Gamma(0.001, 0.001)$, which is a popular choice for a non-informative prior of variance component; and the second INLA model uses $Gamma(0.5, 0.0164)$, as suggested by Fong *et al.* (2010). Based on the fact that when $u_i|\tau_u \sim N(0, \tau_u^{-1})$ and $\tau_u \sim Gamma(a, b)$, the marginal prior of $u_i$ becomes non-standardized Student's $t$, where the degrees of freedom is given as $2a$ and the scale parameter is given as $\sqrt{b/a}$, one can see that $Gamma(0.001, 0.001)$

prior makes the tails of marginal prior for the random effect too much heavy. On the other hand $Gamma(0.5, 0.0164)$ prior produces one of Student's $t$ with 1 degree of freedom (i.e., the Cauchy distribution) and the 95% range of $\exp(u_i)$ is given as $[0.1, 10]$ (see Fong *et al.*, 2010); and hence the marginal prior of the random effect becomes more concentrated on the center.

### *3.4.2 Simulation Results*

We investigate the point estimates of $\beta_0, \beta_1$ from each model, and $\sigma_u$ from the random effect model described in Subsection 3.4.1. For INLA, posterior means of $\beta_0, \beta_1$ and $\sigma_u$ are used for their point estimates. Figure 3.4 shows box plots of point estimates for unknown parameters with small and large values of $\sigma_u$. Here, INLA1 and INLA2 indicate INLA methods with $Gamma(0.001, 0.001)$ and $Gamma(0.5, 0.0164)$ priors for $1/\sigma_u^2$, respectively. In Figure 3.4b three data points beyond $\hat{\sigma}_u > 20$ are removed for the clarity of plotting.

When $\sigma_u$ is small (see Figure 3.4a), the pooled model produces even less biases for estimations of $\beta_0$ and $\beta_1$ than the random effects model because the correlations between observations are almost ignorable and regression coefficients estimates are not influenced by the estimation of $\sigma_u$. On the other hand when $\sigma_u$ is large (see Figure 3.4b), the pooled model shows severe biases in regression coefficients estimates since it ignores large amount of correlation among observations. Table 3.1 summarizes this result more clearly by presenting relative bias of $\hat{\beta}$'s, defined as $(\text{Med}(\hat{\beta}) - \beta)/\beta$ where $\text{Med}(\hat{\beta})$ is the median of estimates from the simulation, along with $\sigma_u$. An absolute value that is close to zero for this relative bias is desired. The table shows that the biasness of estimators from the pooled model quickly escalates as $\sigma_u$ increases. It also shows that estimates from the fixed model produce large bias regardless of the magnitude of $\sigma_u$. On the other hand, three methods of the random effect model

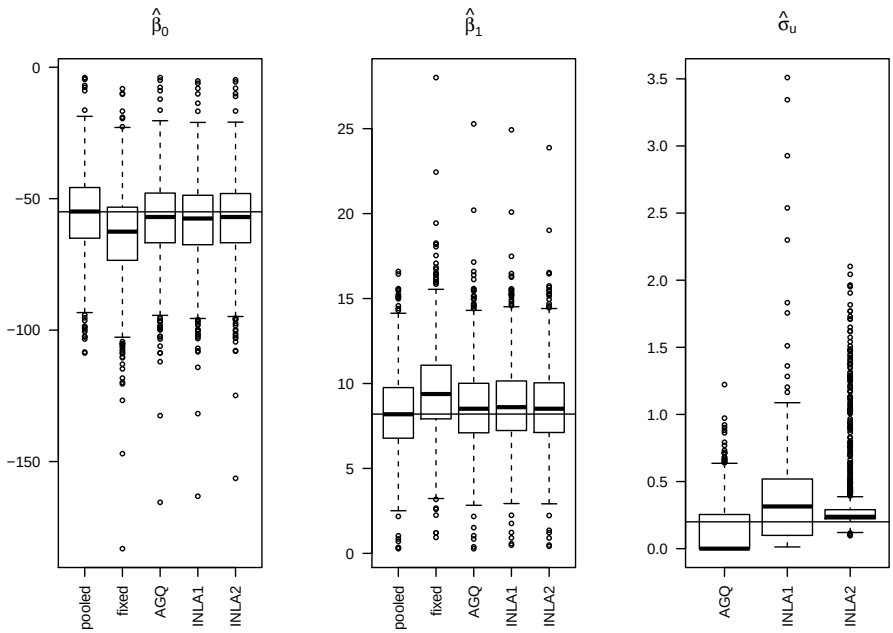


**(a)** $\sigma_u = 0.2$

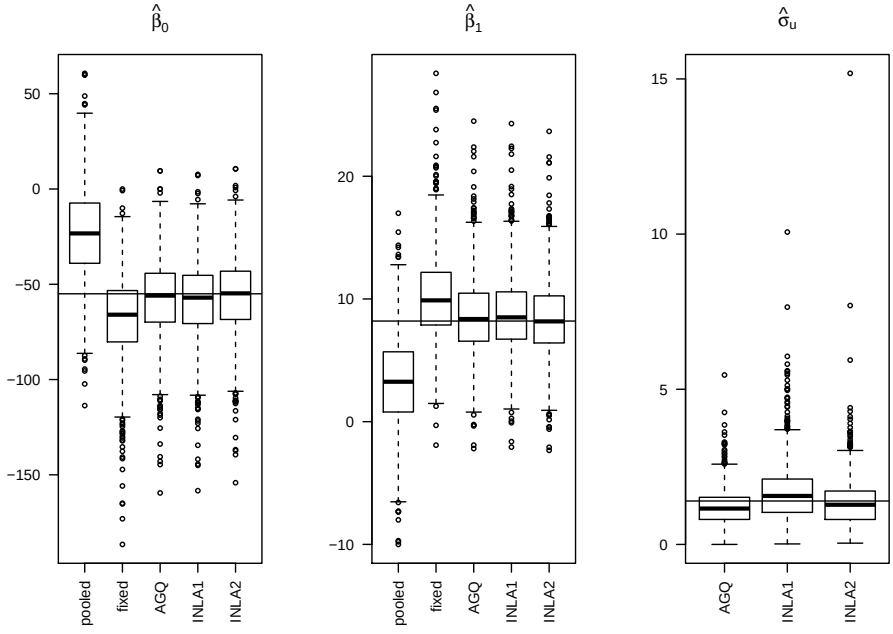


**(b)** $\sigma_u = 1.4$

**Figure 3.4:** Box plots of point estimates for $\beta_0, \beta_1$ and $\sigma_u$ with $\sigma_u = 0.2$ and $\sigma_u = 1.4$, where the horizontal line of each plot indicates the true parameter value.

**Table 3.1:** Relative bias of $\hat{\beta}_0$ and $\hat{\beta}_1$ by $\sigma_u$

| $\sigma_u$ | $(\text{Med}(\hat{\beta}_0) - \beta_0)/\beta_0$ | | | | | $(\text{Med}(\hat{\beta}_1) - \beta_1)/\beta_1$ | | | | |
|---|---|---|---|---|---|---|---|---|---|---|
| | Pooled | Fixed | AGQ | INLA1 | INLA2 | Pooled | Fixed | AGQ | INLA1 | INLA2 |
| 0.2 | −0.002 | 0.137 | 0.036 | 0.046 | 0.036 | −0.001 | 0.144 | 0.038 | 0.049 | 0.038 |
| 0.5 | −0.115 | 0.162 | 0.027 | 0.037 | 0.013 | −0.119 | 0.170 | 0.027 | 0.039 | 0.015 |
| 0.8 | −0.281 | 0.161 | 0.000 | 0.020 | −0.022 | −0.294 | 0.164 | −0.003 | 0.024 | −0.022 |
| 1.1 | −0.422 | 0.178 | 0.013 | 0.028 | −0.005 | −0.440 | 0.179 | 0.012 | 0.030 | −0.004 |
| 1.4 | −0.576 | 0.200 | 0.017 | 0.038 | −0.004 | −0.603 | 0.206 | 0.020 | 0.038 | −0.003 |

provide much improved results. They all maintain small bias across all values of $\sigma_u$. It seems AGQ and INLA2 produce slightly smaller bias than INLA1; and the bias of INLA2 is reduced as $\sigma_u$ increases.

Figure 3.4 displays the estimation of $\sigma_u$ from AGQ, INLA1 and INLA2. One can see that, when $\sigma_u = 0.2$, more than 50% of $\hat{\sigma}_u$ from AGQ is zero, which means AGQ could not detect the small variance component in many cases. On the contrary, two INLA methods produced interquartile ranges (i.e., $Q_3 - Q_1$) of estimates distinguished from zero, which indicates a better performance for detecting small group-to-group variations. This can be thought as the consequence of the priors given to INLA. In fact, $Gamma(0.001, 0.001)$ and $Gamma(0.5, 0.0164)$ prior distributions have peaks near zero although they are very flat priors (see e.g., Grilli *et al.*, 2015). It probably causes some portions of posterior mass for $\sigma_u$ being placed away from zero. Particularly, INLA2 shows more closer estimates to zero than INLA1, which can be also explained by the use of more informative prior in INLA2. Table 3.2 contains the median and interquartile of $\hat{\sigma}_u$ with true values of $\sigma_u$. It shows INLA2, compared to INLA1, consistently produces closer-to-zero estimates and more narrower interquartile ranges across all $\sigma_u$.

**Table 3.2:** Median and interquartile range of $\hat{\sigma}_u$ by true values of $\sigma_u$

| $\sigma_u$ | ASQ | | INLA1 | | INLA2 | |
|---|---|---|---|---|---|---|
| 0.2 | 0.000 | (0.000, 0.254) | 0.315 | (0.099, 0.519) | 0.237 | (0.222, 0.290) |
| 0.5 | 0.369 | (0.000, 0.577) | 0.409 | (0.180, 0.707) | 0.295 | (0.226, 0.590) |
| 0.8 | 0.650 | (0.373, 0.884) | 0.771 | (0.342, 1.144) | 0.594 | (0.270, 1.004) |
| 1.1 | 0.902 | (0.590, 1.213) | 1.151 | (0.642, 1.669) | 0.974 | (0.474, 1.388) |
| 1.4 | 1.157 | (0.805, 1.525) | 1.564 | (1.033, 2.108) | 1.279 | (0.808, 1.722) |

We also investigate interval estimates of AGQ and INLA's. For INLA, the 95% quantile credible intervals from the posterior distributions of $\beta_0$, $\beta_1$ and $\tau_u$ are considered. In AGQ, we adopt a confidence interval based on the profile likelihood (see e.g., Pawitan, 2013). As we can see from Figure 3.4, the distribution of $\hat{\sigma}_u$ is asymmetric in general, especially when $\sigma_u$ is small. In this case, the Wald-type confidence interval based on an asymptotic normality of estimators would perform poorly, especially when we have a small sample. The profile likelihood confidence interval is a better choice. A brief description of this method is as follows. Given the joint likelihood $L(\sigma_u, \boldsymbol{\beta})$ the profile likelihood of $\sigma_u$, for example, is

$$L(\sigma_u) = \max_{\boldsymbol{\beta}} L(\sigma_u, \boldsymbol{\beta}).$$

and a 95% confidence interval for $\sigma_u$ is the set of all values $\sigma_u^*$ such that a two-sided test of the null hypothesis $H_0 : \sigma_u = \sigma_u^*$ would not be rejected at 0.05 significance level. That is $\forall \sigma_u^*$ such that the likelihood ratio statistic $2[\log L(\hat{\sigma}_u, \hat{\boldsymbol{\beta}}) - \log L(\sigma_u^*)] < \chi^2_{1,0.95}$ or

$$\forall \sigma_u^* \quad \text{s.t.} \quad \log L(\sigma_u^*) > \log L(\hat{\sigma}_u, \hat{\boldsymbol{\beta}}) - \chi^2_{1,(1-\alpha)}/2,$$

where $\hat{\sigma}_u$ and $\hat{\boldsymbol{\beta}}$ are the MLE's from $L(\sigma_u, \boldsymbol{\beta})$; and $\chi^2_{1,(1-\alpha)}$ is the $1-\alpha$ quantile of a $\chi^2$ distribution with 1 degree of freedom.

**Table 3.3:** Coverages of 95% interval estimates

| $\sigma_u$ | $\beta_0$ | | | $\beta_1$ | | | $\sigma_u$ ($\tau_u$ for INLA's) | | |
|---|---|---|---|---|---|---|---|---|---|
| | AGQ | INLA1 | INLA2 | AGQ | INLA1 | INLA2 | AGQ | INLA1 | INLA2 |
| 0.2 | 0.954 | 0.946 | 0.955 | 0.950 | 0.946 | 0.955 | 0.986 | 0.959 | 0.984 |
| 0.5 | 0.942 | 0.940 | 0.942 | 0.941 | 0.943 | 0.943 | 0.953 | 0.959 | 0.972 |
| 0.8 | 0.948 | 0.945 | 0.946 | 0.946 | 0.945 | 0.944 | 0.897 | 0.926 | 0.890 |
| 1.1 | 0.958 | 0.953 | 0.951 | 0.956 | 0.952 | 0.948 | 0.879 | 0.913 | 0.854 |
| 1.4 | 0.938 | 0.933 | 0.934 | 0.939 | 0.936 | 0.931 | 0.898 | 0.924 | 0.876 |

Table 3.3 shows the coverage results of 95% interval estimates from each methods. The coverages for $\beta$'s from all three methods look quite close to 0.95, the target coverage, except slightly decreased coverages for $\sigma_u = 1.4$. The coverage of the variance component, however, seems to depend on the estimation method and the magnitude of the parameter's true value. Among the three methods, INLA1 shows relatively consistent and acceptable coverages, while AGQ and INLA2 produce comparable results with large variation. The coverages of both AGQ and INLA2 methods fall under 90% when $\sigma_u \geq 0.8$.

Furthermore, we investigate the effect of sample size on model parameter estimation by using AGQ, INLA1 and INLA2. It is found that when the variance component $\sigma_u$ is small, INLA2 has a better performance than other two methods regardless of sample size. When $\sigma_u$ is relatively large and sample size is small, INLA2 and AGQ have comparable performance and they are better than INLA1, but when sample size is large, all three methods show similar performance.

**Table 3.4:** Stress profiles

| Step | Stress level (kVolts) | Holding time (min.) | | | |
|---|---|---|---|---|---|
| | | Profile 1 | Profile 2 | Profile 3 | Profile 4 |
| 1 | 5.0 | 10 | 10 | 10 | 10 |
| 2 | 10.0 | 10 | 10 | 10 | 10 |
| 3 | 15.0 | 10 | 10 | 10 | 10 |
| 4 | 20.0 | 10 | 10 | 10 | 10 |
| 5 | 26.0 | 15 | 60 | 240 | 960 |
| 6 | 28.5 | 15 | 60 | 240 | 960 |
| 7 | 31.0 | 15 | 60 | 240 | 960 |
| 8 | 33.4 | 15 | 60 | 240 | 960 |
| 9 | 36.0 | 15 | 60 | 240 | 960 |
| 10 | 38.5 | 15 | 60 | 240 | 960 |

## 3.5 Application to Real Data

The dataset of Nelson (1980), introduced in Subsection 3.1.1, have been previously analyzed by several studies (e.g., Nelson, 2008; Lee and Pan, 2010; Hamada, 2015) with different distribution assumptions and methods. We note that Nelson (2008) pointed out significant non-homogeneity among groups of this data by residual analysis and a likelihood ratio test. Lee and Pan (2010) partially considered the non-homogeneity by removing data of groups founded being significantly different from other groups. Regardless, most previous analysis ignored the group effect. In this section, we fully take into account the heterogeneous group effect using GLMM model.

**Table 3.5:** Cable insulation SSALT data

| Test | Thick | Group | Profile | Failure or censored time for each step | | | | | | | | | |
|---|---|---|---|---|---|---|---|---|---|---|---|---|---|
| unit | (mils) | | | 1 | 2 | 3 | 4 | 5 | 6 | 7 | 8 | 9 | 10 |
| 1 | 27 | | | 10+ | 10+ | 10+ | 10+ | 15+ | 15+ | 15+ | 15+ | 2 | |
| 2 | 27 | 1 | 1 | 10+ | 10+ | 10+ | 10+ | 15+ | 15+ | 15+ | 15+ | 13 | |
| 3 | 27 | | | 10+ | 10+ | 10+ | 10+ | 15+ | 15+ | 15+ | 15+ | 13 | |
| 4 | 29.5 | | | 10+ | 10+ | 10+ | 10+ | 60+ | 60+ | 60+ | 60+ | 60+ | 30+ |
| 5 | 29.5 | 2 | 2 | 10+ | 10+ | 10+ | 10+ | 60+ | 60+ | 60+ | 60+ | 60+ | 5+ |
| 6 | 28 | | | 10+ | 10+ | 10+ | 10+ | 60+ | 60+ | 60+ | 60+ | 60+ | 5 |
| 7 | 29 | | | 10+ | 10+ | 10+ | 10+ | 240+ | 240+ | 240+ | 240+ | 240+ | 93 |
| 8 | 29 | 3 | 3 | 10+ | 10+ | 10+ | 10+ | 240+ | 240+ | 240+ | 240+ | 240+ | 9 |
| 9 | 29 | | | 10+ | 10+ | 10+ | 10+ | 240+ | 240+ | 240+ | 240+ | 240+ | 93+ |
| 10 | 29 | | | 10+ | 10+ | 10+ | 10+ | 240+ | 240+ | 240+ | 240+ | 106.4 | |
| 11 | 30 | 4 | 3 | 10+ | 10+ | 10+ | 10+ | 240+ | 240+ | 240+ | 240+ | 240+ | 10.8 |
| 12 | 29 | | | 10+ | 10+ | 10+ | 10+ | 240+ | 240+ | 240+ | 240+ | 97.9 | |
| 13 | 30 | | | 10+ | 10+ | 10+ | 10+ | 960+ | 960+ | 500.9+ | | | |
| 14 | 30 | 5 | 4 | 10+ | 10+ | 10+ | 10+ | 960+ | 960+ | 500.9 | | | |
| 15 | 30 | | | 10+ | 10+ | 10+ | 10+ | 960+ | 960+ | 743.4 | | | |
| 16 | 30 | | | 10+ | 10+ | 10+ | 10+ | 960+ | 960+ | 960+ | 3.9 | | |
| 17 | 30 | 6 | 4 | 10+ | 10+ | 10+ | 10+ | 960+ | 160 | | | | |
| 18 | 30 | | | 10+ | 10+ | 10+ | 10+ | 960+ | 960+ | 2.9 | | | |
| 19 | 30 | | | 10+ | 10+ | 10+ | 10+ | 323.9+ | | | | | |
| 20 | 30 | 7 | 4 | 10+ | 10+ | 10+ | 10+ | 858.4+ | | | | | |
| 21 | 30 | | | 10+ | 10+ | 10+ | 10+ | 960+ | 960+ | 960+ | 960+ | 262.1 | |

Table 3.4 shows the step-stress profiles applied to the test. All four profiles have the same pattern from step 1 to step 4 for the burn-in period, but different stress holding time afterwards. Table 3.5 provides the failure or survived time for each step of each test units, where the plus sign indicates the survived time. As represented in Figure 3.2, observations of 21 test units generate 176 pseudo observations with 15 failure time and 161 censored time.

We assume the exponential distribution for failure time, which has been shown to be a reasonable assumption for this dataset (Lee and Pan, 2010). The inverse power law with consideration of the insulation thickness results in the natural stress variable of log(volts/mils) (Nelson, 1980).

For model comparison, AIC (Akaike Information Criterion) of each model by the frequentist approach is calculated and shown in the first column of Table 3.6. It clearly represents superiority of the random effect model (AGQ). Table 3.6 also shows the result of point estimates for each method. The parameters are estimated in a similar manner as discussed in Section 3.4. The result shows a quite similar pattern with the simulation study. In particular, $\hat{\beta}_1$'s from the pooled model and the fixed model seem to underestimate and overestimate $\beta_1$, respectively, compared to other random effect models. Similarly, $\hat{\beta}_0$'s from the pooled model and the fixed model seem to overestimate and underestimate, respectively. In addition, the estimated $\hat{\sigma}_u$ from the random effect model indicates a substantially large group-to-group variation existed in the dataset. As being expected, AGQ and INLA2 provide $\hat{\sigma}_u$'s more close to zero compared to INLA1.

The impact of discrepancy in parameter estimates between different models becomes even more dramatic when those are extrapolated to the usual stress condition. For instance, Figure 3.5 illustrates the estimated mean failure time of pooled, fixed and random effect model by AGQ. The usual stress level in this example is given

**Table 3.6:** Model comparison for cable insulation data

| | AIC | Parameter estimates | | |
|---|---|---|---|---|
| | | $\hat{\beta}_0$ | $\hat{\beta}_1$ | $\hat{\sigma}_u$ |
| Pooled | 108.3 | −120.45 | 16.15 | – |
| Fixed | 78.8 | −427.09 | 59.50 | – |
| AGQ | 69.2 | −250.56 | 34.57 | 2.61 |
| INLA1 | – | −261.54 | 36.13 | 3.51 |
| INLA2 | – | −237.78 | 32.77 | 2.53 |

as log(400volts/mils) = 5.991. While the estimations are not very different around the stress range $(6.9, 7.2)$ in which most failures are observed, there exists a huge difference at the usual stress condition.

Figure 3.6 depicts the 95% interval estimates of AGQ and INLA's produced by the same methods as in the simulation study. We observe INLA methods present more narrow intervals than AGQ. In particular, the interval for $\hat{\sigma}_u$ by INLA2 is narrower than those by AGQ and INLA1; but we need to consider that the true coverage of this interval may not reach to 95% as we observe from the simulation study.

Lastly, the prediction of random effects for each group, $\tilde{u}_i, i = 1, \ldots, 7$, and 95% prediction intervals are obtained from each method. These are the estimation for the realized values of random variable $u_i$'s. In particular, the prediction of AGQ is obtained from the conditional mode of $u_i$ given data with fixed parameter values, $\hat{\boldsymbol{\beta}}$ and $\hat{\sigma}_u$; and those of INLA's are obtained by the posterior mean of $u_i$'s. Figure 3.7 shows the result and one can observe heterogeneous group effects as their values are different from zero, especially in group 3 and 6. What we found in this study can

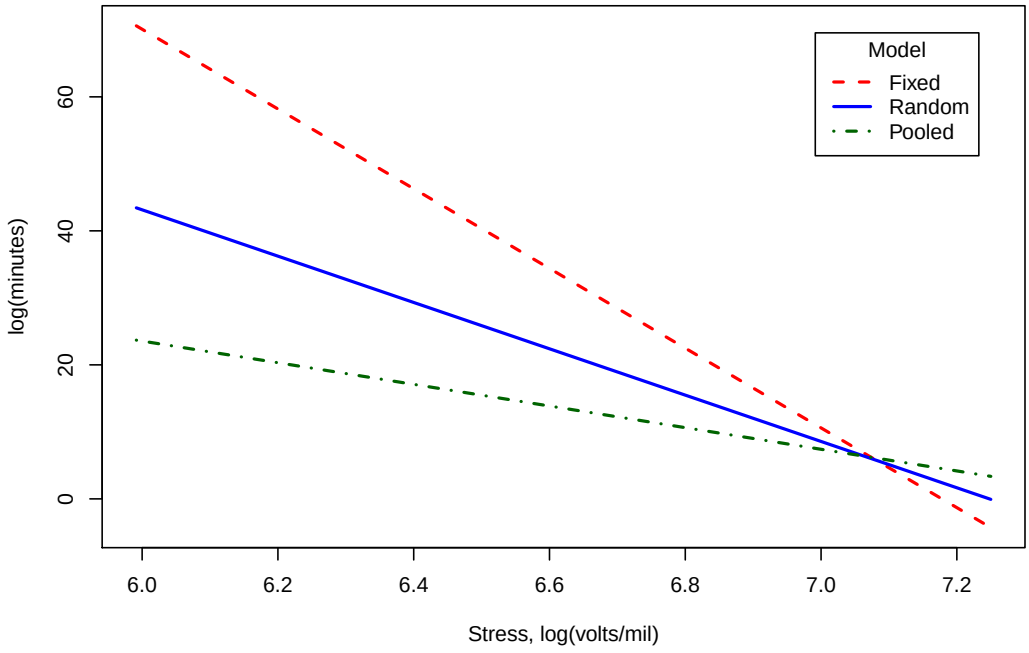


**Figure 3.5:** Estimated mean time to failure

verify arguments from Nelson (2008), where residual plots of the same data have shown big effects of group 3 and 6 (group C and F in Nelson, 2008).

We notice that AGQ provides relatively small intervals compared to INLA's, which is probably due to the different estimation method for $u_i$. That is, the prediction of AGQ is based on the fixed variance component value, while, in INLA, the posterior density of $u_i$ is obtained by the mixture of conditional densities of $u_i$ given the variance component. Even as we consider the wider intervals of INLA's, those of group 3 and 6 are still different from zero.

As one can see from this example, the absence of a random effect in an ALT model may cause a serious misinterpretation of test result. Therefore, reliability test practitioners need to carefully examine any group or cluster structure of a test caused by, e.g., different operators or different test stands, and include this group effect into

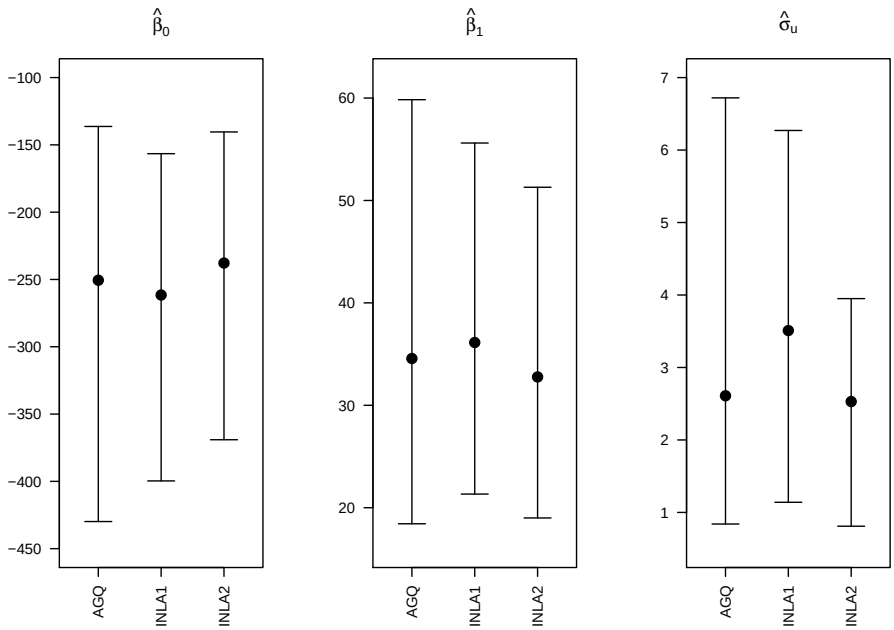


**Figure 3.6:** Point estimates (dots) and 95% interval estimates (corresponding lines) for power cable data

the model. We recommend fitting the data using the traditional model as well as the random effect model, and compare the results.

## 3.6 Conclusion and Future Work

It is always worthwhile to consider the involvement of random effects in SSALT data analysis, because practical experimental protocols are necessary to make a feasible and cost-effective life test. In this chapter, we develop a GLMM approach to the analysis of SSALT data so as to infer the random group effect introduced by subsampling or random blocks. This approach provides the structural framework for modeling lifetime observations from complicated test plans and with censoring. The simulation study has shown that ignoring the group-to-group variation can cause serious problems for the parameter estimation of the acceleration model, which in

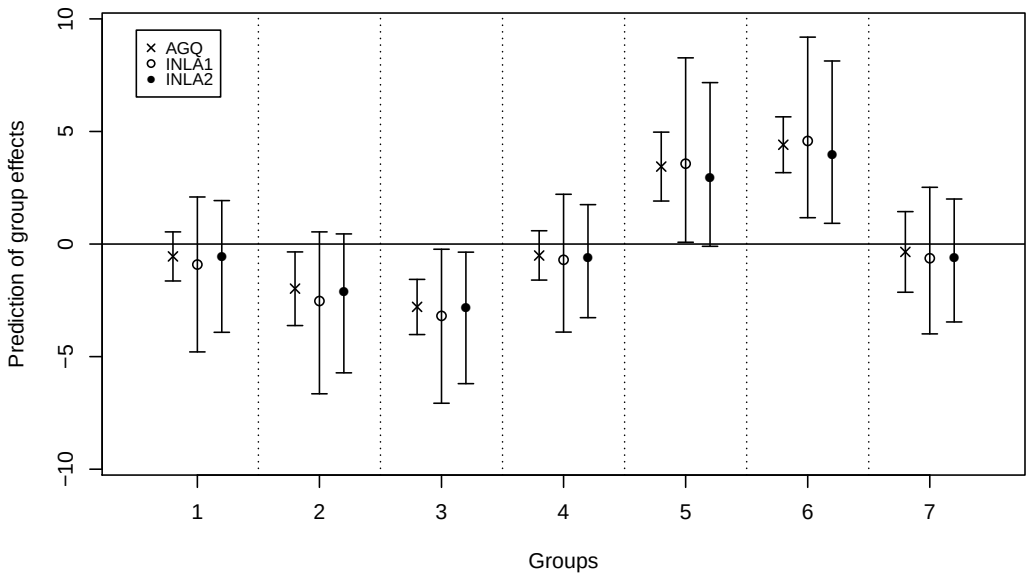


**Figure 3.7:** Prediction of group effects

turn may lead to even more erroneous conclusions for a product's lifetime when it is extrapolated to the usual stress condition. In lieu of the Monte Carlo simulation for approximating the integral involved in parameter estimation, we propose two deterministic approximation methods, AGQ and INLA, from the frequentist's and Bayesian points of view, respectively. Our simulation study shows that both methods have reasonable performance, but the INLA with slightly informative prior could be superior to others at detecting small variance components.

The exponential distribution assumption for failure time used in this chapter may be unrealistic in other ALT applications. Applying the Weibull distribution will allow more flexibility to the model. To do that, we need to estimate an additional parameter that determines the shape of the distribution, which is related to the failure mode. However, if we have knowledge for this shape parameter, say $\alpha$, from the previous or similar products, a simple variable transformation of $t^\alpha$ will make the response follow an exponential distributions again. Therefore, we can still apply the GLMM model

on the transformed failure time. If the shape parameter is unknown, we would need an additional procedure to estimate it and couple it with the GLMM approach to estimating other model parameters. This will be studied in our future research.

Chapter 4

# PLANNING ACCELERATED LIFE TESTS WITH RANDOM EFFECTS OF TEST CHAMBERS

In accelerated life tests (ALTs), test units are often tested in multiple test chambers along with different stress conditions. The non-homogeneity of test chambers precludes the complete randomized experiment, and may affect the life-stress relationship of the tested product. These chamber-to-chamber variations should be taken into account for ALT planning so as to obtain more accurate test results. In this chapter, planning ALTs under a nested design structure with random test chamber effects is studied. First, by a two-phase approach, we illustrate to what extent different test chamber assignments to stress conditions impact the estimation of unknown parameters. Then, the $D$-optimal test plan with two test chambers is considered. To construct the optimal design we establish the generalized linear mixed model (GLMM) for failure time data and apply quasi-likelihood method, where the test chamber assignment is determined as well as the other decision variables required for planning ALTs.

## 4.1 Introduction

### *4.1.1 Background and Motivation*

The accelerated life test (ALT) is a popular testing method in industry which aims to assess product lifetime within an acceptably short period of time. It accelerates the product failure by applying the higher-than-usual levels of environmental stresses

(e.g., temperature, voltage, humidity, etc.), then the data obtained from ALTs would be exploited by reliability practitioners to identify the lifetime-stress relationship and predict the product reliability in the usual stress condition. Planning ALT has a big impact on these statistical inferences and predictions of failure time distribution. As such, optimal experimental designs of ALT, which seek to obtain statistically efficient test plans that satisfy some desirable criteria, have been studied by many researchers (see, e.g., Nelson, 2005a,b). Typical decision variables of optimal ALT design include, given other assumptions, locating test stress conditions and determining the number of test units to be allocated at each stress condition.

Although previous studies on the optimal ALT design have achieved success to some extent, most of them have been derived based on an assumption that lifetime observations are independent of each other. It is, however, extremely expensive and time-consuming to achieve total randomization in a real experimental setting. For instance, reliability engineers often put many test units in the same test chamber and test them at the same time. In addition, multiple test chambers may be used and they are set at different stress levels. In this case observed failure times are not only affected by the stress factor but also by the test chamber, which may cause discordance of actual stress intensity between two chambers. Consequently, failure time observations from the same test chamber may be correlated to each other. In recent literature (e.g., León *et al.*, 2007), it has been shown that the correlation among the observations from the same test chamber or any other group structure in ALT can lead to severe misunderstanding of the lifetime-stress relationship, especially when a large group-to-group variation exists. Therefore, such correlation should be reflected in the ALT plan so as to avoid poor experimental results and to obtain more accurate inference on the acceleration model and reliability prediction.

In this chapter, we consider the effect of heterogeneous test chambers on optimal ALT plans. Specifically we focus on the ALT with two stress factors with the following additional assumptions.

- Two test chambers are available.
- The test chamber effect is assumed to be random; that is, its effect is assumed to be a sample drawn from a population of random test chamber effects. This is a reasonable assumption when the main interest lies in the variation in the population effect rather than the specific chamber.
- We also impose a constraint that two test chambers cannot afford to be run at the same stress level combination. With this constraint, our ALT plan cannot set the same stress condition at different chambers, which is economically impractical in real applications.
- The failure time given the chamber effect follows the Weibull distribution with known shape parameter.
- The right censoring strategy is used.

With these constraints, the experiment can be seen as the two-stage nested design (see, e.g., Montgomery, 2008), where the stress conditions are nested under the test chambers. Figure 4.1 illustrates an instance of a test plan with the nested structure considered in this chapter. Note that the stress conditions nested in the first test chamber (i.e., $j = \{1, 2\}$) are all different from those nested in the second test chamber (i.e., $j = \{3, 4\}$). In addition, because each test chamber may have an unequal number of stress conditions and each stress condition may have an unequal number of observations, it is an unbalanced nested design.

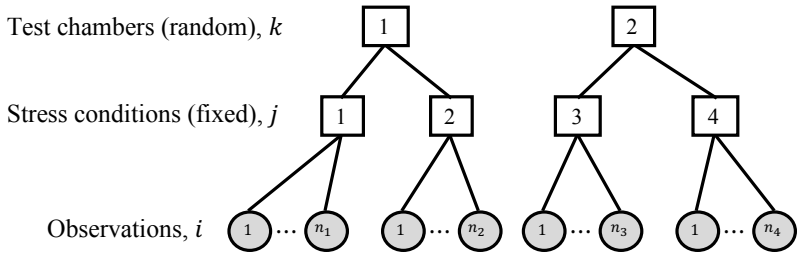


**Figure 4.1:** Nested structure of ALT plan with random test chamber effects

Now the additional decision associated with this problem is "How to assign test chambers to each test location?" and we call it the *chamber assignment problem*. In this chapter we propose two approaches for creating the optimal ALT plans with the consideration of random chamber effect. The first one is a two-phase approach, where the test stress conditions and the number of allocations are determined first, and then the chamber assignment is considered separately. The second one is the quasi-likelihood approach, in which all decisions are made at the same time in an integrated manner.

### *4.1.2 Previous Work*

Unlike the regular experimental design with linear regression model, where the response is normally distributed with a constant variance, ALT design is characterized by some features which shall be taken into account for its modeling. First, the response, i.e., failure time, is not normally distributed. Instead the log-location-scale family distributions such as Weibull or lognormal distribution are usually assumed for the failure time variable. Second, failure time observations almost always include censored data. The limited testing time gives rise to right-censored data; and the periodic monitoring of test produces interval-censored data. Lastly, since the experimental region is deviated from the normal levels of stress variables, the estimated

regression model has to be extrapolated to the use stress condition beyond the test region. Therefore, the regression model should be built under a physically reasonable model corresponded to the type of stress factors, e.g., Arrhenius model for thermal stress factor. For more details on these characteristics of failure-time data, see Meeker and Escobar (2014).

A vast amount of literature has been published on the optimal ALT planning since it was first studied by Chernoff (1962). Traditionally the optimal design for ALT is determined by minimizing the (asymptotic) variance of the maximum likelihood estimator for some unknown parameters of interest, which is usually directly calculated by the likelihood function of the corresponding failure time distribution. Mann (1972) considered a problem of obtaining the minimum variance least squares curve intercept at the use condition for a polynomial function modeled for the Weibull scale parameter. Meeker and Nelson (1975) provided the charts for optimum ALT plans, which had shown that more test units should be allocated at the lower stress condition than at the higher one. Park and Yum (1996) developed optimal ALT plans with two stress factors. Escobar and Meeker (1995) suggested the compromise two-factor ALT plans by splitting the degenerate optimum test plan, where the objective was to balance the prediction variance and the parameter estimation. Tang *et al.* (1999) considered optimal test plans under the failure distribution with failure-free life (e.g., two-parameter exponential distribution). Bai *et al.* (1989) presented the optimal test plan for step-stress ALTs with censoring. For more comprehensive review and list of literature on ALT planning, see Nelson (2005a,b, 2015).

More recently, there have been attempts to approach the ALT planning problem within the framework of optimal design theory of experimental designs. Particularly, the generalized linear model (GLM) (McCullagh and Nelder, 1989) plays an important role for this unification. Aitkin and Clayton (1980) first modeled lifetime data using

GLM. Monroe *et al.* (2011) applied the GLM approach to designing ALT experiments with right censoring plan. Yang and Pan (2013) and Pan and Yang (2014) expanded the GLM approach for optimal ALT planning with the interval censoring strategy. Pan *et al.* (2015) developed ALT plans with uncertainty in model specification using the GLM framework. Furthermore, Seo and Pan (2015a) developed an R package for creating and evaluating optimal ALT plans using the GLM approach.

Despite such a large body of work surrounding ALT planning, most of them assumes the non-correlated data. Although the correlated failure time data were analyzed in recent literature (e.g., León *et al.*, 2007; Kensler *et al.*, 2015; Seo and Pan, 2016), ALT planning, which considers a source of correlation, has not been studied yet in our knowledge.

The rest of this chapter is organized as follows. In Section 4.2, independent and correlated ALT data are modeled by GLM and GLMM, respectively. The two-phase approach to find better assignments of test chambers are demonstrated in Section 4.3. The quasi-likelihood based approach to create $D$-optimal test plan using GLMM is developed and a comparison study is conducted in Section 4.4. Finally, in Section 4.5, the contribution and possible extensions of the proposed method are discussed.

## 4.2 Modeling Failure Time Data using GLM and GLMM

In this section we briefly review the GLM modeling approach for independent ALT observations and the GLMM (see, e.g., McCulloch and Searle, 2001) for correlated ALT observations. GLMM is an expansion of GLM to the mixed model where the linear predictor contains both the random and fixed effect terms.

### 4.2.1 Independent ALT Data with Right Censoring

Consider an ALT with $m$ different stress conditions. At each stress condition $j = 1, \ldots, m$, $n_j$ test units are tested, so the total number of test units is $n = \sum_{j=1}^{m} n_j$. Let $t_{ij}$ be the failure time of the $i$th test unit at the $j$th stress condition and $\mathbf{x}_j = (1, x_{j1}, \ldots, x_{jp})'$ be the vector of the $j$th stress level of $p$ stress factors. We assume $t_{ij}$'s are independent and follow the Weibull distribution such as

$$t_{ij} \sim \text{ind. } Weibull(\lambda_j, \alpha),$$

where $\alpha$ is the shape parameter and it is assumed to be common to all failure times; $\lambda_j$ is the scale parameter, which depends on the stress factor levels by the log-linear relationship as

$$\log \lambda_j = \eta_j = \mathbf{x}_j' \boldsymbol{\beta}, \tag{4.1}$$

where $\boldsymbol{\beta} = (\beta_0, \beta_1, \ldots, \beta_p)'$ is a vector of unknown regression coefficients. The probability density function (pdf) and reliability function of $t_{ij}$ are given as $f(t_{ij}, \mathbf{x}_j) = \alpha \lambda_j t_{ij}^{\alpha-1} \exp(-\lambda_j t_{ij}^{\alpha})$ and $R(t_{ij}, \mathbf{x}_j) = \exp(-\lambda_j t_{ij}^{\alpha})$, respectively. Let $c_{ij}$ be an indicator variable for right censored observation, that is, $c_{ij} = 1$ if $t_{ij}$ is a failure observation and $c_{ij} = 0$ if $t_{ij}$ is a right-censored observation. Then the likelihood function of the entire set of observations is given by

$$\begin{aligned} L(\alpha, \boldsymbol{\beta}; \mathbf{t}, \mathbf{c}, \mathbf{X}) &= \prod_{j=1}^{m} \prod_{i=1}^{n_j} f\left(t_{ij}, \mathbf{x}_j\right)^{c_{ij}} R\left(t_{ij}, \mathbf{x}_j\right)^{(1-c_{ij})} \\ &= \prod_{j=1}^{m} \prod_{i=1}^{n_j} \left(\alpha \lambda_j t_{ij}^{\alpha-1}\right)^{c_{ij}} \exp\left(-\lambda_j t_{ij}^{\alpha}\right), \end{aligned}$$

where $\mathbf{t}$ and $\mathbf{c}$ are vectors of observations; and $\mathbf{X} = (\mathbf{x}_1, \ldots, \mathbf{x}_n)'$ is the design matrix. Let $\mu_{ij} = \lambda_j t_{ij}^{\alpha}$, then the log-likelihood function is given as

$$\log L = \sum_{j=1}^{m} \sum_{i=1}^{n_j} (c_{ij} \log \mu_{ij} - \mu_{ij}) + \sum_{j=1}^{m} \sum_{i=1}^{n_j} c_{ij} \log(\alpha - t_{ij}).$$

Given $\alpha$, the unknown parameters are only included in the first term, which is equivalent, up to constants, to the log-likelihood function of $c_{ij} \sim$ ind. $Poisson(\mu_{ij})$, where $\mu_{ij}$ is the mean of the Poisson distribution. The relationship between $\mu_{ij}$ and the explanatory variables is given by

$$g(\mu_{ij}) = \log \mu_{ij} = \mathbf{x}_j'\boldsymbol{\beta} + \alpha \log t_{ij}$$

where the last term is the offset term.

### *4.2.2 Correlated ALT Data by Test Chamber Effects*

Suppose we now have two test chambers, $k = 1, 2$. Let $j(k)$ be a set of stress levels nested in the $k$th test chamber. For instance, $j(1) = \{1, 2\}$ and $j(2) = \{3, 4\}$, as shown in Figure 4.1. Then $t_{ij(k)}$ is the failure time of the $i$th test unit with $j$th stress level and $\mathbf{x}_{j(k)} = (1, x_{j(k)1}, \ldots, x_{j(k)p})'$ is the vector of $j$th stress level, which is nested in the $k$th test chamber. We introduce random variables $U_k$'s to reflect the chamber effect as follows.

$$U_k \sim \text{i.i.d. } N(0, \sigma_U^2), k = 1, 2,$$

where $\sigma_U^2$ is a variance component of chamber effects. Let $u_k$ be the realized value of chamber effect sampled from the population of $U_k$. The conditional failure time distribution given the chamber effect is the Weibull distribution. That is,

$$t_{ij(k)}|U_k \sim \text{ind.} Weibull(\lambda_{j(k)}, \alpha),$$

where $\lambda_{j(k)}$ is defined as

$$\log \lambda_{j(k)} = \eta_{j(k)} = \mathbf{x}_{j(k)}'\boldsymbol{\beta} + u_k \tag{4.2}$$

and the conditional pdf of $t_{ij(k)}$ is given by

$$f\left(t_{ij(k)}, \mathbf{x}_{j(k)}|U_k\right) = \alpha\lambda_{j(k)}t_{ij(k)}^{\alpha-1} \exp\left(-\lambda_{j(k)}t_{ij(k)}^{\alpha}\right),$$

Let $c_{ij(k)}$ be an indicator variable for right censored observations, then the marginal likelihood of all observations in all test chambers is given as follows.

$$L = \prod_{k=1}^{2} \int_{-\infty}^{\infty} \left( \prod_{j \in j(k)} \prod_{i=1}^{n_j} \left( \alpha \lambda_{j(k)} t_{ij(k)}^{\alpha-1} \right)^{c_{ij(k)}} \exp\left( -\lambda_{j(k)} t_{ij(k)}^{\alpha} \right) \right) \pi(u_k) \mathrm{d}u_k \tag{4.3}$$

Let $\lambda_{j(k)} t_{ij(k)}^{\alpha} = \mu_{ij(k)}$; then the Eq. (4.3) can be rewritten as

$$\begin{aligned} \log L = & \sum_{k=1}^{2} \sum_{j \in j(k)} \sum_{i=1}^{n_j} c_{ij(k)} \left( \log \alpha - \log t_{ij(k)} \right) \\ & + \sum_{k=1}^{2} \log \int_{-\infty}^{\infty} \left( \prod_{j \in j(k)} \prod_{i=1}^{n_j} \mu_{ij(k)}^{c_{ij(k)}} \exp\left( -\mu_{ij(k)} \right) \right) \pi(u_k) \mathrm{d}u_k \end{aligned}$$

As in the GLM case, given $\alpha$, the unknown parameters are only included in the second term, which is equivalent, up to constants, to the log-likelihood function of

$$c_{ij(k)} | U_k \sim \text{ind. } Poisson(\mu_{ij(k)}), \tag{4.4}$$

where $\mu_{ij(k)} = \mathbb{E}\left[ c_{ij(k)} | U_k \right]$ is the conditional mean of the Poisson distribution. The relationship between $\mu_{ij(k)}$ and the explanatory variables, i.e., stress factors and the chamber effect, is given by the link function, $g(\mu_{ij(k)}) = \log \mu_{ij(k)} = \mathbf{x}'_{j(k)} \boldsymbol{\beta} + u_k + \alpha \log t_{ij(k)}$, where the last term is the offset term. Accordingly the inverse link function is given as

$$\mu_{ij(k)} = g^{-1} = \exp\left( \mathbf{x}'_{j(k)} \boldsymbol{\beta} + u_k + \alpha \log t_{ij(k)} \right).$$

## 4.3 Two-phase Approach to Test Chamber Assignment Problem

In this section, we use a modified example of Yang and Pan (2013) to demonstrate the optimal ALT design with random test chamber effects. Suppose an ALT for an electronic device with two stress factors, temperature and humidity. The use condition of this device is given as 30°C, and 25% relative humidity (RH). A total of 100 test units are available for the test, and these test units are all homogeneous. The total

testing time is 30 time units, and the test units that survived until the end of the test are right censored. Two test chambers are used; and once its test chamber is determined, its failure time is assumed to follow the Weibull distribution with a known shape parameter, $\alpha = 1$. Suppose that the accelerated stress conditions can be varied in the range $(60°\text{C}, 110°\text{C})$ for temperature, and $(60\%, 90\%)$ for humidity. According to Eyring model, the natural stress variables of these two factors are defined as $S_1 = 11605/T$, where $T$ is the temperature in degrees Kelvin, and $S_2 = \log(h)$, where $h$ is the percentage of relative humidity. It is convenient to apply coding schemes, $x_1 = (S_1 - S_1^H)/(S_1^L - S_1^H)$; $x_2 = (S_2 - S_2^H)/(S_2^L - S_2^H)$, so that the design space of this experiment becomes a unit square at the first quadrant. The highest stress levels and the lowest stress levels of both stress variables are coded as $(0, 0)$ and $(1, 1)$, accordingly the use condition is located at $(1.758, 3.159)$. For planning ALT, the acceleration model and the parameters in the model should be provided as planning values. In this example we assume the following acceleration model:

$$\eta_{j(k)} = -4.086x^1_{j(k)} - 1.476x^2_{j(k)} + u_k. \tag{4.5}$$

It is also required to have a planning value for the variance component of random chamber effects for planning ALT with correlated observations, and we assume $\sigma_U^2 = 0.25$.

Given all planning values, we must determine (1) the levels of stress factors; (2) the allocations of test units; and (3) the test chamber assignment, satisfying some optimality conditions. For this, our first approach is to separate the whole problem into two, and resolve each problem in greedy manner. In Phase-I, we construct the optimal test plan without consideration of chamber effects (i.e., independent observations). In this phase, the planning variables in (1) and (2) are determined. In Phase-II, we explore the best assignment of test chambers using Monte Carlo

simulation. In this phase, the planning variable in (3) is determined. This approach may seem naive, but it gives useful insight into how many support points are required to identify the test chamber effects; and how much the test chamber assignment may influence on the parameter estimation.

### *4.3.1 Phase-I: Optimal ALT Design using GLM Approach*

Without taking test chamber effects into account, all observations are independent to each other. The optimal test plan in this case can be easily constructed by the GLM approach, which does not consider the source of correlation. Consequently, the ALT data is modeled as in Subsection 4.2.1. With GLM, we now consider the *D*-optimal design, which achieves the minimum general variance of regression coefficients estimates among all test plans. Equivalently, it can be constructed by maximizing the determinant of the information matrix as follows:

$$\psi^* := \arg\max_{\psi} |\mathbf{X}(\psi)'\mathbf{W}\mathbf{X}(\psi)|, \tag{4.6}$$

where $\mathbf{X}(\psi)$ is the design matrix generated from the test plan $\psi$, and $\mathbf{W}$ is the weight matrix derived from the link function of GLM, which is a diagonal matrix due to the independency assumption (for more details, see Seo and Pan, 2015a).

Table 4.1 shows the *D*-optimal test plan generated by ALTopt (Seo and Pan, 2015b), a software package in R; and Figure 4.2 depicts the design plot of the test plan, where the size of each circle is proportional to the test unit allocation. Note that, while the linear predictor in this GLM has only three unknown parameters, $\beta_0$, $\beta_1$, and $\beta_2$, this test plan is supported by four distinct test locations.

**Table 4.1:** *D*-optimal test plan under independent observations

| Design | Temperature | | Humidity | | Allocation |
|---|---|---|---|---|---|
| Point | Actual | Coded | Actual | Coded | |
| $j$ | °C | $x_1$ | RH | $x_2$ | $n_j$ |
| 1 | 110.00 | 0.000 | 90.00 | 0.000 | 34 |
| 2 | 67.74 | 0.826 | 90.00 | 0.000 | 26 |
| 3 | 110.00 | 0.000 | 60.00 | 1.000 | 32 |
| 4 | 87.74 | 0.411 | 60.00 | 1.000 | 8 |

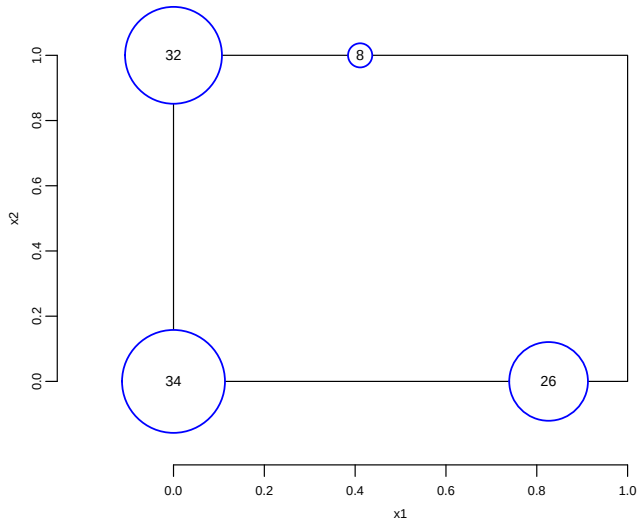


**Figure 4.2:** Design plot of *D*-optimal test plan under independent observations

### ALTopt: an R Package for Optimal ALT Planning using GLM

ALTopt (Seo and Pan, 2015b) is a software package to create and evaluate optimal ALT experimental designs based on the GLM theory. It is capable to handle both of right-censoring and interval-censoring plans, and also accommodates three statistical optimality criteria - $D$-optimal, $U$-optimal and $I$-optimal.

The objective function as in, e.g., Eq. (4.6) for $D$-optimal test plan with right-censoring, is optimized by using stats::optim in R with the "L-BFGS-B" method. This function allows box constraints on design variables. In our case, we have a cuboidal design region where the levels of each stress factor are coded to be between 0 and 1. More details about the"L-BFGS-B" method are available in Byrd *et al.* (1995).

The optimization procedure begins by generating an initial test plan with $n$ design points, which are randomly selected from possible points in the design region. For example, if we have 100 test units and 2 stress factors the optimization process begins from 100 randomly chosen initial points, which spread out over the design region. Throughout the optimization procedure, each of these 100 points converges to its own optimal location.

To create a practical test plan, it is useful to reduce the number of distinct design points by using clustering. Two clustering methods are implemented in the package. First, when the design points are very close, the simple rounding (to the $3^{\text{rd}}$ decimal place) method can be applied to the stress levels. Second, when there exist too many design points, the k-means clustering can be used as an alternative, where the number of clusters should be specified by users. By carefully selecting the number of clusters, it is possible to reduce the number of distinct design points without significantly affecting the objective function value.

The final recommended test plans are provided by a table containing each stress condition and the number of test units for each condition. The corresponding objective values of these plans are also shown. This package also provides graphical functions for evaluating and comparing various test plans.

### *4.3.2 Phase-II: Test Chamber Assignment by Monte Carlo Simulation*

In Phase-II, we further assume $u_1 = 0.5$ and $u_2 = -0.5$, so that the maximum likelihood estimator (MLE) of $\sigma_U^2$ could be matched to 0.25 as we assumed previously. We now consider every possible way to assign two test chamber, $k = 1, 2$, to four test locations, $j = 1, 2, 3, 4$. Table 4.2 enumerates all alternative test chamber assignment plans.

Each chamber assignment is assessed by Monte Carlo simulation with $1,000$ simulated ALT data sets, each of which is generated by the following procedure.

(1) According to Eq. (4.2) and Eq. (4.5), calculate the scale parameter at each test location, so the conditional cdf of failure time is determined. For instance, given the chamber assignment plan A1, they can be calculated as

$$\lambda_{1(1)} = \exp(-4.086(0) - 1.476(0) + 0.5) = 1.649;$$

$$\lambda_{2(2)} = \exp(-4.086(0.826) - 1.476(0) - 0.5) = 0.021;$$

$$\lambda_{3(2)} = \exp(-4.086(0) - 1.476(1) - 0.5) = 0.139;$$

$$\lambda_{4(2)} = \exp(-4.086(0.411) - 1.476(1) - 0.5) = 0.026.$$

(2) Draw 100 samples $z_{ij(k)}$'s from $Unif(0, 1)$.

(3) Obtain $t_{ij(k)}$ by the inverse of conditional cdf for the corresponding test location. That is,

$$t_{ij(k)} = -\frac{\ln(1 - z_{ij(k)})}{\lambda_{j(k)}}$$

**Table 4.2:** Alternatives of test chamber assignments

| Chamber | Test Chamber | |
|---|---|---|
| Assignment | $k = 1$ | $k = 2$ |
| A1 | $j(1) = \{1\}$ | $j(2) = \{2, 3, 4\}$ |
| A2 | $j(1) = \{2\}$ | $j(2) = \{1, 3, 4\}$ |
| A3 | $j(1) = \{3\}$ | $j(2) = \{1, 2, 4\}$ |
| A4 | $j(1) = \{4\}$ | $j(2) = \{1, 2, 3\}$ |
| A5 | $j(1) = \{1, 2\}$ | $j(2) = \{3, 4\}$ |
| A6 | $j(1) = \{1, 3\}$ | $j(2) = \{2, 4\}$ |
| A7 | $j(1) = \{1, 4\}$ | $j(2) = \{2, 3\}$ |
| A8 | $j(1) = \{2, 3\}$ | $j(2) = \{1, 4\}$ |
| A9 | $j(1) = \{2, 4\}$ | $j(2) = \{1, 3\}$ |
| A10 | $j(1) = \{3, 4\}$ | $j(2) = \{1, 2\}$ |
| A11 | $j(1) = \{1, 2, 3\}$ | $j(2) = \{4\}$ |
| A12 | $j(1) = \{1, 2, 4\}$ | $j(2) = \{3\}$ |
| A13 | $j(1) = \{1, 3, 4\}$ | $j(2) = \{2\}$ |
| A14 | $j(1) = \{2, 3, 4\}$ | $j(2) = \{1\}$ |

(4) Generate the indicator variable for censoring; and, for censored observations, replace the failure time with the censored time. That is,

$$c_{ij(k)} = \begin{cases} 1, \text{ if } t_{ij(k)} < 30 \\ 0, \text{ if } t_{ij(k)} \geq 30 \end{cases}, \quad t_{ij(k)} = \begin{cases} t_{ij(k)}, \text{ if } t_{ij(k)} < 30 \\ 30, \text{ if } t_{ij(k)} \geq 30 \end{cases}$$

Each data set is fitted by SAS PROC GLIMMIX using the quadrature method (Littell *et al.*, 2006). The simulation results are illustrated by Figures. 4.3 through 4.6, where the parameter estimates by each test chamber assignment are displayed

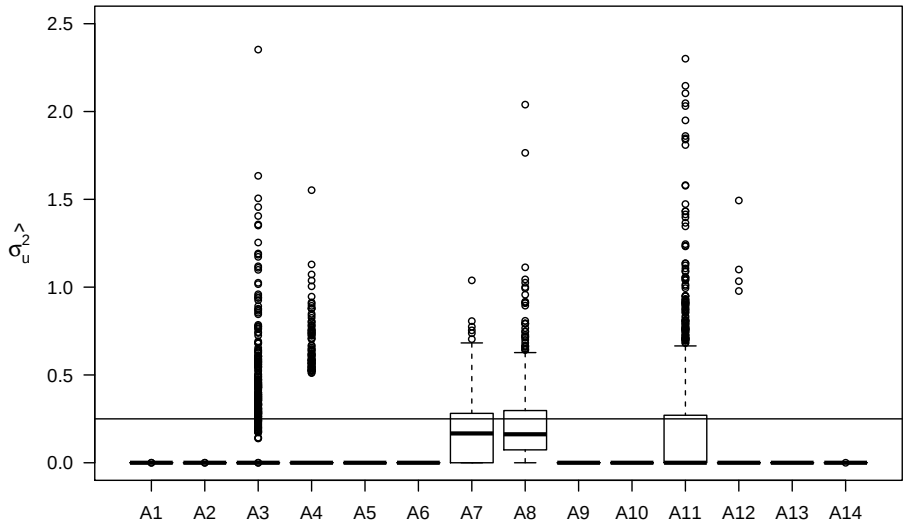


**Figure 4.3:** Box plots for point estimates for $\sigma_U^2$ by each test chamber assignment plan. The horizontal line indicates the true parameter value. Three data points beyond $\hat{\sigma}_U^2 > 2.5$ in A3 and A11 are removed for the clarity of plotting

by box plots. One can see that, in general, test chamber assignment has a big impact on each parameter's estimate. In particular, Figure 4.3 shows the medians of $\hat{\sigma}_U^2$ for A7 and A8 plans are closer to the true value of $\sigma_U^2$, which indicates those plans have relatively better performances to detect random effects among test chambers. On the other hand, chamber assignments of A1, A2, A5, A6, A9, A10, A13 and A14 show an inability to detect random effects for all simulated data sets. There are some other test plans, namely, A3, A4, A11 or A12 resulting non-zero estimates of the variance component for some cases, and yet their medians, so in the majority of cases, are still stuck in zero. Table 4.3 shows the mean squared error (MSE) of $\hat{\sigma}_U^2$ for assignment plans whose squared bias are less than 0.0625 (i.e., assignment plans which have an

**Table 4.3:** Mean squared error of $\hat{\sigma_U^2}$

| Chamber Assignment | $(\mathbb{E}[\hat{\sigma_U^2}] - \sigma_U^2)^2$ | $\text{var}(\hat{\sigma_U^2})$ | $MSE$ |
|---|---|---|---|
| A1 | 0.0625 | – | – |
| A2 | 0.0625 | – | – |
| A3 | 0.0195 | 0.0719 | 0.0914 |
| A4 | 0.0376 | 0.0383 | 0.0759 |
| A5 | 0.0625 | – | – |
| A6 | 0.0625 | – | – |
| A7 | 0.0049 | 0.0305 | 0.0354 |
| A8 | 0.0017 | 0.0380 | 0.0397 |
| A9 | 0.0625 | – | – |
| A10 | 0.0625 | – | – |
| A11 | 0.0040 | 0.2602 | 0.2642 |
| A12 | 0.0602 | 0.0055 | 0.0657 |
| A13 | 0.0625 | – | – |
| A14 | 0.0625 | – | – |

ability, in partial at least, to detect the random effects). As expected from the box plots, A7 and A8 show the best performances.

It would be worth noting that, although it is not shown here, any test plan supported by only three distinct test locations cannot detect random effects at all, no matter how the test chambers are assigned. For instance, one can enforce a $D$-optimal design to produce three test locations by clustering the original test locations in Phase-I, so that the test plan is capable of estimating all unknown parameters in

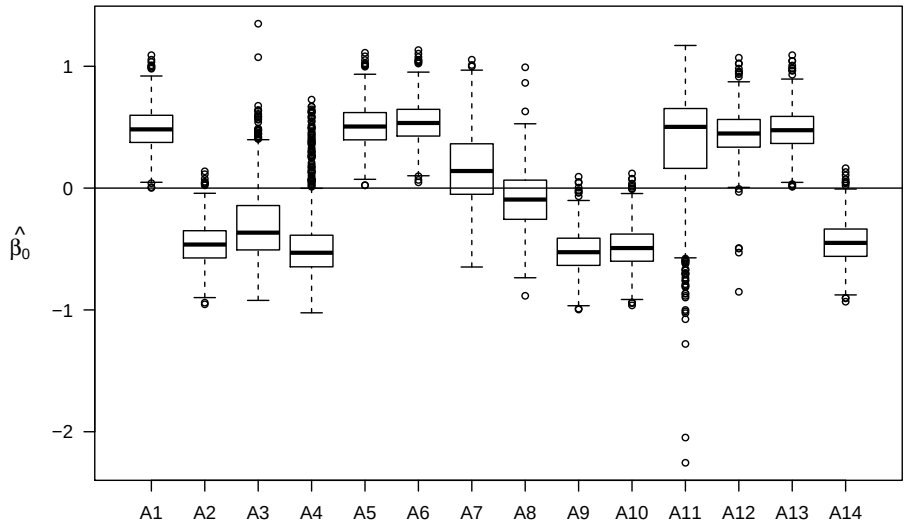


**Figure 4.4:** Box plots for point estimates for $\beta_0$ by each test chamber assignment plan. The horizontal line indicates the true parameter value.

the linear predictor with the smallest number of test locations. However, with three test locations, there is no possible way to distinguish the fixed effects from the random effects. In other words, once three test locations determine the slopes and the intercept of the fitted surface (i.e., fixed effects), then there is no remaining variation requiring the random effects, and hence MLE of GLMM always produces a zero estimate for the variance component. Therefore having four distinct test locations is a necessary condition for the best test plan, and the assignment of test chambers should be chosen based on that condition.

The quality of the variance component estimate directly affects the quality of estimation for the regression coefficients. From Figure. 4.4 to 4.6, A7 and A8 consistently show relatively smaller bias for all regression coefficients than the other assignment plans. Some plans result in better performance for a part of regression coefficients,

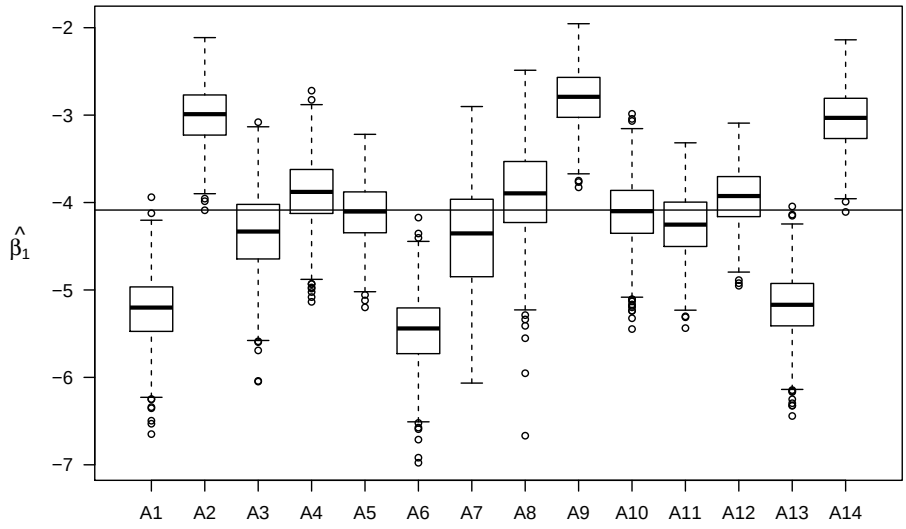


**Figure 4.5:** Box plots for point estimates for $\beta_1$ by each test chamber assignment plan. The horizontal line indicates the true parameter value.

but not overall. For instance, A4 and A11 show small bias for $\beta_1$ and $\beta_2$, but not for $\beta_0$; and A5 and A10 show the smallest bias for $\beta_1$ among all assignment plans, but large bias for $\beta_0$ and $\beta_2$. We can also interpret this result by the analogy with the linear mixed model (LMM) case. In LMM, where the response is normally distributed, it is well-known that orthogonal blocking is an optimal design strategy (Goos, 2012). That is, in a design space with two factors, assigning design points lying in a diagonal direction into the same block makes $D$-optimal design for the uncorrelated model being the same as that for the correlated model. It is certainly not the case that the orthogonal blocking can be applied for the design in Figure 4.2 because the design has an unbalanced number of allocations at each design point, and also some design points are not located at the factorial points ($j = \{2, 4\}$). Nonetheless, it can be seen that A7 and A8 are the most similar plans with the orthogonal blocking. Therefore

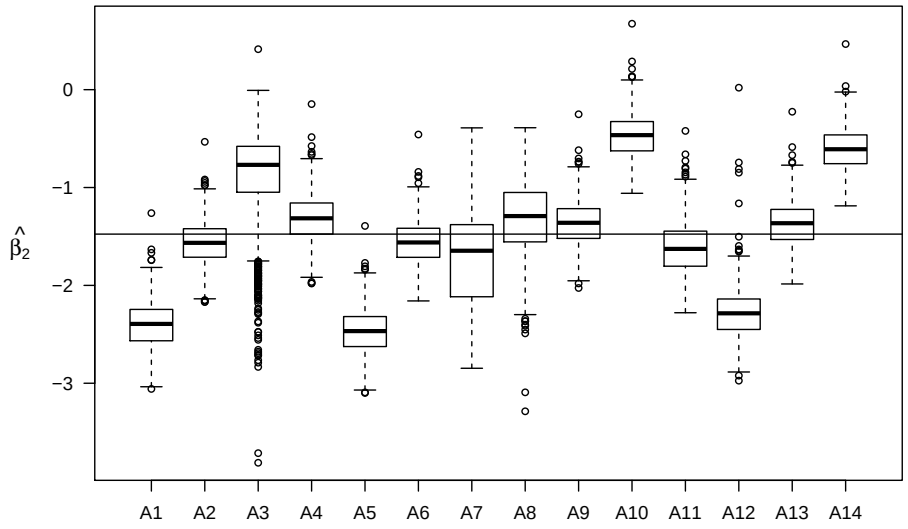


**Figure 4.6:** Box plots for point estimates for $\beta_2$ by each test chamber assignment plan. The horizontal line indicates the true parameter value.

it is not unusual that those plans have good performances. On the other hand, one can see that the variances of regression coefficients estimates of A7 and A8 are consistently larger than those of other plans. This can be seen as an impact of non-zero estimates of the variance component; that is, since A7 and A8 can detect the random effects, these plans may also harbor more uncertainty for regression coefficients.

Overall, the MSE of regression coefficients estimates for each assignment plan are shown in Table 4.4. It shows A4 and A11 are also competitive assignment plans (in terms of $\hat{\boldsymbol{\beta}}$) as well as A7 or A8. While A7 and A8 assign two stress conditions to each test chamber, A4 and A11 assign three stress conditions to one of test chamber and a remaining one to the other test chamber. In next section, we consider these two different cases to find the optimal test plan.

**Table 4.4:** Mean squared error of $\hat{\boldsymbol{\beta}}$

| Chamber Assignment | $\sum(\mathbb{E}[\hat{\beta}] - \beta)^2$ | $\sum \text{var}(\hat{\beta})$ | $MSE$ |
|---|---|---|---|
| A1 | 2.38 | 0.24 | 2.62 |
| A2 | 1.40 | 0.19 | 1.59 |
| A3 | 0.48 | 0.56 | 1.04 |
| A4 | 0.29 | 0.29 | 0.58 |
| A5 | 1.25 | 0.19 | 1.44 |
| A6 | 2.20 | 0.24 | 2.44 |
| A7 | 0.19 | 0.65 | 0.84 |
| A8 | 0.07 | 0.47 | 0.55 |
| A9 | 1.94 | 0.19 | 2.13 |
| A10 | 1.25 | 0.23 | 1.48 |
| A11 | 0.18 | 0.39 | 0.57 |
| A12 | 0.88 | 0.21 | 1.09 |
| A13 | 1.42 | 0.22 | 1.65 |
| A14 | 2.05 | 0.19 | 2.24 |

## 4.4 *D*-optimal Test Plan with Test Chamber Effect

Because the two-phase approach determines decision variables in two separated steps, the outcome is not optimal as a whole. Furthermore, it requires investigation of candidate designs by a simulation study, which is time-consuming. In this section, a completely integrated approach to create the optimal ALT plan with test chamber effects is established, where all required decision variables are determined simultane-

ously. We exploit the GLMM formulation established in Subsection 4.2.2 to find the optimal design.

Though related work on optimal designs under GLMM is sparsely found in the literature, they make a substantial contribution to our study. Among others, the method used in this section is similar to that of Niaparast (2009), where the information matrix based on quasi-likelihood is utilized with the marginalized mean and variance-covariance matrix of the response variable in GLMM. Hassler (2015) illustrates optimal designs for GLM with random blocks via several possible design criteria, and shows that the quasi-likelihood based approach is superior to the other criteria. While Niaparast (2009) presumes the crossed design case with a single variable, we apply the method to the nested design with multiple variables. The number of stress conditions is fixed by four (i.e., $m = 4$) because it is the smallest number of supporting points to detect the non-zero variance component, as discussed in Section 4.3.

### *4.4.1 Variance-covariance Structure*

The marginalized mean and variance of $c_{ij(k)}$ in Eq. (4.4) are given, respectively, by

$$\mu^*_{ij} = E\left[c_{ij(k)}\right] = \exp\left(\mathbf{x}'_{j(k)}\boldsymbol{\beta} + \sigma^2_U/2\right) t^{\alpha}_{ij(k)}, \tag{4.7}$$

$$\text{var}\left(c_{ij(k)}\right) = \mu^*_{ij} + {\mu^*_{ij}}^2 \xi, \tag{4.8}$$

where $\xi = e^{\sigma^2_U} - 1$. We use the notation $\mu^*_{ij}$ for the marginalized mean instead of $\mu^*_{ij(k)}$ since it does not depend on a specific test chamber. As the mean is unequal to the variance, $c_{ij(k)}$ is no longer the Poisson random variable. The covariance of two observations within the same test chamber is given by

$$\text{cov}\left(c_{ij(k)}, c_{i'j'(k)}\right) = \mu^*_{ij}\mu^*_{i'j'}\xi, \quad \forall ij(k) \neq i'j'(k) \tag{4.9}$$

Also, $\mathrm{cov}\left(c_{ij(k)}, c_{i'j'(k')}\right) = 0,\ \forall k \neq k'$. The derivation of Eq. (4.7), (4.8) and (4.9) are inserted in Appendix B. Let $j = \{1,2,3,4\}$; then, without loss of generality, the way to assign two test chambers is either $j(1) = \{1\}, j(2) = \{2,3,4\}$ or $j(1) = \{1,2\}, j(2) = \{3,4\}$. Accordingly the marginal variance-covariance matrix of $c_{ij(k)}$ is given as either

$$\mathbf{V1} = \begin{bmatrix} \mathbf{V_{(1)}} & \mathbf{0} \\ \mathbf{0} & \mathbf{V_{(2)}} \end{bmatrix} = \begin{bmatrix} \mathbf{V_{11}} & \mathbf{0} & \mathbf{0} & \mathbf{0} \\ & \mathbf{V_{22}} & \mathbf{V_{23}} & \mathbf{V_{24}} \\ & & \mathbf{V_{33}} & \mathbf{V_{34}} \\ sym & & & \mathbf{V_{44}} \end{bmatrix}, \tag{4.10}$$

or

$$\mathbf{V2} = \begin{bmatrix} \mathbf{V_{(1)}} & \mathbf{0} \\ \mathbf{0} & \mathbf{V_{(2)}} \end{bmatrix} = \begin{bmatrix} \mathbf{V_{11}} & \mathbf{V_{12}} & \mathbf{0} & \mathbf{0} \\ & \mathbf{V_{22}} & \mathbf{0} & \mathbf{0} \\ & & \mathbf{V_{33}} & \mathbf{V_{34}} \\ sym & & & \mathbf{V_{44}} \end{bmatrix}, \tag{4.11}$$

where $\mathbf{V_{(k)}}, k = 1,2$ is the variance-covariance matrix of observations in $k$th test chamber, and $\mathbf{V_{jj'}}$ is given by

$$\mathbf{V_{jj'}} = \begin{bmatrix} \mu^*_{1j} + {\mu^*_{1j}}^2\xi & {\mu^*_{1j}}^2\xi & \cdots & {\mu^*_{1j}}^2\xi \\ {\mu^*_{2j}}^2\xi & \mu^*_{2j} + {\mu^*_{2j}}^2\xi & \cdots & {\mu^*_{2j}}^2\xi \\ \vdots & \vdots & \ddots & \vdots \\ {\mu^*_{n_jj}}^2\xi & {\mu^*_{n_jj}}^2\xi & \cdots & \mu^*_{n_jj} + {\mu^*_{n_jj}}^2\xi \end{bmatrix}, \quad \mathbf{j} = \mathbf{j'}, \tag{4.12}$$

$$\mathbf{V_{jj'}} = \begin{bmatrix} \mu^*_{1j}\mu^*_{1j'}\xi & \mu^*_{1j}\mu^*_{2j'}\xi & \cdots & \mu^*_{1j}\mu^*_{n_{j'}j'}\xi \\ \mu^*_{2j}\mu^*_{1j'}\xi & \mu^*_{2j}\mu^*_{2j'}\xi & \cdots & \mu^*_{2j}\mu^*_{n_{j'}j'}\xi \\ \vdots & \vdots & \ddots & \vdots \\ \mu^*_{n_jj}\mu^*_{1j'}\xi & \mu^*_{n_jj}\mu^*_{2j'}\xi & \cdots & \mu^*_{n_jj}\mu^*_{n_{j'}j'}\xi \end{bmatrix}, \quad \mathbf{j} \neq \mathbf{j'}. \tag{4.13}$$

In Eq. (4.7), the marginal mean depends on the failure time observation $t_{ij(k)}$, yet it is not available in design phase. Therefore, we replace $\mu^*_{ij}$ with its expected value.

That is,

$$\begin{aligned}\mu_{ij}^{*} &= \mathbb{E}\left[\exp\left(\mathbf{x}'_{j(k)}\boldsymbol{\beta}+\sigma_U^2/2\right)t_{ij(k)}^{\alpha}\right] \\ &= \exp\left(\mathbf{x}'_{j(k)}\boldsymbol{\beta}+\sigma_U^2/2\right)\mathbb{E}\left[\frac{1-\exp\left(-e^{\mathbf{x}'_{j(k)}\boldsymbol{\beta}+U}t_c^{\alpha}\right)}{e^{\mathbf{x}'_{j(k)}\boldsymbol{\beta}+U}}\right], \end{aligned} \tag{4.14}$$

where $t_c$ is the censoring time. For the derivation of Eq. (4.14), see Appendix B. The expected value in Eq. (4.14) can be calculated by Monte Carlo sampling as follows:

$$\mathbb{E}\left[\frac{1-\exp\left(-e^{\mathbf{x}'_{j(k)}\boldsymbol{\beta}+U}t_c^{\alpha}\right)}{e^{\mathbf{x}'_{j(k)}\boldsymbol{\beta}+U}}\right] = \frac{1}{M}\sum_{r=1}^{M}\frac{1-\exp\left(-e^{\mathbf{x}'_{j(k)}\boldsymbol{\beta}+u_r}t_c^{\alpha}\right)}{e^{\mathbf{x}'_{j(k)}\boldsymbol{\beta}+u_r}} \tag{4.15}$$

where $u_1, u_2, \ldots, u_M$ are random draws from $N(0, \sigma_U^2)$. Now $\mu_{1j}^{*} = \ldots = \mu_{n_j j}^{*} = \mu_j^{*}$, and hence Eq. (4.12) and (4.13) can be expressed as

$$\mathbf{V_{jj'}} = \begin{cases} \mu_j^{*}\mathbf{I}_{n_j} + \xi\mu_j^{*2}\mathbf{1}_{n_j}\mathbf{1}'_{n_j}, & \mathbf{j} = \mathbf{j'} \\ \xi\mu_j^{*}\mu_{j'}^{*}\mathbf{1}_{n_j}\mathbf{1}'_{n'_j}, & \mathbf{j} \neq \mathbf{j'} \end{cases}$$

where $\mathbf{I}_{n_j}$ denotes the $n_j \times n_j$ identity matrix and $\mathbf{1}_{n_j}$ is the $n_j \times 1$ vector with all entries equal to 1. Consequently Eq. (4.10) and (4.11) can be written as

$$\mathbf{V1} = \begin{bmatrix} \mu_1^{*}\mathbf{I}_{n_1} + \xi\mu_1^{*2}\mathbf{1}_{n_1}\mathbf{1}'_{n_1} & & \mathbf{0} \\ & \begin{bmatrix} \mu_2^{*}\mathbf{I}_{n_2} & \mathbf{0} & \mathbf{0} \\ \mathbf{0} & \mu_3^{*}\mathbf{I}_{n_3} & \mathbf{0} \\ \mathbf{0} & \mathbf{0} & \mu_4^{*}\mathbf{I}_{n_4} \end{bmatrix} + \xi \begin{bmatrix} \mu_2^{*}\mathbf{1}_{n_2} \\ \mu_3^{*}\mathbf{1}_{n_3} \\ \mu_4^{*}\mathbf{1}_{n_4} \end{bmatrix} \begin{bmatrix} \mu_2^{*}\mathbf{1}'_{n_2} & \mu_3^{*}\mathbf{1}'_{n_3} & \mu_4^{*}\mathbf{1}'_{n_4} \end{bmatrix} \end{bmatrix}$$

$$\mathbf{V2} = \begin{bmatrix} \begin{bmatrix} \mu_1^{*}\mathbf{I}_{n_1} & \mathbf{0} \\ \mathbf{0} & \mu_2^{*}\mathbf{I}_{n_2} \end{bmatrix} + \xi \begin{bmatrix} \mu_1^{*}\mathbf{1}_{n_1} \\ \mu_2^{*}\mathbf{1}_{n_2} \end{bmatrix} \begin{bmatrix} \mu_1^{*}\mathbf{1}'_{n_1} & \mu_2^{*}\mathbf{1}'_{n_2} \end{bmatrix} & & \mathbf{0} \\ & \begin{bmatrix} \mu_3^{*}\mathbf{I}_{n_3} & \mathbf{0} \\ \mathbf{0} & \mu_4^{*}\mathbf{I}_{n_4} \end{bmatrix} + \xi \begin{bmatrix} \mu_3^{*}\mathbf{1}_{n_3} \\ \mu_4^{*}\mathbf{1}_{n_4} \end{bmatrix} \begin{bmatrix} \mu_3^{*}\mathbf{1}'_{n_3} & \mu_4^{*}\mathbf{1}'_{n_4} \end{bmatrix} \end{bmatrix}$$

### 4.4.2 D-optimality Criteria

The unconditioned $c_{ij(k)}$'s do not follow any standard probability distribution, yet we know the mean and the variance of those. In this case the following quasi-score function can be used to estimate the unknown parameters (Myers *et al.*, 2012).

$$\mathbf{D}'\mathbf{V}^{-1}(\mathbf{c}-\boldsymbol{\mu})=\mathbf{0},$$

where $\mathbf{c}$ is $n\times 1$ vector of $c_{ij(k)}$, $\boldsymbol{\mu}$ is the vector of means, $\mathbf{V}$ is $n\times n$ variance-covariance matrix, and $\mathbf{D}$ is $n\times(p+1)$ matrix of derivatives given as

$$\mathbf{D}=\frac{d\boldsymbol{\mu}}{d\boldsymbol{\beta}}=\frac{d\boldsymbol{\mu}}{d\boldsymbol{\eta}}\frac{d\boldsymbol{\eta}}{d\boldsymbol{\beta}}=\boldsymbol{\Delta}\mathbf{X},$$

where $\boldsymbol{\eta}$ is the vector of linear predictor $\eta_{j(k)}$'s in Eq. (4.2), $\boldsymbol{\Delta}=\text{diag}\{\mu_1^*\mathbf{1}'_{n_1},\mu_2^*\mathbf{1}'_{n_2},\mu_3^*\mathbf{1}'_{n_3},\mu_4^*\mathbf{1}'_{n_4}\}$ is the diagonal matrix of the marginal mean of each observation, and $\mathbf{X}$ is the $n\times(p+1)$ design matrix. The information matrix of the quasi-score function is given by

$$\mathbf{D}'\mathbf{V}^{-1}\mathbf{D}=\mathbf{X}'\boldsymbol{\Delta}\mathbf{V}^{-1}\boldsymbol{\Delta}\mathbf{X}.$$

Let $\psi_1$ and $\psi_2$ be, namely, aggregated designs, which are vectors containing decision variables defining design matrix $\mathbf{X}$ (and $\boldsymbol{\Delta}$, $\mathbf{V}$ as well) with variance-covariance structure $\mathbf{V1}$ and $\mathbf{V2}$, respectively. That is,

$$\psi_1=\begin{bmatrix}x^1_{1(1)} & x^2_{1(1)} & p_1\\ x^1_{2(2)} & x^2_{2(2)} & p_2\\ x^1_{3(2)} & x^2_{3(2)} & p_3\\ x^1_{4(2)} & x^2_{4(2)} & p_4\end{bmatrix},\quad \psi_2=\begin{bmatrix}x^1_{1(1)} & x^1_{1(1)} & p_1\\ x^1_{2(1)} & x^1_{2(1)} & p_2\\ x^1_{3(2)} & x^1_{3(2)} & p_3\\ x^1_{4(2)} & x^1_{4(2)} & p_4\end{bmatrix} \tag{4.16}$$

where $0<p_j<1, j=1,2,3,4$ are proportions of test unit allocations for corresponding stress conditions, and $\sum_{j=1}^4 p_j=1$. Note that the order of each row in $\psi_1$ and $\psi_2$ determines the test chamber assignment. For instance, in $\psi_2$, stress conditions at the

first two rows are assigned to the same test chamber and those at the last two rows are assigned to the other test chamber.

The $D$-optimal design is selected as follows.

$$\psi^* = \begin{cases} \psi_1^*, & \text{if } f_1(\psi_1^*) > f_2(\psi_2^*) \\ \psi_2^*, & \text{otherwise} \end{cases}$$

where $\psi_1^* := \arg\max_{\psi_1} f_1(\psi_1) = |\mathbf{X}'\mathbf{\Delta}\mathbf{V1}^{-1}\mathbf{\Delta}\mathbf{X}|$, and $\psi_2^* := \arg\max_{\psi_2} f_2(\psi_2) = |\mathbf{X}'\mathbf{\Delta}\mathbf{V2}^{-1}\mathbf{\Delta}\mathbf{X}|$. That is, two candidate $D$-optimal designs with different variance-covariance matrix structures in Eq. (4.10) and (4.11) are created first, and one of them with the higher determinant is chosen as the final $D$-optimal design.

### *4.4.3 Information Matrix*

We apply Niaparast (2009) for the evaluation of the objective function, which simplifies the calculation of information matrix by avoiding the matrix inversion, and restricts the decision variables to the desired form as in Eq. (4.16). Applying block diagonal structure of $\mathbf{V}$ as in Eq. (4.10) or (4.11), we obtain

$$\begin{aligned} \mathbf{X}'\mathbf{\Delta}\mathbf{V}^{-1}\mathbf{\Delta}\mathbf{X} &= \mathbf{X}'\mathbf{\Delta} \begin{bmatrix} \mathbf{V_{(1)}} & \mathbf{0} \\ \mathbf{0} & \mathbf{V_{(2)}} \end{bmatrix}^{-1} \mathbf{\Delta}\mathbf{X} \\ &= \mathbf{X_{(1)}}'\mathbf{\Delta_{(1)}}{\mathbf{V}_{(1)}}^{-1}\mathbf{\Delta_{(1)}}\mathbf{X_{(1)}} + \mathbf{X_{(2)}}'\mathbf{\Delta_{(2)}}{\mathbf{V}_{(2)}}^{-1}\mathbf{\Delta_{(2)}}\mathbf{X_{(2)}} \\ &= \mathbf{IM}_{(1)} + \mathbf{IM}_{(2)} \end{aligned}$$

where $\mathbf{X_{(k)}}$ and $\mathbf{\Delta_{(k)}}$ are the sub-matrices of $\mathbf{X}$ and $\mathbf{\Delta}$, respectively, corresponding to $k$th test chamber, and $\mathbf{IM}_{(k)} = \mathbf{X_{(k)}}'\mathbf{\Delta_{(k)}}{\mathbf{V_{(k)}}}^{-1}\mathbf{\Delta_{(k)}}\mathbf{X_{(k)}}$ denotes the information matrix from the observations of $k$th test chamber. Using this notation, $\mathbf{V_{(k)}}$ can be rewritten as $\mathbf{V_{(k)}} = \mathbf{\Delta_{(k)}} + \xi \text{diag}(\mathbf{\Delta_{(k)}})\text{diag}(\mathbf{\Delta_{(k)}})'$, where $\text{diag}(\mathbf{\Delta_{(k)}})$ denotes the vector of diagonal elements of $\mathbf{\Delta_{(k)}}$; and, it can be shown that (Lemma 3.1. in

Niaparast, 2009),

$$\mathbf{IM}_{(k)} = \mathbf{X_{(k)}}' \left( \mathbf{\Delta_{(k)}}^{-1} + \xi \mathbf{1}_{n_{(k)}} \mathbf{1}'_{n_{(k)}} \right)^{-1} \mathbf{X_{(k)}} \tag{4.17}$$

where $n_{(k)}$ is the number of test units in $k$th test chamber. Let $\tilde{\mathbf{X}} = (\mathbf{x}_1, \ldots, \mathbf{x}_m)'$ be the $m \times 1$ aggregated design matrix neglecting the number of test units; and $\tilde{\mathbf{\Delta}} = \text{diag}\{n_1\mu_1^*, \ldots, n_m\mu_m^*\}$. Then Eq. (4.17) can be further simplified as (Lemma 3.2. in Niaparast, 2009)

$$\mathbf{IM}_{(k)} = \tilde{\mathbf{X}}'_{(k)} \left( \tilde{\mathbf{\Delta}}_{(k)} - \frac{\xi \tilde{\mathbf{\Delta}}_{(k)} \mathbf{1}_{m_{(k)}} \mathbf{1}'_{m_{(k)}} \tilde{\mathbf{\Delta}}_{(k)}}{1 + \xi \mathbf{1}'_{m_{(k)}} \tilde{\mathbf{\Delta}}_{(k)} \mathbf{1}_{m_{(k)}}} \right) \tilde{\mathbf{X}}_{(k)}$$

where $m_{(k)}$ denotes the number of stress conditions nested in $k$th test chamber. Lastly $n_1, \ldots, n_m$ in $\tilde{\mathbf{\Delta}}$ are replaced by $np_1, \ldots, np_m$ so that decision variables are all continuous.

### *4.4.4 Implementation and Results*

We implement the quasi-likelihood approach for the optimal ALT plan of an example introduced early in this section using R. The initial values of stress conditions in the aggregated design are randomly selected within the range $(0, 1)$; and the proportions of those conditions are produced as follows, so that those are all positive and sum to 1:

$$p_1 = a_1,\ p_2 = a_2 - a_1,\ p_3 = a_3 - a_2,\ p_4 = 1 - a_3,$$

where $a_1 < a_2 < a_3$ are sorted samples from $(0, 1)$. The method "L-BFGS-B" (Byrd *et al.*, 1995) is used for the optimization routines with feasible region $(0, 1)$ for each decision variable. We use $M = 1,000,000$ samples for calculation of Monte Carlo integration in Eq. (4.15) whenever the objective function is evaluated.

Table 4.5 shows $D$-optimal design for the same example discussed in the two-phased approach ($\sigma_U^2 = 0.25$). We found that $f_2(\psi_2^*) > f_1(\psi_1^*)$ and hence $\psi^* = \psi_2^*$.

**Table 4.5:** $D$-optimal test plan with $\sigma_U^2 = 0.25$

| Test chamber | Design | Temperature | | Humidity | | Allocation |
|---|---|---|---|---|---|---|
| Assignment | Point | Actual | Coded | Actual | Coded | |
| $k$ | $j$ | °C | $x_1$ | RH | $x_2$ | $n_j$ |
| 1 | 1 | 110.00 | 0.000 | 90.00 | 0.000 | 22 |
| 1 | 2 | 84.13 | 0.482 | 60.00 | 1.000 | 27 |
| 2 | 3 | 110.00 | 0.000 | 60.00 | 1.000 | 21 |
| 2 | 4 | 65.88 | 0.867 | 90.00 | 0.000 | 30 |

Accordingly first two rows and last two rows in $\psi^*$, respectively, are assigned to the same test chamber as shown from the first column of the table. Figure 4.7 shows the design plot of the test plan. One can see that stress conditions located in diagonal direction are assigned to the same test chamber, which validates the results of the simulation study from the two-phased approach. Although the stress conditions look similar with the $D$-optimal design without consideration of test chamber effects in Figure 4.2, there are big discrepancies in the test unit allocations. While the design in Figure 4.2 does not allocate many test units to the lowest stress level ($n_4 = 8$), the design in Figure 4.7 allocates 27 test units to the lowest stress condition so that the test units are allocated to each test chamber with more balance. This balanced test unit allocation greatly increases the determinant of the information matrix. It turns out that the objective function value of the design in Figure 4.2 with test chamber assignment plan A7 (or A8) is only 785, while that of the design in Figure 4.7 is about $1,500$.

We also create $D$-optimal test plans for different magnitudes of the variance components. Figure. 4.8 through 4.10 show those with $\sigma_U^2 = 0.10, 0.40$ and $0.50$, respec-

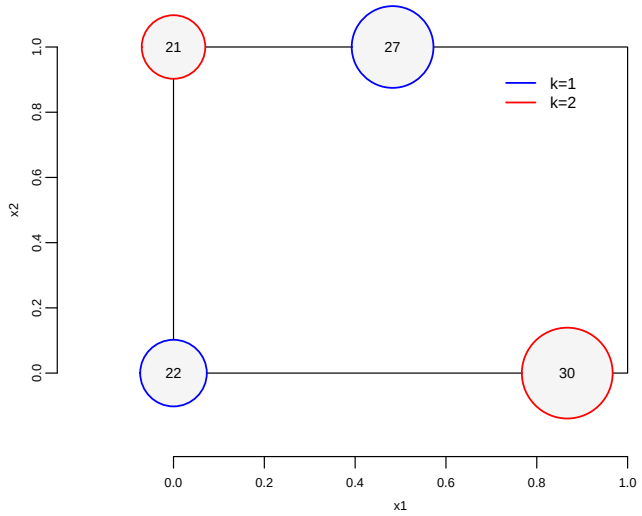


**Figure 4.7:** Design plot of $D$-optimal test plan with $\sigma_U^2 = 0.25$

tively. It seems there is no big difference between these test plans, and therefore this design is robust to the magnitude of chamber-to-chamber variations.

Finally, to validate the $D$-optimal test plan's performance, we conducted a simulation study in the same way as in Subsection 4.3.2. Figure 4.11 shows box plots of $1,000$ estimates for each parameters. For comparison, the four test plans using the two-phased approach with best performance (smallest MSE) are displayed together. For all parameters, the $D$-optimal test plan shows the most smallest bias and the smaller or similar variance. Numerically, the MSE for $\hat{\sigma}_U^2$ of $D$-optimal test plan is 0.0144, and the MSE for $\hat{\boldsymbol{\beta}}$ is 0.24, which are the smallest, in both cases, than any other test plans created by the two-phase approach. Especially, in terms of the variance component, the $D$-optimal test plan is notably superior than the other plans, which implies that it is a good design not only for the regression coefficients estimates but also for the random effects of test chambers.

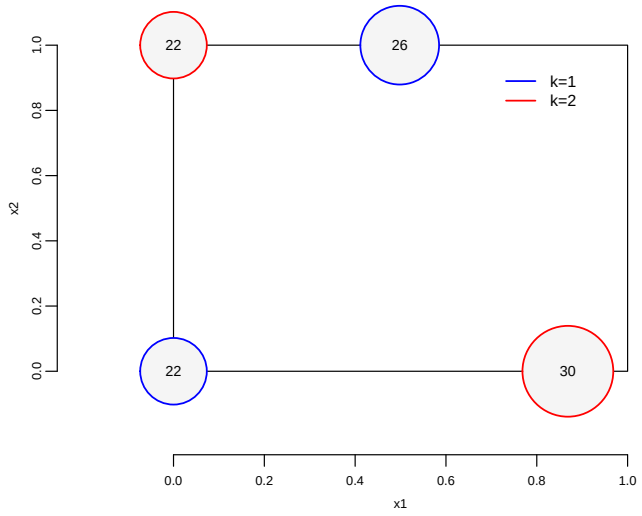


**Figure 4.8:** Design plot of $D$-optimal test plan with $\sigma_U^2 = 0.10$

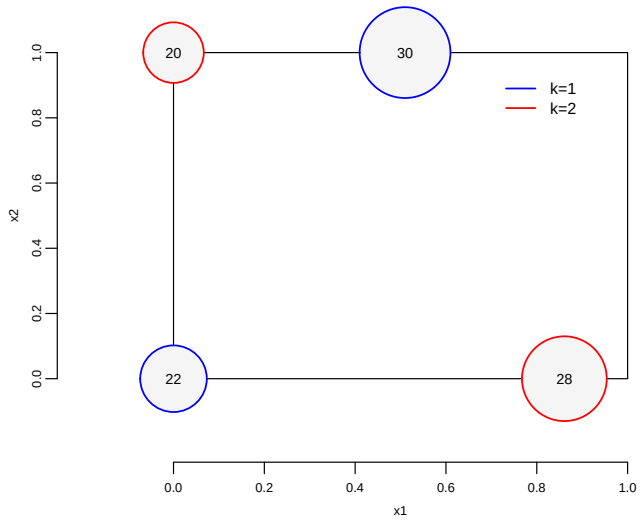


**Figure 4.9:** Design plot of $D$-optimal test plan with $\sigma_U^2 = 0.40$

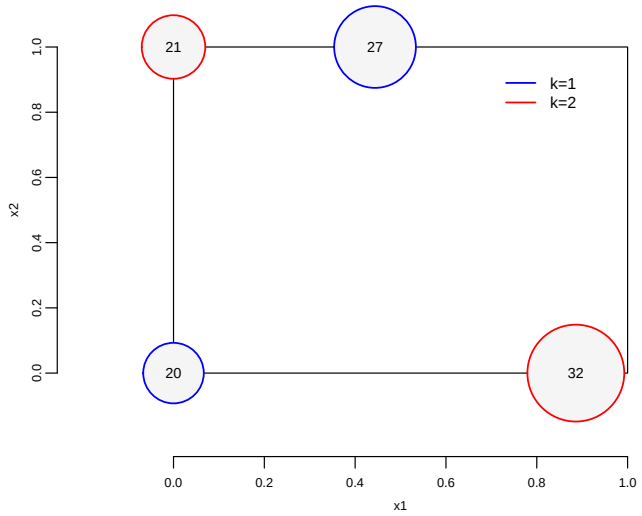


**Figure 4.10:** Design plot of $D$-optimal test plan with $\sigma_U^2 = 0.50$

## 4.5 Conclusion

In this chapter, the problem of planning ALTs under the nested design structure with two heterogeneous test chambers is considered. From the two-phase approach, where decisions on stress conditions along with those test unit allocations and the test chamber assignment are made separately, we paint a picture of how much the test chamber assignment may affect on the estimation of unknown parameters. Then we establish the integrated approach to determine all decision variables simultaneously to build $D$-optimal ALT plan using GLMM and quasi-likelihood techniques, which achieves the remarkable design with smaller bias and variance of the parameter estimates.

There exist apparent opportunities to evolve and expand this research. First, as appeared in other optimal design problems with non-linear regression models, the GLMM approach proposed in this chapter also suffers from the design dependence problem, that is, the information matrix is a function of model parameters, which are

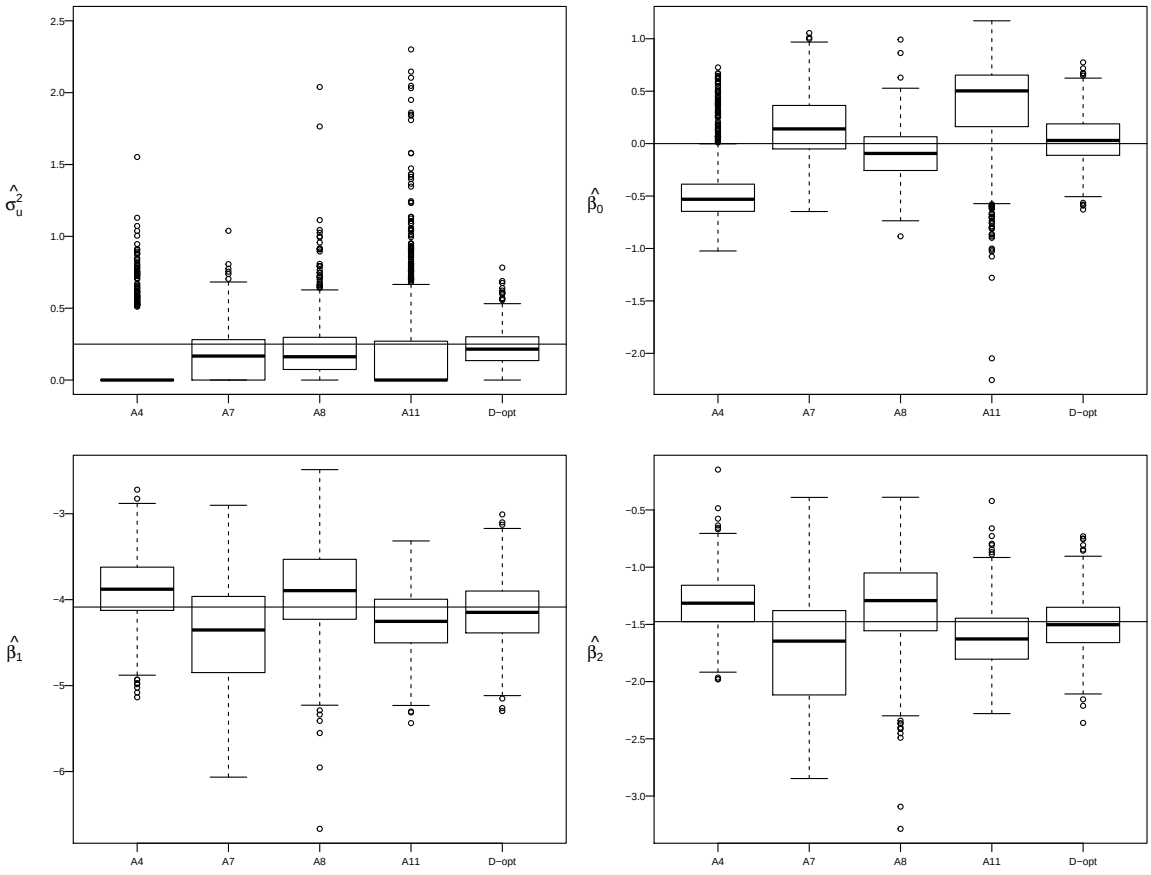


**Figure 4.11:** Parameter estimates of $D$-optimal design

unknown in general. For ALT planning, it is a common practice to presume these parameter values from similar products' experiments or engineers' knowledge, and perform a study to see how different parameter values affect the test plan. Although sensitivity analysis with different values of $\sigma_U^2$ is shown in this chapter, more comprehensive analysis including other parameters (e.g., the shape parameter) are required. Second, more various types of heterogeneity involved in life tests could be taken into account for planning ALTs. The test chamber effects may not be the only source to give rise to correlated observations. For instance, test units manufactured by batch process or different materials may cause correlation between observations from the

same batch or same material. Lastly, different types of censoring or optimality criteria could be studied.

Chapter 5

# PLANNING ACCELERATED LIFE TESTS WITH MULTIPLE SOURCES OF RANDOM EFFECTS

In this chapter, another source of random effects – suppliers of test units – is assumed in addition to the random effects of test chambers. In this case, a crossed structure of suppliers is added to the nested structure of test chambers in the experimental design. The $D$-optimal ALT test plan is constructed by the quasi-likelihood approach. The iterative procedure of three steps of optimization algorithm is developed to determine the test chamber assignment, the number of test unit allocations, and the test locations. The result shows that the $D$-optimal design can be obtained by equally allocating test units of each supplier to test locations.

## 5.1 Introduction

In the previous chapter, the $D$-optimal ALT test plan with test chamber effects was obtained by using the quasi-likelihood approach. The corresponding experimental protocol is a subsampling plan where several test units are located at the same test chamber. Another type of experimental protocol which leads to the grouped structure in reliability tests is a random block. In real applications, test units might be manufactured in different manufacturing batches or supplied by different suppliers. In these cases, test units from the same manufacturer or supplier produce another group structure in addition to the one by the test chamber, and it leads to an additional source of random effects. For more about the experimental protocols in reliability tests, see Vining (2013).

In this chapter, expanding the previous chapter, we consider multiple sources of random effects, which are different test chambers and suppliers, for the optimal ALT planning. Suppose we have the following assumptions in addition to those in Chapter 4.

- Test units are supplied by two different manufacturers.
- The total number of test units is given as $n$, but no restriction is assumed for the number of test units provided by each manufacturer. That is, we assume each manufacturer is capable of supplying any number of test units suggested by the optimal design.
- The supplier's effect is assumed to be random.

Figure 5.1 illustrates the group structures of these two sources of random effects. Whereas the test units at the same stress conditions are nested in one of two test chambers, the test units from different suppliers can be placed on the same stress condition, which adds the crossed structure of suppliers to the nested structure of test chambers.

## 5.2 Quasi-likelihood Approach

### *5.2.1 Modeling ALT Data with Multiple Random Effects*

The ALT data with multiple random effects is modeled by GLMM similarly as in the previous chapter, but with an additional random effect term. We introduce two independent random variables, $U^c$ and $U^s$, to reflect the random effects due to test

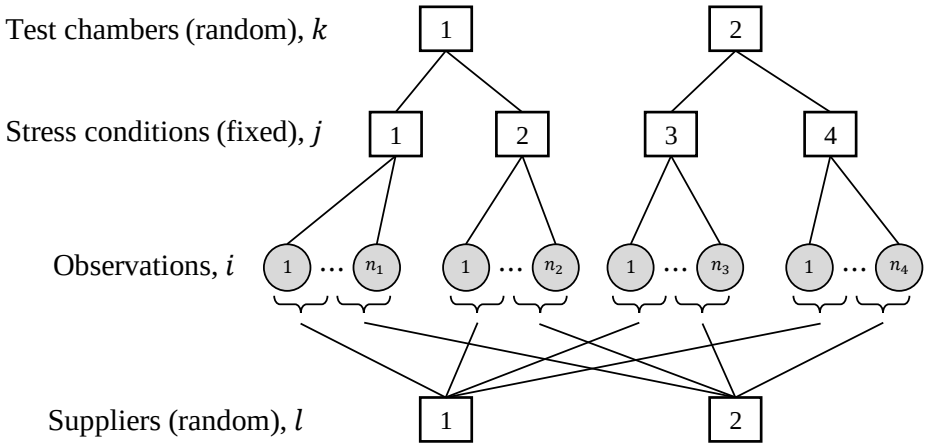


**Figure 5.1:** Nested and crossed structure of ALT plan with random test chamber effects and random supplier effects

chambers and suppliers, respectively. That is,

$$U_k^c \sim \text{i.i.d. } N(0, \sigma_{U^c}^2), k = 1, 2,$$

$$U_l^s \sim \text{i.i.d. } N(0, \sigma_{U^s}^2), l = 1, 2,$$

$$\text{cov}\,(U_k^c, U_l^s) = 0,\ \forall k, l$$

where $\sigma_{U^c}^2$ and $\sigma_{U^s}^2$ are, respectively, variance components of chamber effects and supplier effects. The conditional failure time distribution is given as

$$t_{ij(k)l} | U_k^c, U_l^s \sim \text{ind.} Weibull(\lambda_{j(k)l}, \alpha),$$

where $\lambda_{j(k)l}$ is defined as

$$\log \lambda_{j(k)l} = \eta_{j(k)l} = \mathbf{x}'_{j(k)}\boldsymbol{\beta} + u_k^c + u_l^s$$

and it can be rewritten, using matrix notation, as

$$\boldsymbol{\eta} = \mathbf{X}\boldsymbol{\beta} + \mathbf{Z}\boldsymbol{u}$$

or

$$\begin{bmatrix} \eta_{1(1)1} \\ \eta_{2(1)1} \\ \eta_{3(2)1} \\ \eta_{4(2)1} \\ \eta_{1(1)2} \\ \eta_{2(1)2} \\ \eta_{3(2)2} \\ \eta_{4(2)2} \end{bmatrix} = \begin{bmatrix} 1 & x^1_{1(1)} & x^2_{1(1)} \\ 1 & x^1_{2(1)} & x^2_{2(1)} \\ 1 & x^1_{3(2)} & x^2_{3(2)} \\ 1 & x^1_{4(2)} & x^2_{4(2)} \\ 1 & x^1_{1(1)} & x^2_{1(1)} \\ 1 & x^1_{2(1)} & x^2_{2(1)} \\ 1 & x^1_{3(2)} & x^2_{3(2)} \\ 1 & x^1_{4(2)} & x^2_{4(2)} \end{bmatrix} \begin{bmatrix} \beta_0 \\ \beta_1 \\ \beta_2 \end{bmatrix} + \begin{bmatrix} 1 & 0 & 1 & 0 \\ 1 & 0 & 1 & 0 \\ 0 & 1 & 1 & 0 \\ 0 & 1 & 1 & 0 \\ 1 & 0 & 0 & 1 \\ 1 & 0 & 0 & 1 \\ 0 & 1 & 0 & 1 \\ 0 & 1 & 0 & 1 \end{bmatrix} \begin{bmatrix} u^c_1 \\ u^c_2 \\ u^s_1 \\ u^s_2 \end{bmatrix}$$

By a similar argument as in the previous chapter, we can treat the indicator variable for censoring as if

$$c_{ij(k)l} | U^c_k, U^s_l \sim \text{ind. } Poisson(\mu_{ij(k)l}),$$

where $\mu_{ij(k)l} = \mathbb{E}\left[c_{ij(k)l} | U^c_k, U^s_k\right]$ is the conditional mean of the Poisson distribution.

### *5.2.2 Information Matrix*

It can be shown that the marginal mean of $c_{ij(k)l}$ is given as

$$\begin{aligned} \mu^*_{ij(k)l} &= \mathbb{E}\left[c_{ij(k)l}\right] \\ &= \exp\left(\mathbf{x}'_{j(k)}\boldsymbol{\beta} + \frac{\sigma^2_{U^c} + \sigma^2_{U^s}}{2}\right) t^\alpha_{ij(k)l} \end{aligned}$$

As in the previous chapter, $t^\alpha_{ij(k)l}$ is replaced by its expected value, which is,

$$\mathbb{E}\left[t^\alpha_{ij(k)l}\right] = \mathbb{E}\left[\frac{1 - \exp\left(-e^{\mathbf{x}'_{j(k)}\boldsymbol{\beta} + U^c + U^s} t^\alpha_c\right)}{e^{\mathbf{x}'_{j(k)}\boldsymbol{\beta} + U^c + U^s}}\right],$$

and it is calculated by a large number of samples of two random effects from the following distribution.

$$\begin{bmatrix} u^c \\ u^s \end{bmatrix} \sim N_2\left(\begin{bmatrix} 0 \\ 0 \end{bmatrix}, \quad \begin{bmatrix} \sigma^2_{U^c} & 0 \\ 0 & \sigma^2_{U^s} \end{bmatrix}\right) \tag{5.1}$$

The marginal variance is given as

$$\text{var}\left(c_{ij(k)l}\right) = \mu^*_{ij(k)l} + {\mu^*_{ij(k)l}}^2\xi,$$

where $\xi = e^{\sigma^2_{U^c}+\sigma^2_{U^s}} - 1$. Accordingly the covariances of two observations are given as

$$\begin{aligned}
\text{cov}\left(c_{ij(k)l}, c_{i'j'(k)l}\right) &= \mu^*_{ij}\mu^*_{i'j'}\xi, \quad \forall ij(k)l \neq i'j'(k)l \\
\text{cov}\left(c_{ij(k)l}, c_{i'j'(k')l}\right) &= \mu^*_{ij}\mu^*_{i'j'}\xi_s, \quad \forall ij(k)l \neq i'j'(k')l \\
\text{cov}\left(c_{ij(k)l}, c_{i'j'(k)l'}\right) &= \mu^*_{ij}\mu^*_{i'j'}\xi_c, \quad \forall ij(k)l \neq i'j'(k)l' \\
\text{cov}\left(c_{ij(k)l}, c_{i'j'(k')l'}\right) &= 0, \quad \forall ij(k)l \neq i'j'(k')l'
\end{aligned}$$

where $\xi_s = e^{\sigma^2_{U^s}} - 1$ and $\xi_c = e^{\sigma^2_{U^c}} - 1$.

Let $n$ be the total number of test units and $p$ be the number of stress factors. The information matrix from the quasi-score function is given by

$$\mathbf{X}'\mathbf{\Delta}\mathbf{V}^{-1}\mathbf{\Delta}\mathbf{X} \tag{5.2}$$

where $\mathbf{X}$ is the $n \times (p+1)$ design matrix, $\mathbf{\Delta}$ is the $n \times n$ diagonal matrix of $\mu^*_{ij(k)l}$'s, and $\mathbf{V}$ is the $n \times n$ variance-covariance matrix. In Chapter 4, two different variance-covariance structures, **V1** and **V2**, according to the number of stress conditions assigned to each test chamber, were considered. The optimal design, however, was always obtained by using **V2**, in which two stress conditions were assigned to each test chamber. In this chapter, therefore, we consider only the case of $j(1) = \{1, 2\}, j(2) = \{3, 4\}$ in general. The variance-covariance matrix then is given as

$$\mathbf{V} = \begin{bmatrix}
\mathbf{V}_{(1)1} & \mathbf{V}_{(12)1} & \mathbf{V}_{(1)12} & \mathbf{0} \\
 & \mathbf{V}_{(2)1} & \mathbf{0} & \mathbf{V}_{(2)12} \\
 & & \mathbf{V}_{(1)2} & \mathbf{V}_{(12)2} \\
sym & & & \mathbf{V}_{(2)2}
\end{bmatrix} \tag{5.3}$$

where $\mathbf{V}_{(k)l}$ is the variance-covariance matrix of observations for the same test chamber and supplier, $\mathbf{V}_{(kk')l}$ is the covariance matrix of observations for the different test chamber but the same supplier, and $\mathbf{V}_{(k)ll'}$ is the one for the same test chamber but for different suppliers. Accordingly $\mathbf{\Delta}$ can be represented by

$$\mathbf{\Delta} = \begin{bmatrix} \mathbf{\Delta}_{(1)1} & & & \mathbf{0} \\ & \mathbf{\Delta}_{(2)1} & & \\ & & \mathbf{\Delta}_{(1)2} & \\ \mathbf{0} & & & \mathbf{\Delta}_{(2)2} \end{bmatrix}$$

where $\mathbf{\Delta}_{(k)l} = \text{diag}\{\mu^*_{j(k)l}\mathbf{1}'_{n_{j(k)l}}, \mu^*_{j'(k)l}\mathbf{1}'_{n_{j'(k)l}}\}$. Then

$$\begin{aligned} \mathbf{V}_{(k)l} &= \mathbf{\Delta}_{(k)l} + \xi \text{diag}\left(\mathbf{\Delta}_{(k)l}\right) \text{diag}\left(\mathbf{\Delta}_{(k)l}\right)' \\ \mathbf{V}_{(kk')l} &= \xi_s \text{diag}\left(\mathbf{\Delta}_{(k)l}\right) \text{diag}\left(\mathbf{\Delta}_{(k')l}\right)' \\ \mathbf{V}_{(k)ll'} &= \xi_c \text{diag}\left(\mathbf{\Delta}_{(k)l}\right) \text{diag}\left(\mathbf{\Delta}_{(k)l'}\right)' \end{aligned}$$

## 5.3 *D*-optimal Design Construction

### *5.3.1 Initial Design Generation*

Recall the example of ALT with two stress factors, temperature and humidity, in Chapter 4. In this section, an additional random effect term of a supplier is included in the acceleration model, that is

$$\eta_{j(k)l} = -4.086x^1_{j(k)} - 1.476x^2_{j(k)} + u^c_k + u^s_l.$$

The *D*-optimal design is constructed by selecting the locations of four stress conditions, the assignment of two test chambers, and the number of test units allocations for each combination of stress conditions and suppliers, such that the determinant of the information matrix in (5.2) is maximized. The aggregated design is defined as

the following form.

$$\psi = \begin{bmatrix} x^1_{1(1)} & x^2_{1(1)} & n_{1(1)1} \\ x^1_{2(1)} & x^2_{2(1)} & n_{2(1)1} \\ x^1_{3(2)} & x^2_{3(2)} & n_{3(2)1} \\ x^1_{4(2)} & x^2_{4(2)} & n_{4(2)1} \\ x^1_{1(1)} & x^2_{1(1)} & n_{1(1)2} \\ x^1_{2(1)} & x^2_{2(1)} & n_{2(1)2} \\ x^1_{3(2)} & x^2_{3(2)} & n_{3(2)2} \\ x^1_{4(2)} & x^2_{4(2)} & n_{4(2)2} \end{bmatrix}, \tag{5.4}$$

where $n_{j(k)l}$, $j = 1, 2, 3, 4; k = 1, 2; l = 1, 2$ represents the number of test units allocated at the $j$th stress condition, nested in the $k$th test chamber, from the $l$th supplier; and $\sum_l \sum_k \sum_j n_{j(k)l} = n$. The initial design for the input of the optimization procedure is created by randomly selecting $x^1_{j(k)}$, $x^2_{j(k)}$, $j(k) = 1(1), 2(1), 3(2), 4(2)$ from the range of $(0, 1)$. Note that the first four stress conditions in (5.4) are simply copied to the last four stress conditions. The initial values of the last column of (5.4) is generated by follows:

$$n_{1(1)1} = a_1,\ n_{2(1)1} = a_2 - a_1,\ n_{3(2)1} = a_3 - a_2,\ n_{4(2)1} = a_4 - a_3,$$

$$n_{1(1)2} = a_5 - a_4,\ n_{2(1)2} = a_6 - a_5,\ n_{3(2)2} = a_7 - a_6,\ n_{4(2)2} = n - a_7$$

where $a_1 < a_2 < a_3 < a_4 < a_5 < a_6 < a_7$ are sorted integers sampled from $(0, n)$.

### *5.3.2 Optimization*

The optimization is conducted by iterations of three separate steps as follows.

1. **Exchange the test chamber assignment**

   The first step is to find the best test chamber assignment. The first two stress conditions in the initial design are assigned to the same test chamber and the

others to the another chamber, that is $j(1) = \{1, 2\},\ j(2) = \{3, 4\}$. We evaluate the objective function for alternative test chamber assignment plans, which are $j(1) = \{1, 3\},\ j(2) = \{2, 4\}$ and $j(1) = \{1, 4\},\ j(2) = \{2, 3\}$, and choose one with the highest objective function value.

2. **Exchange the number of allocations**

   The second step is to exchange the number of test unit allocations between all pairs of stress conditions. For each pair of $n_{j(k)l}$'s in (5.4), one test unit is exchanged in a way to increase the objective value. For example, for the pair of $n_{1(1)1}$ and $n_{2(1)1}$, we consider two cases, $(n_{1(1)1} + 1, n_{2(1)1} - 1)$ and $(n_{1(1)1} - 1, n_{2(1)1} + 1)$, and evaluate the objective function for both cases. If any case produces a better objective value, the design is replaced. Once these exchanges are finished for all pairs, the entire procedure is repeated until there is no more change in the third column of the right hand side of (5.4).

3. **Optimize the stress conditions**

   The third step is to find the locations of four stress conditions which produce the best objective function value given the current test chamber assignment and the number of allocations. Since decision variables are continuous in the range of $(0, 1)$, we can use a general non-linear optimization routine. The method "L-BFGS-B" (Byrd *et al.*, 1995) provided by R is used for this purpose.

For an initial design, these three steps are repeated until there is no improvement of the objective value. This entire process is conducted multiple times with several different initial designs to find the global optimal design.

This optimization procedure can be adapted to some different cases with deviations of assumptions in Subsection 5.1. First, it can be applied to the case of more than two suppliers by extending the variance-covariance matrix in (5.3) and corre-

sponding $\mathbf{\Delta}$ matrix, which is obvious. Second, if the number of test units from each manufacturer is limited by some capacities, the second optimization step is separated to two sub-steps, one for the first supplier and the other one for the second supplier. In this case, the number of test units is only exchanged within the rows of the corresponding supplier.

## 5.4 Implementation and Results

### *5.4.1 D-optimal Test Plan*

The $D$-optimal design for the case of $\sigma^2_{U^c} = 0.25$ and $\sigma^2_{U^s} = 0.25$ was obtained by the procedure described in Subsection 5.3.2 with 10 randomly generated initial designs. The objective function was calculated by $M = 2,000,000$ samples of $(U^c, U^s)$ in Eq. (5.1). Table 5.1 and Figure 5.2 show the result. It can be seen that the test locations of two stress factors are quite similar to the case of the single source of random effect in Chapter 4 (see Table 4.5); and also two test chambers are allocated in a similar way with the one in the previous chapter, where the two test locations in a diagonal direction in Figure 5.2 are assigned to the same test chamber. In terms of the number of test unit allocations, the sum of test unit allocations of both suppliers for each test location is very close to the case in Chapter 4. For example, the sum of 10 and 11 test units, which is 21, from supplier 1 and 2, respectively, for a test location $j = 1$ is close to the number of test units allocated at the corresponding test location in the previous chapter, which is 22, as can be seen from Figure 4.7. We also observe that test units from two suppliers are almost equally allocated to each test locations. For example, 10 test units from supplier 1 and 11 test units from supplier 2 have been allocated for the test location $j = 1$.

**Table 5.1:** $D$-optimal test plan with $\sigma^2_{Uc} = 0.25$ and $\sigma^2_{Us} = 0.25$

| Supplier | Test chamber Assignment | Design Point | Temperature | | Humidity | | Allocation |
|---|---|---|---|---|---|---|---|
| | | | Actual | Coded | Actual | Coded | |
| $l$ | $k$ | $j$ | °C | $x_1$ | RH | $x_2$ | $n_{j(k)l}$ |
| 1 | 1 | 1 | 110.00 | 0.000 | 60.00 | 1.000 | 10 |
| 1 | 1 | 2 | 66.87 | 0.845 | 90.00 | 0.000 | 14 |
| 1 | 2 | 3 | 84.08 | 0.483 | 60.00 | 1.000 | 15 |
| 1 | 2 | 4 | 110.00 | 0.000 | 90.00 | 0.000 | 11 |
| 2 | 1 | 1 | 110.00 | 0.000 | 60.00 | 1.000 | 11 |
| 2 | 1 | 2 | 66.87 | 0.845 | 90.00 | 0.000 | 15 |
| 2 | 2 | 3 | 84.08 | 0.483 | 60.00 | 1.000 | 14 |
| 2 | 2 | 4 | 110.00 | 0.000 | 90.00 | 0.000 | 10 |

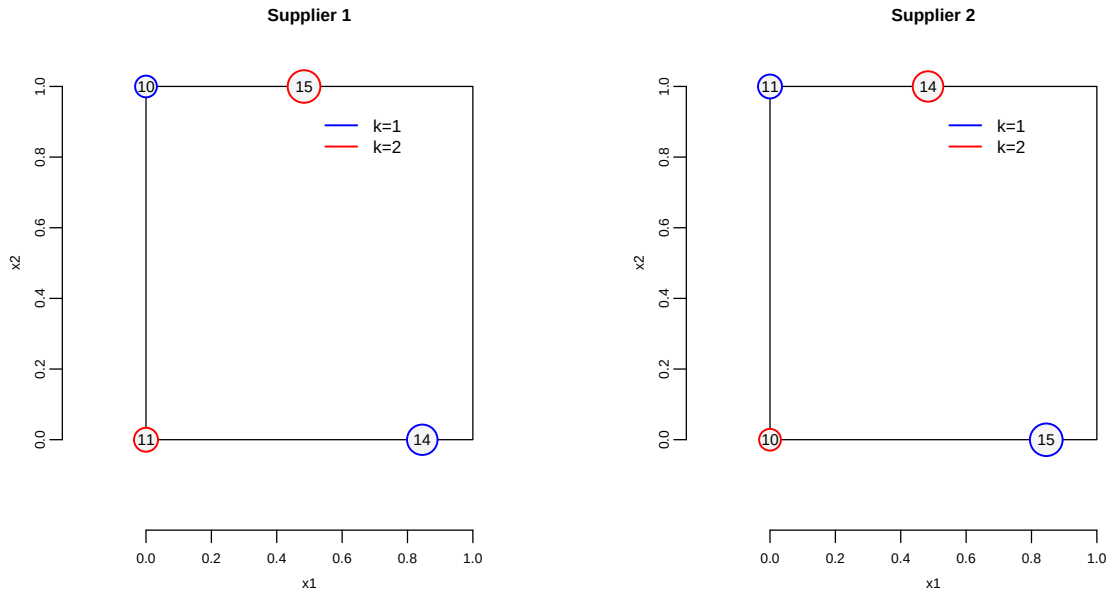


**Figure 5.2:** Design plot of $D$-optimal test plan with $\sigma^2_{Uc} = 0.25$ and $\sigma^2_{Us} = 0.25$

In short, the $D$-optimal design of multiple random effects shown in Figure 5.2 seems to be constructed by splitting the $D$-optimal design of the nested structure shown in Figure 4.7 equally into two parts so that the effect of different suppliers can be measured in each test location with balanced number of test units. In fact Theorem 3.1. in Niaparast (2009) has shown that the optimal population design (i.e., optimal design for all suppliers) is obtained by the *uniform* optimal individual design (i.e., optimal design for a supplier) in a crossed design structure; and our results verify the theorem numerically.

### *5.4.2 Optimization Process*

It would be worth observing how the optimization process described in Subsection 5.3.2 actually works for this example. In this subsection, we follow each step of the search process from the initial design to the optimal design.

Figure 5.3a shows the initial test plan, where four stress conditions and the test unit allocations are randomly generated. The test chamber assignment is exchanged in Figure 5.3b so as to increase the objective function value. According to the second step of Subsection 5.3.2, test unit allocations are updated in Figure 5.3c, which produces much more balanced allocations between two suppliers compared to the initial design. The next step is to find the optimal stress conditions, and Figure 5.3d shows the result. This step improves the objective function value from 12.566 to 924.217, which is the largest improvement among those by a single step in the entire process. The first iteration is finished, and all three steps are repeated in the next iteration. For the second iteration, the result of the exchange of test chamber assignment (i.e., the first step) is not depicted since there is no change. However the objective function keeps increasing on the second and third steps. Figure 5.3 depicts the test plans until the fourth iteration and the objective function value reaches to 1006.711. In fact, the

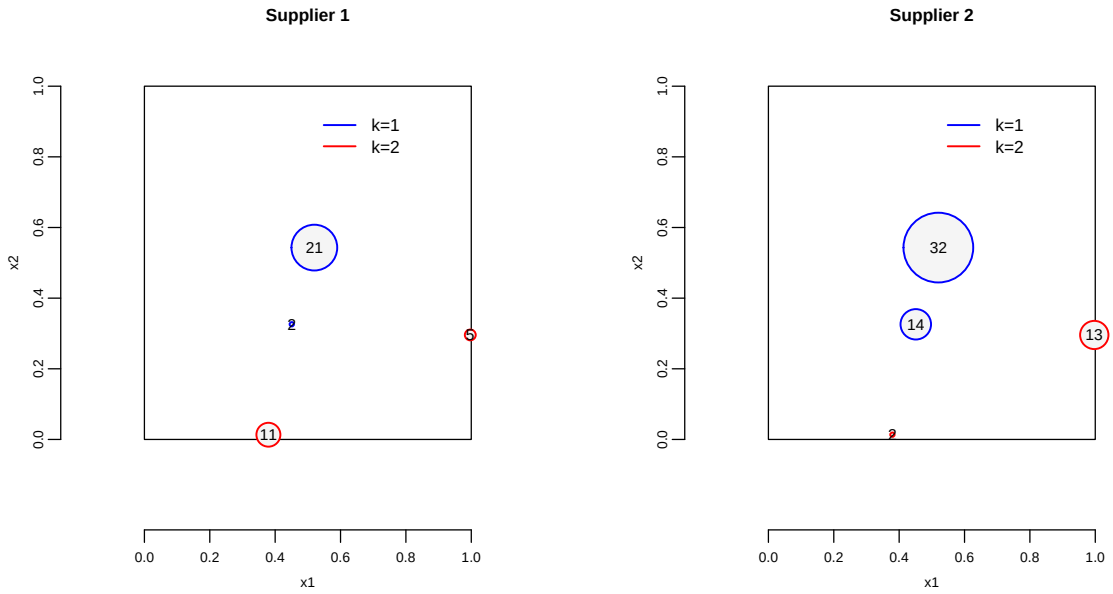


**(a)** Initial design: stress conditions and the number of test units are randomly generated (objective function value:= 3.599)

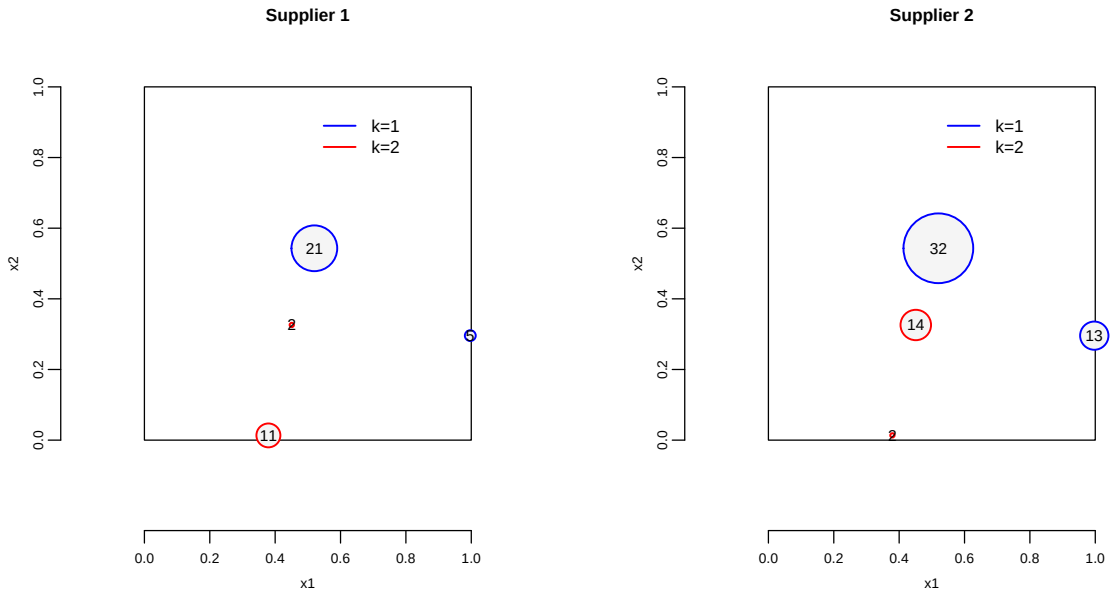


**(b)** Iteration 1 (step 1): chamber assignment is updated (4.107)

**Figure 5.3:** Optimization process

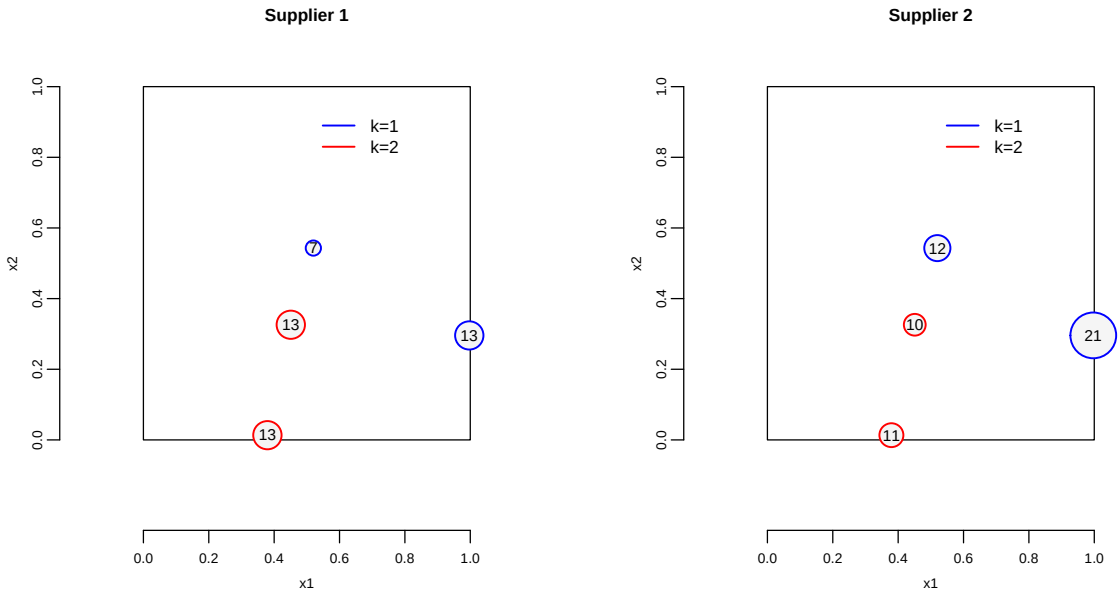


**(c)** Iteration 1 (step 2): number of test units is updated (12.566)

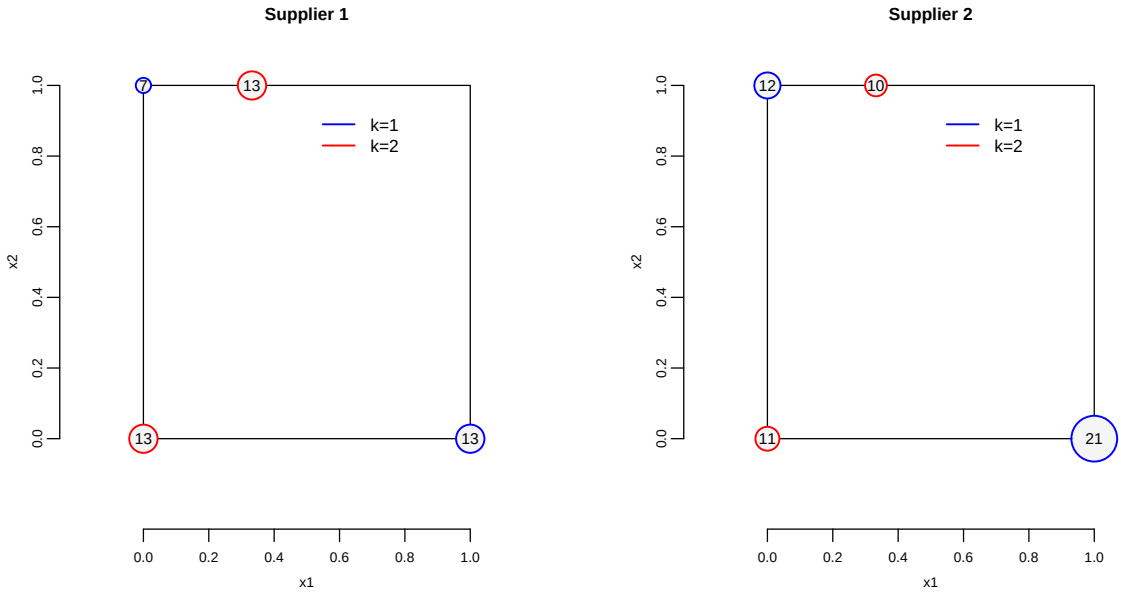


**(d)** Iteration 1 (step 3): stress conditions are updated (924.217)

**Figure 5.3:** Optimization process (continued)

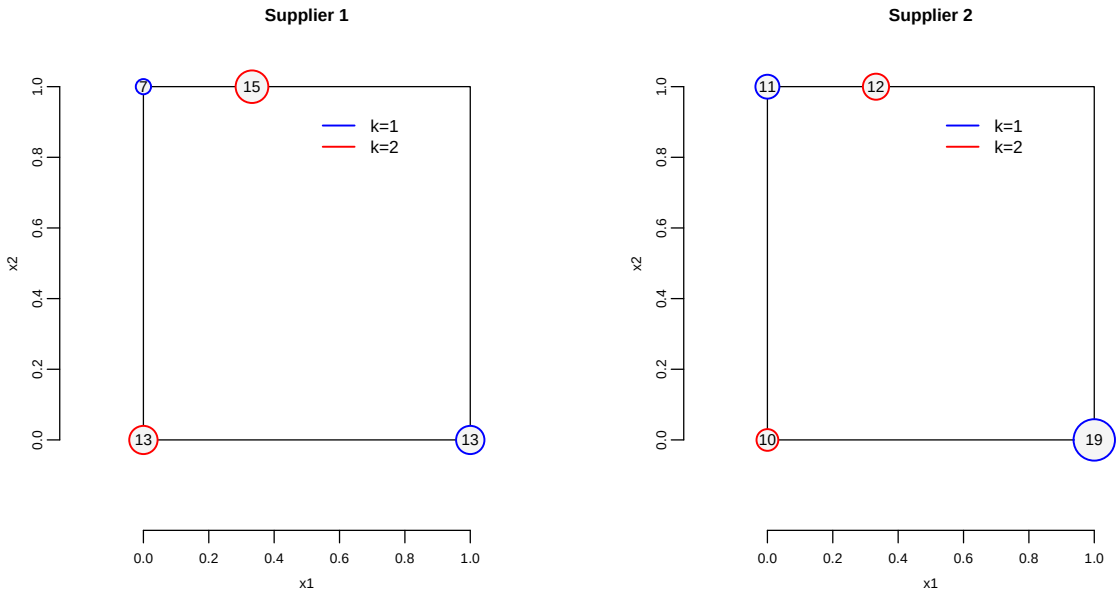


**(e)** Iteration 2 (step 2): number of test units is updated (939.283)

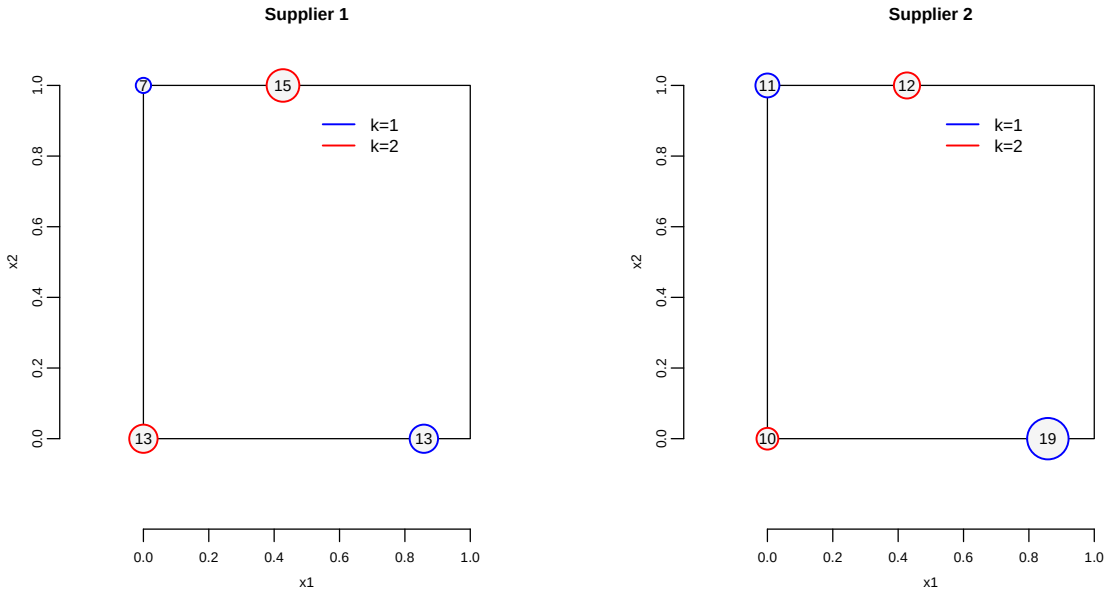


**(f)** Iteration 2 (step 3): stress conditions are updated (988.394)

**Figure 5.3:** Optimization process (continued)

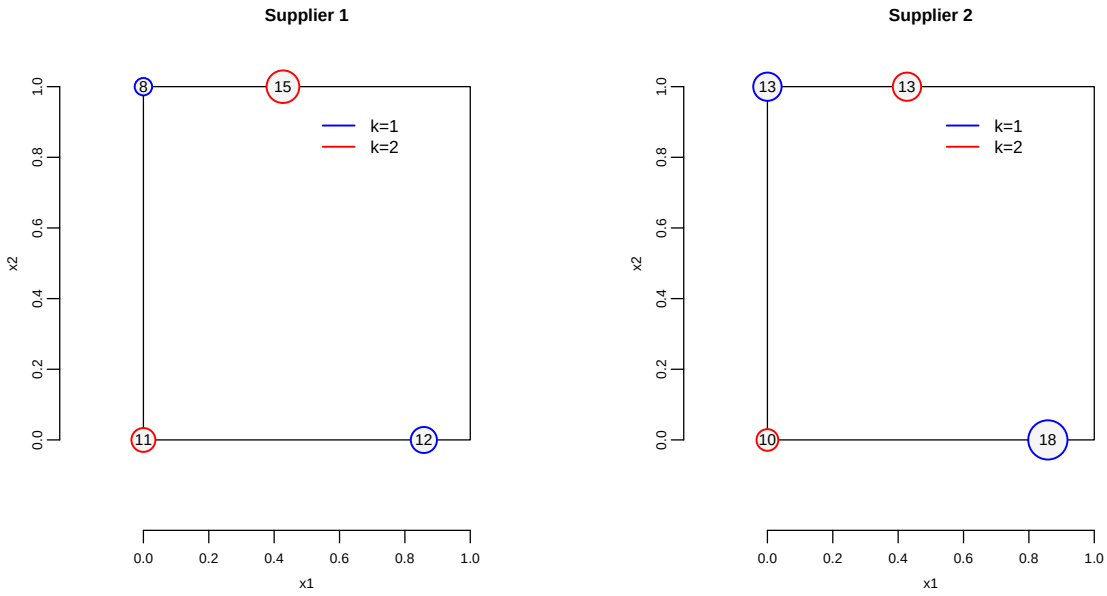


**(g)** Iteration 3 (step 2): number of test units is updated (1002.090)

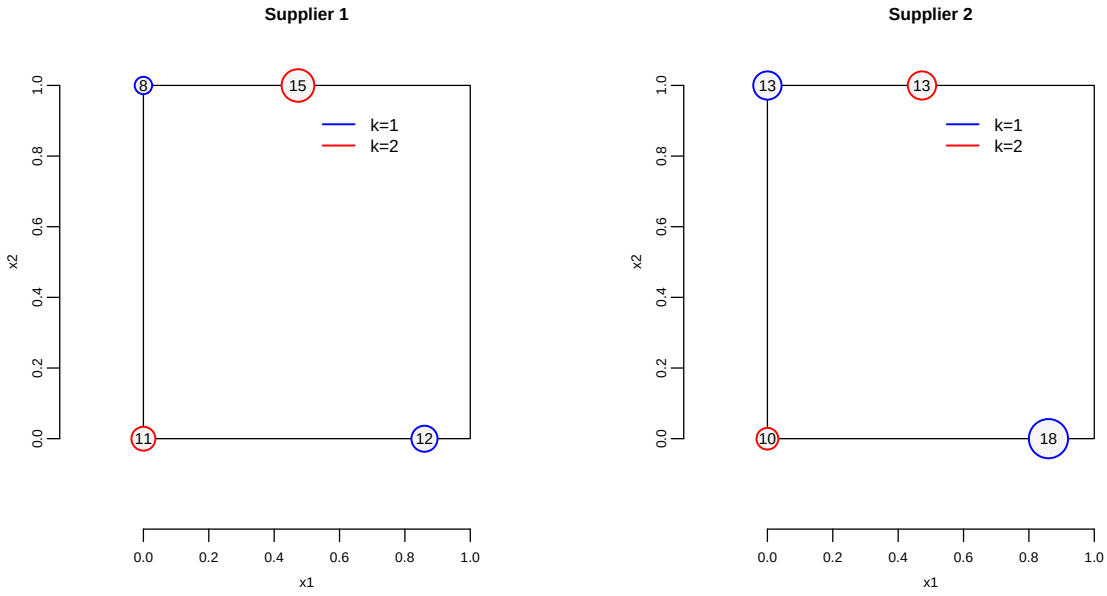


**(h)** Iteration 3 (step 3): stress conditions are updated (1005.143)

**Figure 5.3:** Optimization process (continued)

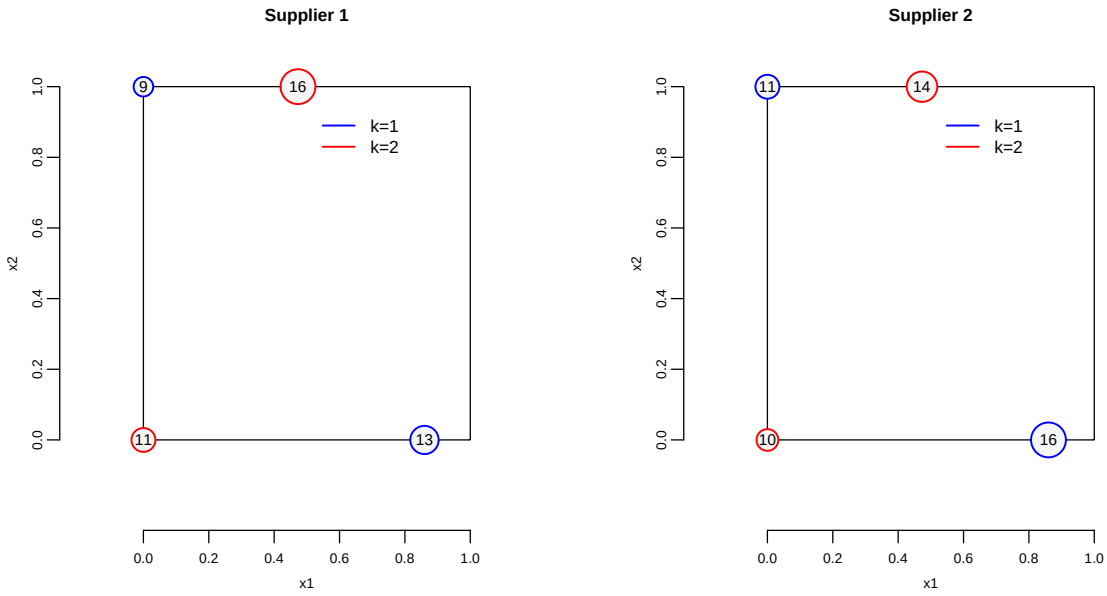


**(i)** Iteration 4 (step 2): number of test units is updated (1006.288)

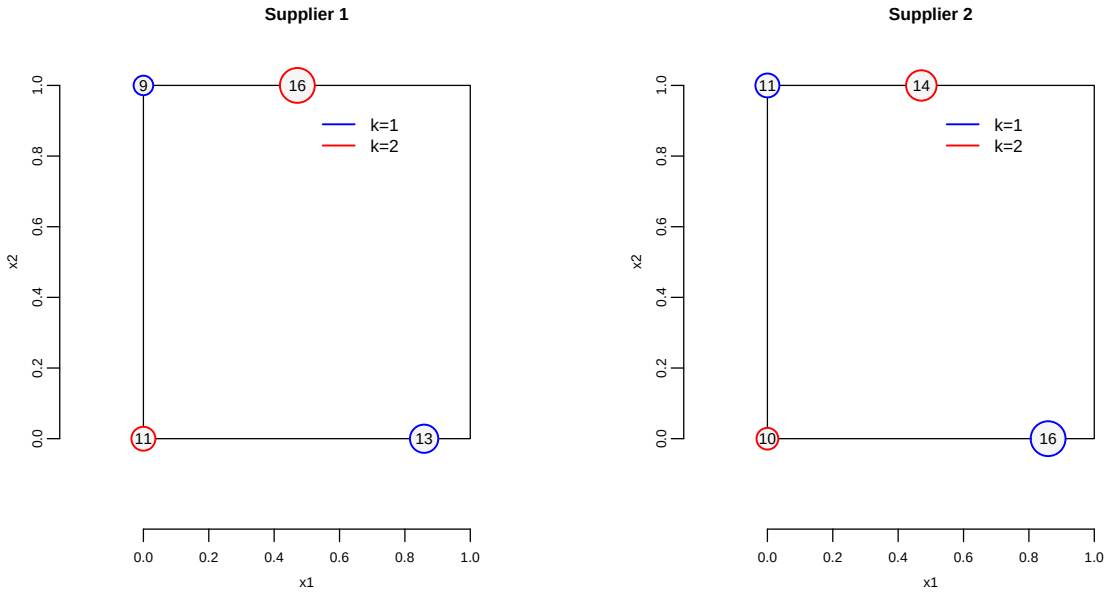


**(j)** Iteration 4 (step 3): stress conditions are updated (1006.711)

**Figure 5.3:** Optimization process (continued)

entire optimization process was completed at the seventh iteration and the optimal objective function value was 1007.673.

## 5.5 Conclusion

In this chapter, the $D$-optimal ALT test plan was constructed with multiple sources of random effects. We considered the crossed design structure by different suppliers of test units as well as the nested design structure by different test chambers. It has been shown that the $D$-optimal design could be obtained by mixing similar numbers of test units from different suppliers for each test condition. Also the optimal test conditions were slightly different from those in the case of single random effect by test chambers, which was seemingly caused by increased random effects in the acceleration model.

Extending this chapter, it would be worthwhile to investigate the optimal test plans for various cases with different combinations of $\sigma^2_{U^c}$ and $\sigma^2_{U^s}$. Also any improvement of the optimization procedure proposed in this chapter, in terms of computational time or $D$-efficiency, would be another opportunity for future research.

# Chapter 6

# CONCLUSIONS AND FUTURE WORK

A product's reliability assessment affects all different aspects of reliability-related decision making in industries. For a precise evaluation of the product's lifetime, it is important to reflect a possible influential factor caused by the experimental setting in real world to the mathematical model. This dissertation considered the effects from heterogeneous groups in a sample of reliability tests. In ALTs, test observations are likely to be constructed by several different groups due to, e.g., the discordance between the experimental unit (i.e., test chamber) and observational unit (i.e., test unit) or different sources of materials. In this dissertation, the effects of those groups were treated as a random variable, and ALT data was modeled upon a framework of GLMM. The first half of this thesis studied reliability data analysis and the second half described the optimal test plan, taking heterogeneous random group effects into account.

In Chapter 2, lifetime observations with constrained randomization from a constant-stress ALT were modeled by a Poisson GLMM. The iterative maximum likelihood was developed for the parameter estimation, and the variance-covariance matrix was calculated by the quadrature approximation. The GLMM provides several advantages. First, it is a structured framework for censored failure time data with random effects. Second, it can be easily implemented in statistical software. Third and most importantly, owing to the recent studies of experimental designs for GLMM, the optimal ALT planning can be derived.

Chapter 3 examined the exploitation of GLMM for a step-stress ALT data analysis. According to the memoryless property of exponential random variable, the

SSALT data was transformed to the pseudo CSALT data. Both maximum likelihood and Bayesian approaches were used for the parameter estimation. Deterministic approximation methods, AGQ and INLA, were applied in this chapter. The proposed model was compared to other traditional models by a simulation study, and applied to the SSALT data of power cable insulation. From the results, we observed that the random group effect should be considered in the model to avoid highly biased parameter estimation, which might significantly affect the reliability assessment when the model was extrapolated to the normal use condition. The prediction of each group effect was also provided from the estimation results of GLMM, and it enabled us to examine an abnormal group without an additional residual analysis.

Since life tests are expensive and require long period of time, it is also essential to plan ALTs in an efficient way where information for statistical inference of an acceleration model could be extracted as much as possible from those tests. Chapter 4 and Chapter 5 tackled such problems by pursuing the optimal experimental design for GLMM. Particularly in Chapter 4 the test chamber assignment problem was studied where observations from the same test chamber were likely to be correlated. We observed the test chamber assignment to test locations had a substantial impact on the parameter estimation under the nested design structure. Also $D$-optimal test plan was obtained by using quasi-likelihood approach, and it performed better than any test plan constructed by the greedy approach.

Chapter 5 dealt with an additional random effect caused by heterogeneous test units for ALT planning. We postulated a situation for which test units were supplied by two different manufacturers, and failure time observations of those from the same manufacturer were correlated. The objective function of $D$-optimal test plan could be derived by the similar manner as Chapter 4 using quasi-likelihood, while the optimization was carried out by iterations of updating each decision variable. As a result

the $D$-optimal design was obtained by uniformly allocating test units from different suppliers to each test location.

There are some limitations of this thesis and future research opportunities. First, many different types of sensitivity analysis could be conducted with violations, to a small or large extent, of assumptions in this dissertation. For example, the normality assumption for the random effect may be violated in a real world application. We may be able to conduct a simulation study to see how the GLMM approach is sensitive to deviations from the normal distribution of random effects. Another opportunity for the sensitivity analysis lies in cases with incorrect planning values for the experimental design study, i.e., the presumed model of the linear predictor and the value of the variance component. An optimal design derived from a specific planning value would not be optimal for a different planning value, and it would be worth to observe how sensitive the optimal design is to changes of each parameter in the linear predictor and the variance of random effects. Besides, this dissertation only deals with the first order model with main effects of stress factors for the acceleration model. However, we may consider some other acceleration models, such as a quadratic model, as a true life-stress relationship. As an alternative to the sensitivity study, the Bayesian approach (DuMouchel and Jones, 1994) could be adapted to tackle such dependency problems due to the uncertainty in the acceleration model.

Second, some practical constraints for planning ALTs could be taken into account. For example, a manufacturer may have a limited budget and time for a test; test chambers may have a limited capacity for the number of test units to be tested at the same time; or the number of test units provided by each supplier may be limited. In these cases, we may consider restricting a feasible region of a design space by including a suitable constraints in terms of cost, time, and number of test units into the optimization problem. Alternatively, an additional objective function could be

added so as to e.g., minimize the total cost or testing time with maintaining the least acceptable $D$-efficiency, which leads to an optimization with dual objective functions where one is related to the statistical efficiency and the other one controls the practical constraints.

Lastly, this dissertation only dealt with failure time data. These days, however, a product's failure is hardly observed even with elevated environmental stresses. For this reason, a product's degradation data is widely used for diagnostic and prediction tools, and the heterogeneous group effects could be taken into account for degradation data analysis. In addition, thanks to modern sensor technologies and the Internet of things (IoT), it is easy and inexpensive to collect data on the state of machinery being operated. With such abundant data from all different environments, it would be more important to consider heterogeneous effects in the model. Based on this dissertation's findings, these topics will be studied in the future.

# REFERENCES


Achcar, J. A., "Approximate Bayesian methods: some applications in life testing problems", Brazilian Journal of Probability and Statistics **7**, 2, 135–158 (1993).

Aitkin, M. and D. Clayton, "The fitting of exponential, Weibull and extreme value distributions to complex censored survival data using GLIM", Applied Statistics **29**, 2, 156–163 (1980).

Bai, D., M. Kim and S. Lee, "Optimum simple step-stress accelerated life tests with censoring", IEEE transactions on reliability **38**, 5, 528–532 (1989).

Breslow, N. E. and D. G. Clayton, "Approximate inference in generalized linear mixed models", Journal of the American Statistical Association **88**, 421, 9–25 (1993).

Byrd, R. H., P. Lu, J. Nocedal and C. Zhu, "A limited memory algorithm for bound constrained optimization", SIAM Journal on Scientific Computing **16**, 5, 1190–1208 (1995).

Chernoff, H., "Optimal accelerated life designs for estimation", Technometrics **4**, 3, 381–408 (1962).

Cox, D. R., "Regression models and life-tables", Journal of the Royal Statistical Society. Series B (Methodological) **34**, 2, 187–220 (1972).

DuMouchel, W. and B. Jones, "A simple Bayesian modification of D-optimal designs to reduce dependence on an assumed model", Technometrics **36**, 1, 37–47 (1994).

Escobar, L. A. and W. Q. Meeker, "Planning accelerated life tests with two or more experimental factors", Technometrics **37**, 4, 411–427 (1995).

Escobar, L. A. and W. Q. Meeker, "A review of accelerated test models", Statistical Science **21**, 4, 552–577 (2006).

Fong, Y., H. Rue and J. Wakefield, "Bayesian inference for generalized linear mixed models", Biostatistics **11**, 3, 397–412 (2010).

Freeman, L. J. and G. G. Vining, "Reliability data analysis for life test experiments with subsampling", Journal of Quality Technology **42**, 3, 233–241 (2010).

Freeman, L. J. and G. G. Vining, "Reliability data analysis for life test designed experiments with sub-sampling", Quality and Reliability Engineering International **29**, 4, 509–519 (2013).

Gerstle, F. P. and S. C. Kunz, "Prediction of long-term failure in kevlar 49 composites", ASTM Special Technical Publication pp. 263–292 (1983).

Goos, P., *The optimal design of blocked and split-plot experiments*, vol. 164 (Springer Science & Business Media, 2012).

Grilli, L., S. Metelli and C. Rampichini, "Bayesian estimation with integrated nested Laplace approximation for binary logit mixed models", Journal of Statistical Computation and Simulation **85**, 13, 2718–2726 (2015).

Hamada, M., "Bayesian analysis of step-stress accelerated life tests and its use in planning", Quality Engineering **27**, 3, 276–282 (2015).

Hassler, E., *Bayesian D-optimal design issues and optimal design construction methods for generalized linear models with random blocks*, Ph.D. thesis, Arizona State University (2015).

Holand, A. M., I. Steinsland, S. Martino and H. Jensen, "Animal models and integrated nested Laplace approximations", G3: Genes, Genomes, Genetics **3**, 8, 1241–1251 (2013).

Kensler, J. L. K., L. J. Freeman and G. G. Vining, "Analysis of reliability experiments with random blocks and subsampling", Journal of Quality Technology **47**, 3, 235–251 (2015).

Khamis, I. H. and J. J. Higgins, "An alternative to the Weibull step-stress model", International Journal of Quality & Reliability Management **16**, 2, 158–165 (1999).

Lee, J. and R. Pan, "Bayesian inference model for step-stress accelerated life testing with type-ii censoring", in "2008 Annual Reliability and Maintainability Symposium (RAMS)", pp. 91–96 (IEEE, 2008).

Lee, J. and R. Pan, "Analyzing step-stress accelerated life testing data using generalized linear models", IIE Transactions **42**, 8, 589–598 (2010).

Lee, J. and R. Pan, "Bayesian analysis of step-stress accelerated life test with exponential distribution", Quality and Reliability Engineering International **28**, 3, 353–361 (2012).

León, R. V., R. Ramachandran, A. J. Ashby and J. Thyagarajan, "Bayesian modeling of accelerated life tests with random effects", Journal of quality technology **39**, 1, 3–16 (2007).

Littell, R. C., W. W. Stroup, G. A. Milliken, R. D. Wolfinger and O. Schabenberger, *SAS for mixed models* (SAS institute, 2006).

Lv, S., Z. Niu, L. Qu, S. He and Z. He, "Reliability modeling of accelerated life tests with both random effects and nonconstant shape parameters", Quality Engineering **27**, 3, 329–340 (2015).

Mann, N. R., "Design of over-stress life-test experiments when failure times have the two-parameter Weibull distribution", Technometrics **14**, 2, 437–451 (1972).

McCullagh, P. and J. A. Nelder, *Generalized linear models*, vol. 37 (CRC press, 1989).

McCulloch, C. E. and S. R. Searle, *Generalized, linear, and mixed models* (Wiley, 2001).

McCulloch, C. E., S. R. Searle and J. M. Neuhaus, *Generalized linear mixed models, Second Edition* (Wiley, New Jersey, 2008).

Meeker, W. Q. and L. A. Escobar, *Statistical methods for reliability data* (John Wiley & Sons, 2014).

Meeker, W. Q. and W. Nelson, "Optimum accelerated life-tests for the Weibull and extreme value distributions", IEEE Transactions on Reliability **24**, 5, 321–332 (1975).

Monroe, E. M., R. Pan, C. M. Anderson-Cook, D. C. Montgomery and C. M. Borror, "A generalized linear model approach to designing accelerated life test experiments", Quality and Reliability Engineering International **27**, 4, 595–607 (2011).

Montgomery, D. C., *Design and analysis of experiments* (John Wiley & Sons, 2008).

Myers, R. H., D. C. Montgomery, G. G. Vining and T. J. Robinson, *Generalized linear models: with applications in engineering and the sciences*, vol. 791 (John Wiley & Sons, 2012).

Nelson, W. B., "Accelerated life testing-step-stress models and data analyses", Reliability, IEEE Transactions on **29**, 2, 103–108 (1980).

Nelson, W. B., "A bibliography of accelerated test plans", IEEE Transactions on Reliability **54**, 2, 194–197 (2005a).

Nelson, W. B., "A bibliography of accelerated test plans part ii-references", IEEE transactions on Reliability **54**, 3, 370–373 (2005b).

Nelson, W. B., "Residuals and their analyses for accelerated life tests with step and varying stress", Reliability, IEEE Transactions on **57**, 2, 360–368 (2008).

Nelson, W. B., *Accelerated testing: statistical models, test plans, and data analysis*, vol. 344 (John Wiley & Sons, 2009).

Nelson, W. B., "An updated bibliography of accelerated test plans", in "2015 Annual Reliability and Maintainability Symposium (RAMS)", pp. 1–6 (IEEE, 2015).

Niaparast, M., "On optimal design for a poisson regression model with random intercept", Statistics & Probability Letters **79**, 6, 741–747 (2009).

Pan, R. and Y. Kozakai, "Semiparametric model and Bayesian analysis for clustered accelerated life testing data", Statistics Research Letters **2**, 1, 1–11 (2013).

Pan, R. and T. Yang, "Design and evaluation of accelerated life testing plans with dual objectives", Journal of Quality Technology **46**, 2, 114 (2014).

Pan, R., T. Yang and K. Seo, "Planning constant-stress accelerated life tests for acceleration model selection", IEEE Transactions on Reliability **64**, 4, 1356–1366 (2015).

Park, J.-W. and B.-J. Yum, "Optimal design of accelerated life tests with two stresses", Naval Research Logistics (NRL) **43**, 6, 863–884 (1996).

Pawitan, Y., *In all likelihood: statistical modelling and inference using likelihood* (OUP Oxford, 2013).

Pinheiro, J. C. and D. M. Bates, "Approximations to the log-likelihood function in the nonlinear mixed-effects model", Journal of computational and Graphical Statistics **4**, 1, 12–35 (1995).

Rodríguez-Borbón, M. I., M. A. Rodríguez-Medina, L. A. Rodríguez-Picón, A. Alvarado-Iniesta and N. Sha, "Reliability estimation for accelerated life tests based on a Cox proportional hazard model with error effect", Quality and Reliability Engineering International (2017).

Rue, H., S. Martino and N. Chopin, "Approximate Bayesian inference for latent Gaussian models by using integrated nested Laplace approximations", Journal of the royal statistical society: Series b (statistical methodology) **71**, 2, 319–392 (2009).

Seo, K. and R. Pan, "ALTopt: An R package for optimal experimental design of accelerated life testing.", R Journal **7**, 2 (2015a).

Seo, K. and R. Pan, *ALTopt: Optimal Experimental Designs for Accelerated Life Testing*, URL `https://CRAN.R-project.org/package=ALTopt`, R package version 0.1.1 (2015b).

Seo, K. and R. Pan, "Data analysis for accelerated life tests with constrained randomization", in "2016 Annual Reliability and Maintainability Symposium (RAMS)", pp. 489–495 (IEEE, 2016).

Sha, N. and R. Pan, "Bayesian analysis for step-stress accelerated life testing using Weibull proportional hazard model", Statistical Papers **55**, 3, 715–726 (2014).

Sinharay, S., "Experiences with Markov chain Monte Carlo convergence assessment in two psychometric examples", Journal of Educational and Behavioral Statistics **29**, 4, 461–488 (2004).

Tang, L., T. Goh, Y. Sun and H. Ong, "Planning accelerated life tests for censored two-parameter exponential distributions", Naval Research Logistics (NRL) **46**, 2, 169–186 (1999).

Vining, G. G., "Technical advice: experimental protocol and the basic principles of experimental design", Quality Engineering **25**, 3, 307–311 (2013).

Wang, G., Z. Niu, S. Lv, L. Qu and Z. He, "Bootstrapping analysis of lifetime data with subsampling", Quality and Reliability Engineering International (2015).

Xiao, L. and L. C. Tang, "Analysis of reliability experiments with blocking", Quality Technology and Quantitiative Management **10**, 2, 141–160 (2013).

Xu, A., S. Basu and Y. Tang, "A full Bayesian approach for masked data in step-stress accelerated life testing", Reliability, IEEE Transactions on **63**, 3, 798–806 (2014).

Yang, T. and R. Pan, "A novel approach to optimal accelerated life test planning with interval censoring", IEEE Transactions on Reliability **62**, 2, 527–536 (2013).

Zelen, M., "Factorial experiments in life testing", Technometrics **1**, 3, 269–288 (1959).

Zhao, W. and E. A. Elsayed, "A general accelerated life model for step-stress testing", IIE Transactions **37**, 11, 1059–1069 (2005).

# APPENDIX A

# FURTHER DETAILS IN CHAPTER 3

## A.1 Derivation of Gaussian Approximation

The first and second derivatives of $g(u_i)$ are

$$\frac{\partial g(u_i)}{\partial u_i} = -\frac{u_i}{\sigma_u^2} + \sum_{s=1}^{q_i}(c_{is} - \mu_{is}) \tag{A.1}$$

$$\frac{\partial^2 g(u_i)}{\partial u_i^2} = -\left(\frac{1}{\sigma_u^2} + \sum_{s=1}^{q_i}\mu_{is}\right) \tag{A.2}$$

Since Eq. (A.2) is negative, there is a unique point $u_i^*$ such that $u_i^* = \arg\max_{u_i} g(u_i)$. As Eq. (A.1) is vanished at $u_i^*$, one can determine $u_i^*$ by the following iterations.

$$u_i^{(k+1)} = \sigma_u^2 \sum_{s=1}^{q_i}(c_{is} - \mu_{is}^{(k)}), \quad \mu_{is}^{(k)} = \exp(\beta_0 + \beta_1 x_{is} + u_i^{(k)})$$

where the iteration can be started with the initial value $u_i^{(0)} = 0$. Let $\mu_{is}^* = \exp(\beta_0 + \beta_1 x_{is} + u_i^*)$, then it can be shown that, by the second-order Taylor expansion at $u_i^*$, the Gaussian approximation of $\exp\{g(u_i)\}$, without normalizing constant, is given as

$$\exp\left\{-\frac{u_i^2}{2\sigma_u^2} + \sum_{s=1}^{q_i}(c_{is}\log\mu_{is} - \mu_{is})\right\} \approx \exp\left\{-\frac{(u_i - u_i^*)^2}{2\sigma^{2*}}\right\}$$

which is the kernel of the normal density with the mean $u_i^*$ and the variance $\sigma^{2*} = \left(\sum_{s=1}^{q_i}\mu_{is}^* + \frac{1}{\sigma_u^2}\right)^{-1}$.

## A.2 Laplace Approximation

The Laplace approximation of the posterior marginal of $\pi(\tau_u|\mathbf{D})$ refers to

$$\tilde{\pi}_{LA}(\tau_u|\mathbf{D}) \propto \left.\frac{\pi(\boldsymbol{z}, \tau_u, \mathbf{D})}{\tilde{\pi}_G(\boldsymbol{z}|\tau_u, \mathbf{D})}\right|_{\boldsymbol{z}=\boldsymbol{z}^*(\tau_u)} \tag{A.3}$$

where $\tilde{\pi}_G(\boldsymbol{z}|\tau_u, \mathbf{D})$ is the Gaussian approximation to the full conditional density of $\boldsymbol{z}$; and $\boldsymbol{z}^*(\tau_u)$ is the mode of the full conditional of $\boldsymbol{z}$, for a given $\tau_u$. The mode $\boldsymbol{z}^*(\tau_u)$ has to be recalculated for each given value of $\tau_u^k$, which will be used for the numerical integration in Eq. (3.14). For the problem in this paper, the full conditional of $\boldsymbol{z}$ is

given as

$$\pi(\boldsymbol{z}|\tau_u, \mathbf{D}) \propto \exp\left\{-\frac{1}{2}\boldsymbol{z}^T\mathbf{Q}(\tau_u)\boldsymbol{z} + \sum_{i=1}^{m}\sum_{s=1}^{q_i}(c_{is}\log\mu_{is} - \mu_{is})\right\}$$

which has the similar form with Eq. (3.8) of AGQ; but now it is a multidimensional version. The Gaussian approximation of this form is known particularly being accurate (Rue *et al.*, 2009). The major reason of the use of Laplace approximation in INLA is $\pi(\tau_u|\mathbf{D})$ in Eq. (3.13) would not be well approximated to the Gaussian density directly; but by introducing the Gaussian variable $\boldsymbol{z}$ from Eq. (A.3), it achieves substantially accurate results.

We can conduct the Gaussian approximation by the similar way of AGQ. Then we obtain

$$\tilde{\pi}_G(\boldsymbol{z}|\tau_u, \mathbf{D}) \propto \exp\left\{-\frac{1}{2}(\boldsymbol{z} - \boldsymbol{z}^*(\tau_u))^T(\mathbf{Q}(\tau_u) + \mathbf{C}^*)(\boldsymbol{z} - \boldsymbol{z}^*(\tau_u))\right\}$$

where $\mathbf{Q}(\tau_u) + \mathbf{C}^*$ is the precision matrix.

The other density $\tilde{\pi}_{LA}(z_p|\tau_u, \mathbf{D})$ in Eq. (3.14) is calculated by the similar manner, but now the full conditional density depends on two variables as follows.

$$\tilde{\pi}_{LA}(z_p|\tau_u, \mathbf{D}) \propto \left.\frac{\pi(\boldsymbol{z}, \tau_u, \mathbf{D})}{\tilde{\pi}_G(\boldsymbol{z}_{\setminus p}|z_p, \tau_u, \mathbf{D})}\right|_{\boldsymbol{z}_{\setminus p}=\boldsymbol{z}^*_{\setminus p}(z_p,\tau_u)}$$

where $\boldsymbol{z}_{\setminus p}$ is the Gaussian variables except the $p$th element. Therefore, the mode $\boldsymbol{z}^*_{\setminus p}(z_p, \tau_u)$ has to be calculated for each combination of $(z_p, \tau_u^k)$.

**Algorithm 1** Simulation data generation

$pseudoData \leftarrow NULL$; ▷ matrix including columns of stress level, failure time, censoring indicator and group index
**for** $i = 0$ to $m$ **do**
  draw a sample $u_i$ from $N(0, \sigma_u^2)$;
  **for** $k = 1$ to $4$ **do** ▷ determine the conditional cdf of each group
    calculate $\lambda_{ijk}$, $j = 1, \ldots, n$, by Eq. (3.16);
  **end for**
  **for** $j = 1$ to $n$ **do**
    draw a sample $z_{ij}$ from $Unif(0, 1)$; ▷ random samples in y-axis of the conditional cdf
    obtain $t_{ij}$ by the inverse of conditional cdf of SSALT (Eq. (A.4)); ▷ projecting $z_{ij}$ into x-axis
    **if** $t_{ij} \leq \xi_1$ **then** ▷ pseudo data generation
      append $(x_1, t_{ij}, 1, i)$ to $pseudoData$;
    **else if** $t_{ij} \leq \xi_2$ **then**
      append $(x_1, \xi_1, 0, i)$ to $pseudoData$;
      append $(x_2, t_{ij} - \xi_1, 1, i)$ to $pseudoData$;
    **else if** $t_{ij} \leq \xi_3$ **then**
      append $(x_1, \xi_1, 0, i)$ to $pseudoData$;
      append $(x_2, \xi_2 - \xi_1, 0, i)$ to $pseudoData$;
      append $(x_3, t_{ij} - \xi_2, 1, i)$ to $pseudoData$;
    **else if** $t_{ij} \leq \xi_4$ **then**
      append $(x_1, \xi_1, 0, i)$ to $pseudoData$;
      append $(x_2, \xi_2 - \xi_1, 0, i)$ to $pseudoData$;
      append $(x_3, \xi_3 - \xi_2, 0, i)$ to $pseudoData$;
      append $(x_4, t_{ij} - \xi_3, 1, i)$ to $pseudoData$;
    **else**
      append $(x_1, \xi_1, 0, i)$ to $pseudoData$;
      append $(x_2, \xi_2 - \xi_1, 0, i)$ to $pseudoData$;
      append $(x_3, \xi_3 - \xi_2, 0, i)$ to $pseudoData$;
      append $(x_4, \xi_4 - \xi_3, 0, i)$ to $pseudoData$;
    **end if**
  **end for**
**end for**

where the inverse cdf is given as

$$
\begin{aligned}
t_{ij} &= F_{\text{ss}}^{-1}(z_{ij}|u_i) \\
&= \begin{cases}
-\frac{\ln(1-z_{ij})}{\lambda_{i1}},\ 0 \leq z_{ij} < 1 - \mathrm{e}^{-\lambda_{i1}\xi_1} \\
-\frac{\ln(1-z_{ij})+\lambda_{i1}\xi_1}{\lambda_{i2}} + \xi_1,\ 1 - \mathrm{e}^{-\lambda_{i1}\xi_1} \leq z_{ij} < 1 - \mathrm{e}^{-\lambda_{i2}(\xi_2-\xi_1)-\lambda_{i1}\xi_1} \\
-\frac{\ln(1-z_{ij})+\lambda_{i2}(\xi_2-\xi_1)+\lambda_{i1}\xi_1}{\lambda_{i3}} + \xi_2, \\
\quad 1 - \mathrm{e}^{-\lambda_{i2}(\xi_2-\xi_1)-\lambda_{i1}\xi_1} \leq z_{ij} < 1 - \mathrm{e}^{-\lambda_{i3}(\xi_3-\xi_2)-\lambda_{i2}(\xi_2-\xi_1)-\lambda_{i1}\xi_1} \\
-\frac{\ln(1-z_{ij})+\lambda_{i3}(\xi_3-\xi_2)+\lambda_{i2}(\xi_2-\xi_1)+\lambda_{i1}\xi_1}{\lambda_{i3}} + \xi_3, \\
\quad 1 - \mathrm{e}^{-\lambda_{i3}(\xi_3-\xi_2)-\lambda_{i2}(\xi_2-\xi_1)-\lambda_{i1}\xi_1} \leq z_{ij} < 1.
\end{cases}
\end{aligned} \tag{A.4}
$$

# APPENDIX B

# FURTHER DETAILS IN CHAPTER 4

## B.1 Derivation of Marginal Mean, Variance, and Covariance

The marginalized mean, variance and covariance for Poisson GLMM can be expressed as closed forms (McCulloch and Searle, 2001). The marginal mean is calculated as

$$\begin{aligned}
\mu^*_{ij(k)} = \mathbb{E}\left[c_{ij(k)}\right] &= \mathbb{E}\left[\mathbb{E}\left[c_{ij(k)}|U_k\right]\right] \\
&= \exp\left(\mathbf{x}'_{j(k)}\boldsymbol{\beta} + \alpha \log t_{ij(k)}\right) \mathbb{E}\left[\exp(U_k)\right] \\
&= \exp\left(\mathbf{x}'_{j(k)}\boldsymbol{\beta} + \alpha \log t_{ij(k)}\right) M_U(1) \\
&= \exp\left(\mathbf{x}'_{j(k)}\boldsymbol{\beta} + \alpha \log t_{ij(k)}\right) \exp\left(\sigma^2_U/2\right) \\
&= \exp\left(\mathbf{x}'_{j(k)}\boldsymbol{\beta} + \alpha \log t_{ij(k)} + \sigma^2_U/2\right)
\end{aligned}$$

where $M_U(1)$ is the moment generating function (MGF) of $U$ evaluated at 1. Recall the MGF of normal random variable $U$ is given as $M_U(t) = \exp(\mu_u t + \sigma^2_u t^2/2)$.

Accordingly the marginal variance is calculated as

$$
\begin{aligned}
&\operatorname{var}\left(c_{ij(k)}\right) \\
&\quad = \operatorname{var}\left(\mathbb{E}\left[c_{ij(k)}|U_k\right]\right) + \mathbb{E}\left[\operatorname{var}\left(c_{ij(k)}|U_k\right)\right] \\
&\quad = \operatorname{var}\left(\mu_{ij(k)}\right) + \mathbb{E}\left[\mu_{ij(k)}\right] \\
&\quad = \operatorname{var}\left(\exp\left(\mathbf{x}'_{j(k)}\boldsymbol{\beta} + \alpha \log t_{ij(k)} + U_k\right)\right) + \mathbb{E}\left[\exp\left(\mathbf{x}'_{j(k)}\boldsymbol{\beta} + \alpha \log t_{ij(k)} + U_k\right)\right] \\
&\quad = \mathbb{E}\left[\exp\left\{2\left(\mathbf{x}'_{j(k)}\boldsymbol{\beta} + \alpha \log t_{ij(k)} + U_k\right)\right\}\right] - \left[\mathbb{E}\left[\exp\left(\mathbf{x}'_{j(k)}\boldsymbol{\beta} + \alpha \log t_{ij(k)} + U_k\right)\right]\right]^2 \\
&\qquad + \mathbb{E}\left[\exp\left(\mathbf{x}'_{j(k)}\boldsymbol{\beta} + \alpha \log t_{ij(k)} + U_k\right)\right] \\
&\quad = \exp\left\{2\left(\mathbf{x}'_{j(k)}\boldsymbol{\beta} + \alpha \log t_{ij(k)}\right)\right\} M_U(2) - \exp\left\{2\left(\mathbf{x}'_{j(k)}\boldsymbol{\beta} + \alpha \log t_{ij(k)}\right)\right\} M_U^2(1) \\
&\qquad + \exp\left(\mathbf{x}'_{j(k)}\boldsymbol{\beta} + \alpha \log t_{ij(k)}\right) M_U(1) \\
&\quad = \exp\left\{2\left(\mathbf{x}'_{j(k)}\boldsymbol{\beta} + \alpha \log t_{ij(k)} + \sigma_U^2/2\right)\right\} \exp\left(\sigma_U^2\right) \\
&\qquad - \exp\left\{2\left(\mathbf{x}'_{j(k)}\boldsymbol{\beta} + \alpha \log t_{ij(k)} + \sigma_U^2/2\right)\right\} + \exp\left(\mathbf{x}'_{j(k)}\boldsymbol{\beta} + \alpha \log t_{ij(k)} + \sigma_U^2/2\right) \\
&\quad = \mathbb{E}\left[c_{ij(k)}\right]^2 \left(e^{\sigma_U^2} - 1\right) + \mathbb{E}\left[c_{ij(k)}\right] \\
&\quad = \mu^*_{ij(k)} + {\mu^*_{ij(k)}}^2 \xi
\end{aligned}
$$

The marginal covariance of two observations in the same test chamber is calculated as

$$
\begin{aligned}
&\operatorname{cov}\left(c_{ij(k)}, c_{ij'(k)}\right) \\
&\quad = \operatorname{cov}\left(\mathbb{E}\left[c_{ij(k)}|U_k\right], \left[c_{ij'(k)}|U_k\right]\right) + \mathbb{E}\left[\operatorname{cov}\left(c_{ij(k)}, c_{ij'(k)}|U_k\right)\right] \\
&\quad = \operatorname{cov}\left(\mu_{ij(k)}, \mu_{ij'(k)}\right) + \mathbb{E}[0] \\
&\quad = \operatorname{cov}\left(\exp\left(\mathbf{x}'_{j(k)}\boldsymbol{\beta} + \alpha \log t_{ij(k)} + U_k\right), \exp\left(\mathbf{x}'_{j'(k)}\boldsymbol{\beta} + \alpha \log t_{ij'(k)} + U_k\right)\right) \\
&\quad = \exp\left(\mathbf{x}'_{j(k)}\boldsymbol{\beta} + \mathbf{x}'_{j'(k)}\boldsymbol{\beta} + \alpha \log t_{ij(k)} + \alpha \log t_{ij'(k)}\right) \operatorname{cov}\left(\exp(U_k), \exp(U_k)\right) \\
&\quad = \exp\left(\mathbf{x}'_{j(k)}\boldsymbol{\beta} + \mathbf{x}'_{j'(k)}\boldsymbol{\beta} + \alpha \log t_{ij(k)} + \alpha \log t_{ij'(k)}\right) \operatorname{var}\left(\exp(U_k)\right) \\
&\quad = \exp\left(\mathbf{x}'_{j(k)}\boldsymbol{\beta} + \mathbf{x}'_{j'(k)}\boldsymbol{\beta} + \alpha \log t_{ij(k)} + \alpha \log t_{ij'(k)}\right) \left(\mathbb{E}\left[\exp(2U_k)\right] - \mathbb{E}\left[\exp(U_k)\right]^2\right) \\
&\quad = \exp\left(\mathbf{x}'_{j(k)}\boldsymbol{\beta} + \mathbf{x}'_{j'(k)}\boldsymbol{\beta} + \alpha \log t_{ij(k)} + \alpha \log t_{ij'(k)}\right) \left(M_U(2) - M_U^2(1)\right) \\
&\quad = \exp\left(\mathbf{x}'_{j(k)}\boldsymbol{\beta} + \mathbf{x}'_{j'(k)}\boldsymbol{\beta} + \alpha \log t_{ij(k)} + \alpha \log t_{ij'(k)}\right) \left(e^{2\sigma_U^2} - e^{\sigma_U^2}\right) \\
&\quad = \exp\left(\mathbf{x}'_{j(k)}\boldsymbol{\beta} + \alpha \log t_{ij(k)} + \sigma_U^2/2\right) \exp\left(\mathbf{x}'_{j'(k)}\boldsymbol{\beta} + \alpha \log t_{ij'(k)} + \sigma_U^2/2\right) \left(e^{\sigma_U^2} - 1\right) \\
&\quad = \mu^*_{ij(k)}\mu^*_{ij'(k)}\xi
\end{aligned}
$$

## B.2 Derivation of Expected Value of $t_{ij(k)}^{\alpha}$

Let $y_{ij(k)} = t_{ij(k)}^{\alpha}|U_k$, $y_c = t_c^{\alpha}$. Given $\alpha$, then $y_{ij(k)} \sim Exp(\lambda_{j(k)})$.

$$
\begin{aligned}
&\mathbb{E}\left[t_{ij(k)}^{\alpha}\right] \\
&= \mathbb{E}\left[\mathbb{E}\left[t_{ij(k)}^{\alpha}|U_k\right]\right] \\
&= \mathbb{E}\left[\mathbb{E}\left[y_{ij(k)}\right]\right] \\
&= \mathbb{E}\left[P(y_{ij(k)} < y_c)\mathbb{E}\left[y_{ij(k)}|y_{ij(k)} < y_c\right] + P(y_{ij(k)} \geq y_c)\mathbb{E}\left[y_{ij(k)}|y_{ij(k)} \geq y_c\right]\right] \\
&= \mathbb{E}\left[P\left(y_{ij(k)} < y_c\right)\frac{\int_0^{y_c} y_{ij(k)}\lambda_{j(k)}\exp\left(-\lambda_{j(k)}y_{ij(k)}\right)\mathrm{d}y_{ij(k)}}{P\left(y_{ij(k)} < y_c\right)} + \exp\left(-\lambda_{j(k)}y_c\right)y_c\right] \\
&= \mathbb{E}\left[\frac{1-\exp\left(-\lambda_{j(k)}y_c\right)}{\lambda_{j(k)}}\right] \\
&= \mathbb{E}\left[\frac{1-\exp\left(-\lambda_{j(k)}t_c^{\alpha}\right)}{\lambda_{j(k)}}\right] \\
&= \mathbb{E}\left[\frac{1-\exp\left(-e^{\mathbf{x}'_{j(k)}\boldsymbol{\beta}+U}t_c^{\alpha}\right)}{e^{\mathbf{x}'_{j(k)}\boldsymbol{\beta}+U}}\right]
\end{aligned}
$$

Thus, it follows that

$$
\begin{aligned}
&\mathbb{E}\left[\exp\left(\mathbf{x}'_{j(k)}\boldsymbol{\beta}+\sigma_U^2/2\right)t_{ij(k)}^{\alpha}\right] \\
&= \exp\left(\mathbf{x}'_{j(k)}\boldsymbol{\beta}+\sigma_U^2/2\right)\mathbb{E}\left[t_{ij(k)}^{\alpha}\right] \\
&= \exp\left(\mathbf{x}'_{j(k)}\boldsymbol{\beta}+\sigma_U^2/2\right)\mathbb{E}\left[\mathbb{E}\left[t_{ij(k)}^{\alpha}|U_k\right]\right] \\
&= \exp\left(\mathbf{x}'_{j(k)}\boldsymbol{\beta}+\sigma_U^2/2\right)\mathbb{E}\left[\frac{1-\exp\left(-e^{\mathbf{x}'_{j(k)}\boldsymbol{\beta}+U}t_c^{\alpha}\right)}{e^{\mathbf{x}'_{j(k)}\boldsymbol{\beta}+U}}\right]
\end{aligned}
$$